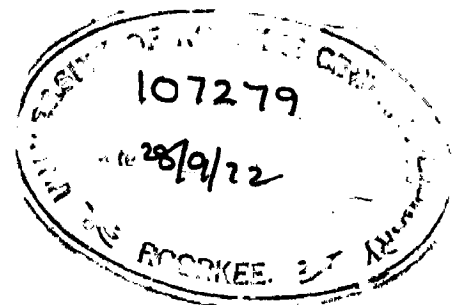


H41-72  
PRA

# EARTHQUAKE RESPONSE OF CONCRETE GRAVITY DAMS WITH LIGHT STRUCTURAL SYSTEM AT THE TOP

*A Dissertation*  
*submitted in partial fulfilment*  
*of the requirement for the Degree*  
*of*  
MASTER OF ENGINEERING  
*in*  
EARTHQUAKE ENGINEERING  
*with Specialization in Structural Dynamics*

by  
**G. I. PRAJAPATI**



DEPARTMENT OF EARTHQUAKE ENGINEERING  
UNIVERSITY OF ROORKEE  
ROORKEE  
JULY 1972

CERTIFICATE

Certified that thesis entitled "Earthquake Response of Concrete Gravity Dams with Light Structural System at the Top", which is being submitted by Mr. Gunvantprasad Ishwarlal Prajapati in partial fulfilment for the award of the degree of Master of Engineering in Earthquake Engineering with specialization in STRUCTURAL DYNAMICS, of the University of Roorkee, Roorkee, is a record of student's own work carried out by him under our supervision and guidance. The matter embodied in this thesis has not been submitted for the award of any other degree or diploma.

---

This is further to certify that he has worked for a period of seven months from January 1972 to July 1972 for preparing this thesis for Master of Engineering Degree at the University.

*S.K. Thakkar*

S.K. Thakkar  
Lecturer in Structural Dynamics  
Department of Earthquake Engineering  
University of Roorkee  
Roorkee

*Manya*

Dr. A.S. Arya 3.8.72  
Professor and Head  
Department of Earthquake  
Engineering  
University of Roorkee  
Roorkee

## SYNOPSIS

The more critical tensile stresses occur in the upper parts of the dams due to earthquakes. The extra concrete near the crest of the dam to support roadway etc., is found to be responsible for this. An attempt has been made to reduce crest mass by developing several light structural systems to support the roadway and perform other necessary functions.

The dynamic response of the dam is calculated for different earthquakes by shear bending beam approach using Holzer's technique. Root Mean Square combination of the first three modes is used for this purpose. ~~The principal stresses due to static and~~ dynamic vertical stresses are worked out for both reservoir full and empty conditions at upstream and downstream faces of the dam.

The reduction of the weight at the top results in the reduction of the tensile principal stresses as compared to the dam with the solid crest. The reduction in tensile principal stresses is significant at the crest level as compared to the base section.

ACKNOWLEDGEMENTS

The author wishes to express his sincere thanks to Dr. A.S. Arya, Professor and Head, and Mr. S.K. Thakkar, Lecturer in Structural Dynamics, Earthquake Engineering Department, University of Roorkee for their valuable guidance and constant encouragement throughout this investigation.

Thanks are due to Mr. K. Loganathan and Mr. R.C. Gupta for their help at various stages of the work.

Thanks are also due to the staff of Computer Centre, ~~Structural Engineering Research Centre, Roorkee,~~ and School of Economics, University of Delhi, Delhi for their help in digital computer work.

# CONTENTS

CHAPTER		PAGE NO.
	CERTIFICATE	(i)
	SYNOPSIS	(ii)
	ACKNOWLEDGEMENTS	(iii)
1	INTRODUCTION	1-8
	1.1 Introduction	1
	1.2 Review of Past Work	1-3
	1.3 Object of Thesis	3
	1.4 Scope of Investigation	4-5
	1.5 Outline of Thesis	5
	1.6 Notations	5-8
2	METHOD OF ANALYSIS	9-18
	2.1 Gravity Method of Stress Analysis	9
	2.2 Dynamical Analysis	9-14
	2.3 Evaluation of Response	14-15
	2.4 Load Combinations	15-16
	<del>2.5 Stress Calculations</del>	<del>16-18</del>
3	RESULTS OF ANALYSIS	19-33
	3.1 Basic Section of Dam	19
	3.2 Problems Considered	19-21
	3.3 Earthquakes Considered	21-23
	3.4 Static Stresses	23-24
	3.5 Dynamic Deflections	24-27
	3.6 Dynamic Shears	27-28
	3.7 Dynamic Moments	28-29
	3.8 Combined Principal Stresses	30-33
4	SUMMARY AND CONCLUSIONS	34-39
	4.1 Summary of Results	34-36
	4.2 Conclusions	36-38
	4.3 Scope for further Investigation	39
5	REFERENCES	40-42
	APPENDIX-A	T1-T2
	Tables	
	APPENDIX-B	P1-P12
	Computer Programs	

## 1. INTRODUCTION

### 1.1 INTRODUCTION

The concrete gravity dams are constructed for irrigation, water supply, hydroelectric power, control of flood and sediment, recreation and navigation or combination of all. The dams are important structures, hence they should be designed for anticipated earthquake forces which are going to induce much larger tensile stresses as compared to static stresses caused due to dead load, hydrostatic pressure, wind load, wave pressure and uplift pressure. Dynamic analyses of stresses in concrete gravity dams during earthquakes demonstrate that more critical tensile stresses occur in upper parts of dam. The principal aim of this investigation is to reduce the tensile stresses caused due to earthquakes.

### 1.2 REVIEW OF PAST WORK

An attempt of reducing stresses due to earthquake was made by Saini<sup>(18)</sup> by reducing mass at the top portion of dam. The profile of the dam used is shown in Fig. 1. Since the maximum acceleration occurs at the top of the dam due to earthquake, the mass near the top contributes most to the inertia forces. The portion from which the mass was removed is shown by shaded lines.

Due to the removal of material at the top, the fundamental natural period was reduced from 0.34 seconds to 0.285 seconds.

The stresses due to earthquake were reduced only in a small portion near top of the dam but were increased elsewhere. The total stresses were slightly lowered in a small portion near the top of the dam but were generally increased at other sections. He concluded that the removal of the material from the top portion of dam would generally not improve the situation because of decrease in the natural period of vibration, hence increase in earthquake forces. As a further step, the finite element method was used for the analysis taking the combined effect of horizontal and vertical components of ground motion as well as horizontal ground motion alone and it was found that there was little difference in the dynamic response.

Chopra and Chakrabarti<sup>(5)</sup> have analysed the overflow and non overflow sections of Koyna Dam as shown in Fig. 1. The finite element method has been used and the stresses are computed by time wise combination of the first four fundamental modes for Koyna earthquake. The periods of the first four modes of vibration of non overflow and overflow sections are 0.326, 0.122, 0.093, 0.063 and 0.205, 0.088, 0.078, 0.051 sec respectively. The maximum tensile stress in case of overflow section was considerably smaller as compared to non overflow section. It was not, however, obvious whether the apparently high stresses developed because of untypical section of this dam or because the ground motion at Koyna had large accelerations and relatively strong high frequency components, or because of both.

They have further analysed a typical concrete gravity Pine Flat Dam of California as shown in Fig. 2. The properties of concrete in this dam are : modulus of elasticity =  $3.5175 \times 10^5 \text{ kg/cm}^2$ , unit weight =  $2.475 \text{ t/m}^3$ , and Poission's ratio = 0.20. The analysis has been carried out for transverse and vertical components of Koyna earthquake. Damping was assumed to be 5 percent of critical in each of the first four fundamental modes. The time periods of the first four modes of vibration were worked out as 0.256, 0.125, 0.092 and 0.072 sec.

The structural section of the Pine Flat Dam i.e., triangular profile is also shown in Fig. 2 after removing the concrete of shaded portion. The time periods of this section in the first four modes were found as 0.22, 0.099, 0.087 and 0.060 sec. As a result of the reduced weight at the crest, much smaller tensile stresses developed in the structural section and the reduction was about 40 percent at the downstream face and about 60 percent at the upstream face. The dynamic interaction between the dam and reservoir was ignored in these computations.

### 1.3 OBJECT OF THESIS

The principal object of this thesis is to study the nature of dynamic response and principal stresses developed due to earthquake forces when the mass at crest level is reduced by providing suitable light structural system at the top so as to support the roadway and perform other necessary functions like providing the free board.



#### 1.4 SCOPE OF INVESTIGATION

Method of Analysis : The Gravity Method is used for computing static normal vertical stresses. The concept of treating the dam as shear bending beam is used for computing dynamic response. The whole structure is discretized into a lumped mass system in order to calculate the dynamic response.

Structural Systems : The concrete gravity dam considered for analysis is modified Pine Flat Dam shown in Fig. 4. Seven systems with different arrangements at the top are considered, varying from a dam with solid crest to a dam having structural section i.e., triangular profile as shown in Fig. 5.

Earthquake Motions : The following earthquakes are considered for the analysis :

- |       |                              |   |                          |
|-------|------------------------------|---|--------------------------|
| (i)   | Koyna-Longitudinal component | ) | Spectral Intensity made  |
| (ii)  | El Centro- N-S component     | ) | equal for 5% of critical |
| (iii) | Average Spectra              | ) | damping                  |
| (iv)  | Koyna elongated              | ) |                          |

Results : The principal stresses due to static loads for both reservoir full and empty conditions are calculated at upstream and downstream faces at various sections from neck to base.

The dynamic response i.e., moment, shear, slope, deflection and acceleration are obtained in each mode. The combined

response, of first three modes is obtained by mode superposition using Root Mean Square technique. The principal stresses due to static and dynamic forces for both reservoir empty and full conditions are obtained at upstream and downstream faces at various sections from neck to base.

## 1.5 OUTLINE OF THESIS

Chapter 2 deals with the method of analysis for computing stresses due to static and dynamic loading and combination of both. The various assumptions involved in the method and the procedure of computations are discussed.

Chapter 3 deals with the results of analysis. The number of cases considered for the analysis, dynamic response and the combined principal stresses developed in each case are discussed.

Chapter 4 deals with summary and conclusions derived from the investigation. The scope for further investigation is also given.

## 1.6 NOTATIONS

A	dynamic response in a particular mode, area of the section
$A_t$	total superimposed response of various modes
a	modal value for a particular mode
C	pressure coefficient varying with shape and depth
$C_{11}$ $C_{12}$ $C_{21}$ $C_{22}$	constants of frequency determinant
$C_m$	maximum value of C

E	modulus of elasticity
G	modulus of rigidity
g	acceleration due to gravity
H	height of the dam
h	maximum depth of the reservoir
$h_n$	length of $n^{\text{th}}$ segment
I	moment of inertia
$I_n$	moment of inertia of member section in $n^{\text{th}}$ segment
M	moment
$M_n, M_{n-1}$	moments at $n^{\text{th}}$ and $(n-1)^{\text{th}}$ mass points
$M_o$	moment at the fixed end of the beam
$M_f$	moment at the free end of the beam
$m_n$	concentrated mass of the beam section at $n^{\text{th}}$ point
n	no. of joint or division point
$P_e$	hydrodynamic pressure at depth $y_1$ , normal to the face
p	circular natural frequency
$p'$	assumed circular natural frequency
$P_{en}$	hydrodynamic pressure acting in the horizontal direction at the u/s face
$P_{ev}'' , P_{ev}'$	dynamic vertical normal stress for reservoir full and empty conditions at u/s and d/s faces
$P_n$	normal water loading at u/s face
$P_v$	vertical normal stress
$P_v'' , P_v'$	static vertical normal stress at u/s and d/s faces
$P_1$	major principal stress
$P_2$	minor principal stress

	mode of vibration
$S_a$	spectral acceleration
$S_d$	spectral displacement
$S_I$	spectral intensity
$S_v$	spectral velocity
$T$	natural period of vibration
$t$	time variable
$V$	shear
$V_f$	shear at the free end of the beam
$V_n$	shear at the $n^{\text{th}}$ section
$V_o$	shear at the fixed end of the beam
$W$	vertical load
$w$	unit weight of water
$x$	distance measured along the height
$Y$	total deflection
$Y_b$	bending deflection
$Y_s$	shear deflection
$y$	distance of the c. g. of the section from remote fibre
$y_f$	deflection at free end of beam
$y_n$	deflection at $n^{\text{th}}$ mass point
$y_o$	deflection at fixed end of beam
$y_1$	depth of section below the water surface
$\alpha$	slope at downstream face
$\alpha_h$	horizontal seismic coefficient
$\beta$	slope at upstream face

$\gamma_r$	mode participation factor $r^{\text{th}}$ mode
$\rho$	mass density
$\zeta$	damping factor
$\sigma$	shape factor
$\theta_f$	inclination of tangent at the free end of beam
$\theta_n, \theta_{n-1}$	inclination of tangent at $n^{\text{th}}$ and $n-1^{\text{th}}$ division point
$\theta_o$	inclination of tangent at the fixed end of beam
$\phi_j^{(r)}$	mode shape factor at point $j$ in $r^{\text{th}}$ mode
$\phi''$	angle between u/s face and vertical
$\phi'$	angle between d/s face and vertical

## 2. METHOD OF ANALYSIS

### 2.1 THE GRAVITY METHOD OF STRESS ANALYSIS

The Gravity Method <sup>(24)</sup> provides an approximate means for determination of stresses in a cross section of gravity dam. The method is applicable to a gravity section with a variable batter on both faces. The following assumptions are made :

- (1) The transverse contraction joints in the dam are neither keyed nor grouted.
- (2) All loads are carried by the gravity section, that is, parallel cantilevers which receive no support from the adjacent elements on either side.
- (3) Unit vertical pressures, or normal stresses on horizontal planes, are assumed to vary linearly from the upstream to downstream face.
- (4) A parabolic variation of shear stresses is assumed on horizontal planes from upstream to downstream face.

### 2.2 DYNAMICAL ANALYSIS

The dam is assumed to be a tapered cantilever as a shear bending beam <sup>(2, 3, 12, 15)</sup> for determining frequencies and mode shapes.

The equations of motion for free undamped vibration of a cantilever can be written as follows wherein bending and shearing

deformations are considered and effect of rotary inertia is also included.

$$\frac{\partial}{\partial x} \left( EI \frac{\partial^2 Y_b}{\partial x^2} \right) + \sigma AG \frac{\partial Y_s}{\partial x} = \frac{P I \partial^3 Y_b}{\partial x \partial t^2} \quad (1)$$

$$\frac{\partial}{\partial x} \left( \sigma AG \frac{\partial Y_s}{\partial x} \right) = P A \frac{\partial^2 Y}{\partial t^2} \quad (2)$$

where,

- Y = total deflection due to shear and bending
- $Y_b$  = bending deflection
- $Y_s$  = shear deflection
- A = area of the section
- x = distance measured along the height
- t = time variable
- E = modulus of elasticity
- G = modulus of rigidity
- I = moment of inertia
- $\sigma$  = shape factor, 1.2 for rectangular section

Transfer matrix approach has been used to obtain the solution of Equations 1 and 2 numerically.

Consider the cantilever beam as shown in Fig. 3(a) vibrating in classical natural mode of circular natural frequency  $p$  with zero damping. If the beam is divided into a number of segments of length  $h_{n-1}$ ,  $h_n$  etc. as shown in Fig. 3(b) and the mass included within

the half segments on either side of division point is concentrated at division points, the shear  $V_n$  and slope  $\theta_n$  in  $n^{\text{th}}$  segment, moment  $M_n$  and deflection  $y_n$  at  $n^{\text{th}}$  mass point will be related to corresponding values at just previous segment and point by certain transfer function<sup>(2)</sup> as defined below :

If on one end of an elastic straight member, there is imposed a harmonic exciting function ( $A \sin pt$ ), where  $A$  is one and only one of the following :

Shear  $V$ , bending moment  $M$ , slope  $\theta$  and displacement  $y$  .

Then the values of these four quantities that are necessary to hold it in dynamic equilibrium at the given frequency are the transfer functions which can be derived for the vibrating cantilever for which a free body diagram is shown in Fig. 3(c). The transfer equations, corresponding to equations 1 and 2, where in the deformations due to shear, bending and the rotary inertia have been included are as follows :

$$V_n = V_{n-1} + m_{n-1} p^2 y_{n-1}$$

$$M_n = M_{n-1} + V_n h_n - p^2 I_n h_n^2 \theta_{n-1}$$

$$\theta_n = \theta_{n-1} + \frac{h_n}{2EI_n} (M_n + M_{n-1})$$

$$y_n = y_{n-1} + h_n \theta_{n-1} + \frac{h_n^2}{3EI_n} \left( M_{n-1} + \frac{M_n}{2} \right) - \frac{6 V_n h_n}{GA_n}$$



where,

$V_n$	=	shear force in $n^{\text{th}}$ segment
$M_n$	=	bending moment on $n^{\text{th}}$ mass point
$\theta_n$	=	slope at $n^{\text{th}}$ mass point
$y_n$	=	deflection at $n^{\text{th}}$ mass point
$m_n$	=	mass lumped at $n^{\text{th}}$ point
$p$	=	natural frequency in radians per second
$h_n$	=	length of $n^{\text{th}}$ segment
$\rho$	=	mass density
$I_n$	=	moment of inertia of member section in $n^{\text{th}}$ segment
$E$	=	modulus of elasticity
$G$	=	modulus of rigidity
$\sigma$	=	shape factor, 1.2 for rectangular section.

These equations are successively applied to the segments proceeding from free end of the beam to the fixed end. Out of the four boundary values at free end, two will be known, that is, moment  $M_f$  and shear  $V_f$  are zero, and two unknowns which are slope  $\theta_f$  and deflection  $y_f$ . Thus the transfer quantities will be in terms of two unknowns  $\theta_f$  and  $y_f$ .

At the base or fixed end, slope  $\theta_0$  and deflection  $y_0$  are zero while moment  $M_0$  and shear  $V_0$  exist.

Thus, if the values of  $p$ ,  $\theta_f$  and  $y_f$  are known, the shear, moment, slope and deflection can be computed for each point successively from free to fixed end of beam. The proper values of  $p$ ,  $\theta_f$  and  $y_f$  are determined by process of successive approximation.

An arbitrary trial value for  $p$  is chosen, say  $p'$ . The total deflection at free end is assumed to be unity while the slope is zero. The resulting deflection and slope are evaluated at the fixed end.

At free end  $y_f = 1$  and  $\theta_f = 0$ . The deflection at fixed end is given by

$$y_o = C_{11} y_f + C_{12} \theta_f \quad (1)$$

Similarly the slope at free end is assumed to be unity while deflection is zero and the resulting slope and deflection are evaluated at the fixed end.

When  $y_f = 0$  and  $\theta_f = 1$ , the slope at fixed end is given by

$$\theta_o = C_{21} y_f + C_{22} \theta_f \quad (2)$$

The equations 1 and 2 can be written in the matrix form as given below :

$$\begin{Bmatrix} y_o \\ \theta_o \end{Bmatrix} = \begin{bmatrix} C_{11} & C_{12} \\ C_{21} & C_{22} \end{bmatrix} \begin{Bmatrix} y_f \\ \theta_f \end{Bmatrix}$$

The boundary conditions for a cantilever beam require that slope  $\theta_o$  and deflection  $y_o$  should be zero at the fixed end, therefore, the condition for  $\theta_f$  and  $y_f$  to be non-zero is the vanishing of the determinant.

$$\Delta \equiv \begin{vmatrix} C_{11} & C_{12} \\ C_{21} & C_{22} \end{vmatrix}$$

where  $C_{11}$ ,  $C_{12}$ ,  $C_{21}$  and  $C_{22}$  are constants of frequency determinant and their values depend upon the value of  $p$ .

The requirement specifies the correct value of  $p$  and, by successive trials, the appropriate value of  $p$  can be determined. When the value of  $p$  has been found for which  $\Delta$  is sufficiently close to zero, the corresponding mode shape is determined by deflected shape of vibrating beam when the base moment is  $M_0$  and the base shear,  $V_0$ , is

$$V_0 = -M_0 \left( \frac{C_2}{C_1} \right)$$

### 2.3 EVALUATION OF RESPONSE

The responses evaluated for the concrete gravity dam section<sup>(1)</sup> are dynamic moments, dynamic shears, dynamic deflections and the accelerations. These are evaluated for the first three modes. The damping is assumed to be 5 % of critical in all modes. The properties of concrete are : modulus of elasticity =  $1.462 \times 10^5 \text{ kg/cm}^2$ , unit weight =  $2400 \text{ kg/m}^3$  and Poisson's ratio = 0.15.

The expressions used for responses and superposition of modal values are given below :

$$A = a \gamma_r S_d$$

$$A_T = \sqrt{A_1^2 + A_2^2 + A_3^2 + \dots + A_n^2}$$

$$\gamma_r = \frac{\sum_{j=1}^n m_j \phi_j^{(r)}}{\sum_{j=1}^n m_j (\phi_j^{(r)})^2}$$

where,

- A = dynamic response in a particular mode corresponding to shear, moment etc.
- a = modal value for any particular mode
- S<sub>d</sub> = spectral displacement
- A<sub>T</sub> = total superimposed response of various modes
- γ<sub>r</sub> = mode participation factor in r<sup>th</sup> mode
- m<sub>j</sub> = concentrated mass at point j
- φ<sub>j</sub><sup>(r)</sup> = mode shape factor at point j in r<sup>th</sup> mode.

The root mean square technique is used in order to get combined response of first three modes.

#### 2.4 LOAD COMBINATIONS

The dead load, hydrostatic pressure and uplift pressures are considered for static analysis. In addition to these, hydrodynamic and inertia forces due to earthquake are also considered for static and dynamic analyses. The uplift pressure is assumed to be maximum at the upstream face and reduces to zero at downstream face.

Zangaar's <sup>(19)</sup> approach given by IS: 1893 <sup>(22)</sup> is used for evaluating hydrodynamic pressure. The hydrodynamic effect of reservoir is taken into account by virtual mass <sup>(19, 23)</sup> concept.

The following extreme combinations are considered :

- (1) Reservoir full without earthquake
- (2) Reservoir empty without earthquake
- (3) Reservoir full plus earthquake, inertia force acting from upstream to downstream.
- (4) Reservoir empty plus earthquake, inertia force acting from downstream to upstream.

## 2.5 STRESS CALCULATIONS

The normal vertical stress due to static and dynamic loading is given by

$$p_v = \frac{W}{A} \pm \frac{My}{I}$$

where,

- $p_v$  = vertical stress
- $W$  = total vertical load
- $A$  = area of section considered
- $M$  = moment of all forces about c. g. of the section
- $y$  = distance of the c. g. of the section from remote fibre
- $I$  = moment of inertia

The tensile and compressive stresses are indicated by -ve and +ve signs respectively.

The principal stresses are given by :

- (1) Reservoir full condition without earthquake

upstream face

$$P_1 = p_n$$

$$P_2 = p_v'' \sec^2 \phi'' - p_n \tan^2 \phi''$$

downstream face

$$P_1 = 0$$

$$P_2 = p_v' \sec^2 \phi'$$

- (2) Reservoir empty condition without earthquake

upstream face

$$P_1 = 0$$

$$P_2 = p_v'' \sec^2 \phi''$$

downstream face

$$P_1 = 0$$

$$P_2 = p_v' \sec^2 \phi'$$

- (3) Reservoir full condition plus earthquake

Upstream face

$$P_1 = p_n + p_{en} \sec \phi''$$

$$P_2 = (p_v'' - p_{ev}'') \sec^2 \phi'' - (p_n + p_{en} \sec \phi'') \tan^2 \phi''$$

downstream face

$$P_1 = p_n$$

$$P_2 = (p_v' + p_{ev}') \sec^2 \phi'$$

- (4) Reservoir empty condition plus earthquake

upstream face

$$P_1 = 0$$

$$P_2 = (p_v'' + p_{ev}'') \sec^2 \phi''$$

downstream face

$$P_1 = 0$$

$$P_2 = (p_v' - p_{ev}') \sec^2 \phi'$$

where,

- $P_1$  = major principal stress
- $P_2$  = minor principal stress
- $P_v''$  = static vertical normal stress at u/s face
- $P_v'$  = static vertical normal stress at d/s face
- $P_n$  = normal water loading at u/s face
- $P_{en}$  = hydrodynamic pressure acting in the horizontal direction at u/s face
- $P_{ev}''$  = dynamic vertical normal stress for reservoir full and empty conditions at u/s face
- $P_{ev}'$  = dynamic vertical normal stress for reservoir full and empty conditions at d/s face
- $\phi''$  = angle between u/s face and vertical
- $\phi'$  = angle between d/s face and vertical

### 3. RESULTS OF ANALYSIS

#### 3.1 BASIC SECTION OF DAM

The dam section selected for the analysis is Pine Flat Dam of California, U.S.A. The section is slightly modified and is shown in Fig. 4. The height of the dam is 129 m. The width of the roadway is 10.5 m. The maximum depth of reservoir is 125 m. The upstream slope is 0.05 to 1 and begins from maximum water level. The downstream slope is 0.78 to 1.0. Fig. 4 gives the details about modified Pine Flat Dam section while original dam section is shown in Fig. 2. The portion above the plane 'aa' in Fig. 4 will be called as crest of the dam.

#### 3.2 PROBLEMS CONSIDERED

Several alternatives are considered to reduce the crest weight. The main object of providing the crest is to support the roadway, to resist impact of floating objects and to provide the necessary free board. These points are also taken into account while reducing the crest weight. The following cases are considered :

Case 1            The crest of the dam is solid as in the case of typical concrete gravity dam, shown in Fig. 5(a) without modification.

Case 2            The concrete above the maximum water level is removed and roadway is lowered upto this level. A cantilever projection having thickness 1 m and height 4 m is provided on upstream face.



A parapet wall having thickness 0.25 m and height 1 m is provided at d/s face as shown in Fig. 5(b).

Case 3            A bridge-pier system is provided at the crest as shown in Fig. 5(c). The piers having thickness of 0.9 m are placed at 7.5 m c/c distance. A slab having thickness of 0.4 m is provided at maximum water level to support roadway. The wall at the upstream may be designed as a counterfort retaining wall to resist water pressure and impact of floating objects.

Case 4            The crest is made hollow by providing vertical walls at upstream and downstream faces. A slab having thickness 0.4 m is provided at the top to support roadway. The parapet walls having thickness 0.25 m and height 1.0 m are provided at upstream and downstream faces as shown in Fig. 5(d).

Case 5            The structural section is indeed the triangular section of the dam in which hydraulic and structural heights of the dam are same. In this case the portion above the structural profile consists of a bridge pier system. The piers are placed at a distance of 7.5 m c/c having thickness 0.9 m. The portion below the structural profile is solid. The slab having thickness 0.4 m is provided at the top to support roadway. A wall having thickness 1.0 m is provided between top and maximum water level. A parapet wall having thickness 0.25 m and height 1.0 m is provided on the downstream face at the top as shown in Fig. 5(e).

Case 6                    The portion above the structural profile is made hollow by providing a vertical wall of thickness 1.0 m at downstream face. A wall having thickness 1.0 m is provided between top and maximum water level. The level of roadway is lowered by 1.0 m. The slab having thickness 0.4 m supports the roadway. The parapet wall having thickness 0.25 m and height 1.0 m is provided at the top on downstream face as shown in Fig. 5(f).

Case 7                    The crest is made triangular. The free-board and roadway are not provided in this case. The dam section is shown in Fig. 5(g). The hydraulic and structural heights are made equal.

The crest may be reinforced in cases 2 to 6 if required.

The geometrical properties like area and moment of inertia of the cross sections are calculated by considering the section as a rectangular section, having unit width and depth equal to the width of the section in Case 1, Case 2, Case 4, and Case 7. In Case 3 and Case 5, the channel sections shown in Fig. 5(c) and Fig. 5(e) are considered for calculating the cross section properties. The area and moment of inertia are found for a channel having depth equal to 7.5 m. Finally, the properties are evaluated for unit width by dividing them by 7.5.

### 3.3                    EARTHQUAKES CONSIDERED

The following four earthquakes are taken for analysis :

- (1) Koyna, India : - The earthquake took place on December 11, 1967. The longitudinal component along dam axis is taken for the analysis. The maximum acceleration was 63.0 percent of that due to gravity.
- (2) El Centro, California : - This earthquake occurred on May 18, 1940. The North-South component is taken for the analysis. The maximum acceleration was 33.0 percent of gravity.
- (3) Average Spectra: - The average spectra given by IS: 1893<sup>(23)</sup> are also considered for the analysis. The velocity spectrum<sup>(22)</sup> for 5 percent of critical damping is considered for evaluating the displacement spectra.
- (4) Koyna elongated: - This earthquake is obtained from original data of Koyna earthquake.

The time periods and displacements are elongated by the factors 1.5 and 2.25 respectively and displacement spectrum for Koyna elongated earthquake is obtained.

The spectral intensity represents a measure of the intensity of ground motion. It is defined as the area under the velocity spectrum curve between 0.1 sec and 2.5 sec and is denoted by  $SI_{\xi}$ , where  $\xi$  is the fraction of critical damping.

The spectral intensities of Koyna, El Centro, Average spectra earthquakes are 98.2 cm/sec, 151.72 cm/sec, 37.94 cm/sec respectively. The SI of El Centro and Average Spectra are brought

equal to Koyna level i.e., 98.2 cm/sec in using the first three earthquakes. The fourth earthquake has SI 0.05 of 117.98 cm/sec, hence much more severe as compared with the other three normalised earthquakes.

The displacement spectra for above four earthquakes are shown in Fig. 6 for 5.0 percent of critical damping.

### 3.4 STATIC STRESSES

The static vertical and principal stresses on upstream and downstream faces are calculated at eleven sections as shown in Fig. 4. The first section is situated at the neck, at height of 111.5 m from base. The eleventh section is situated at the base. The stresses are calculated for reservoir full and empty conditions. The vertical stresses and principal stresses are calculated by preparing a digital computer program given in Appendix A using the relevant equations as given in Section 2.5.

The values of principal stresses are given in Table 3 for Case 1, Case 3 and Case 7 for both the conditions. The magnitude of the principal stresses remains approximately same for all cases. Slight tensile principal stresses are developed at the bottom in Cases 1 and 2 on the upstream face. In Cases 3 to 7, tensile principal stresses are developed approximately at all the sections, the maximum value being  $1.73 \text{ kg/cm}^2$ .

The nature of the principal stresses developed at downstream face is compressive. The magnitude of the stresses remains more or less same for all cases at all sections except at the neck section. The magnitudes are minimum and maximum at the first and eleventh section respectively in Case 3 through Case 7.

Under reservoir empty condition, the compressive principal stresses are developed on the upstream face in all cases. The values are minimum and maximum at the crest and base. The values are more or less same for all cases.

On the downstream face, compressive principal stresses are developed in all cases except a tensile stress of  $0.564 \text{ kg/cm}^2$  occurs only at the first section in Case 3.

### 3.5 DYNAMIC DEFLECTIONS

The Case 1 and Case 7 are extreme cases of solid crest and triangular crest. Case 3 represents the crest system with minimum top weight as compared to remaining cases. The results of cases 2, 4, 5 and 6 fall in the range of Case 1 and Case 3. Therefore cases 1, 3 and 7 are generally studied in greater detail.

The modal deflections for the first three modes are plotted for Case 1, Case 3 and Case 7 for both reservoir full and empty conditions in Fig. 7(a) and Fig. 7(b).

In the first mode, modal deflection values for Case 3 and Case 7 are greater than the Case 1, the maximum being for Case 7 along the height of the dam, for reservoir full condition. The same variation holds good for reservoir empty condition with increase in the values of Case 3 and Case 7 as compared to Case 1.

The modal deflection in second mode for Case 3 and Case 7 are greater than the Case 1 at and near the top of the dam. The values are minimum for Case 1 and maximum for Case 3 in the upper middle portion of the dam while in the lower middle portion and at and near the bottom the values are minimum for Case 7 and maximum for Case 3. Similar type of variation is also seen for reservoir empty condition.

In the third mode, modal deflections are greater in Case 3 and Case 7 as compared to Case 1, maximum being for Case 7, at and near the top. The values are minimum for Case 1 and maximum for Case 3 in the upper middle portion of the dam. In the upper middle portion the values are minimum for Case 1 and maximum for Case 3 while at the middle portion the values are minimum for Case 7 and maximum for Case 1. At and near the bottom, the values are minimum for Case 3 and maximum for Case 1 for reservoir full condition. The same relation holds good for reservoir empty condition with change in values.

The height versus dynamic deflections for Cases 1, 2, 3, 5 and 7 are plotted in Fig. 8 for reservoir full and empty conditions.

The results of the Cases 4 and 6 are more or less similar to Case 3 and Case 5, therefore they are ignored for further analysis.

The dynamic deflection is minimum for Case 1 and maximum for Case 3 at the top. The values for the remaining cases are in between Case 1 and Case 3. The trend remains same throughout the height of the dam for reservoir full condition.

In reservoir empty condition, the maximum deflection at the top occurs in Case 1 and minimum in Case 7. The minimum deflection occurs in Case 3 below crest level.

The results of Case 1, Case 3 and Case 7 are also plotted for all the four earthquakes for both conditions. The deflections caused by Koyna Elongated earthquake are largest as compared to others for all the three cases as shown in Fig. 9(a) to Fig. 9(c). The spectral intensities of 'El Centro' and 'Average Spectra' earthquakes are brought equal to that of Koyna earthquake, hence it is reasonable to compare the horizontal dynamic deflections for the above three cases for both the conditions. The maximum deflection at top in Case 1 is caused by 'El Centro' earthquake while the minimum is due to 'Average Spectra' earthquake. The trend remains the same along the height of the dam for reservoir full condition. For reservoir empty condition the maximum deflection at top is caused by 'Koyna' earthquake while minimum is due to 'Average Spectra' earthquake. This trend remains the same along the height of the dam. The effect of reservoir is to increase the deflection but in case of 'Koyna'

earthquake, large deflection is seen for Case 1 in Fig. 9(a) for reservoir empty condition. The major contribution to the dynamic deflection is mainly due to first two modes. The time periods for the first two modes with reservoir full are 0.474 sec and 0.219 sec, the corresponding mode participation factors are 2.54 and -2.88. The  $S_d$  values for these time periods can be obtained from Fig. 6 and the values are 0.0265 m and 0.014 m. Similarly for reservoir empty condition, the time periods, mode participation factors and  $S_d$  values are 0.37 sec., 0.182 sec., 2.66, -2.93, 0.033 m, 0.0095 m respectively. The increase in the deflection may be due to increase in mode participation factor and  $S_d$  value in first mode while in the second mode participation factor is increased but the  $S_d$  value is decreased.

For Cases 3 and 7, the deflection at the top caused by 'Average Spectra' and 'Koyna' earthquakes are minimum and maximum for reservoir full condition. The same variation is observed for reservoir empty condition with decrease in values as shown in Fig. 9(b) and Fig. 9(c).

### 3.6 DYNAMIC SHEARS

The dynamic shears in tonnes are plotted along the height of the dam in Fig. 10(a) and Fig. 10(b) for reservoir full and empty conditions for Cases 1, 2, 3, 5 and 7. The dynamic shears are reduced in all cases near the top as compared to Case 1. While the values are increased near the base as compared to Case 1 for reservoir full condition, the maximum being for Case 7.



For reservoir empty condition, the dynamic shears are reduced upto the mid-height of the dam measured from the top. The reduction is greater as compared to the reservoir full condition as shown in Fig. 10(b). The dynamic shears are also reduced at and near the base as compared to Case 1.

The maximum dynamic shears are naturally caused due to 'Koyana Elongated' earthquake. Comparing 'El Centro' and 'Average Spectra' earthquakes for the above three cases as shown in Fig. 11(a) through Fig. 11(f), it is seen that the maximum and minimum shears are due to 'Koyana' and 'Average Spectra' earthquakes at and near the base for reservoir full condition. The same is also true for reservoir empty condition with decrease in values at and near the base.

### 3.7 DYNAMIC MOMENTS

The dynamic moments are plotted along the height of the dam for both conditions as shown in Fig. 10(a) and Fig. 10(b). For reservoir full condition, it is seen that the moments are reduced as compared to Case 1 at the top upto one-third height of the dam. The values are found to be increased at and near the base as compared to Case 1 as shown in Fig. 10(a). For reservoir empty condition, the moments are reduced in all cases as compared to Case 1 along the height from top to base. The differences in the values are also reduced near the base as compared to full reservoir condition as shown in Fig. 10(b).

The moments caused by 'Koyana Elongated' earthquake is maximum for all cases and for both the conditions because of large  $S_d$  values as compared to other earthquakes. Comparing the moments caused by 'Koyana', 'El Centro' and 'Average Spectra' earthquakes, it is seen that the maximum and minimum moments are caused by 'El Centro' and 'Average Spectra' earthquakes near the base as shown in Fig. 11(a) for Case 1 for reservoir full condition. The time periods in the first and second modes are 0.474 and 0.219 sec. The corresponding  $S_d$  values for 'Koyana', 'El Centro' and 'Average Spectra' earthquakes are 0.0265 m, 0.0357 m, 0.025 m and 0.014 m, 0.0072 m, 0.0055 m respectively. The  $S_d$  values for 'Average Spectra' earthquake are minimum as compared to the other two for these periods. In the first mode  $S_d$  value for 'El Centro' is higher than the 'Koyana' while it is smaller in the second mode. Because of the greater  $S_d$  value in the first mode, the moment is also maximum as compared to 'Koyana' and 'Average Spectra'.

For empty reservoir condition, maximum and minimum moments are caused due to 'Koyana' and 'Average Spectra' earthquakes, as shown in Fig. 11(b). The values are also found to be decreased for Case 1 except that due to 'Koyana' earthquake as compared to the values of full reservoir condition. In cases 3 and 7, the maximum and minimum moments are caused due to 'Koyana' and 'Average Spectra' earthquakes as shown in Fig. 11(c) to Fig. 11(f) for both conditions at the base. The moments at the base are relatively decreased for empty reservoir condition.

### 3.8 COMBINED PRINCIPAL STRESSES

The combined principal stresses due to static and dynamic effects are evaluated for all the cases for the four earthquakes with and without the reservoir. The principal stresses are calculated on u/s as well as d/s face at the eleven horizontal sections of the dam, the first and eleventh being at the crest and base respectively as shown in Fig. 4.

The compressive principal stresses occur on the upstream face of the dam for reservoir full condition. These stresses are due to external pressure of water i.e., hydrostatic and hydrodynamic pressures. The hydrostatic pressure is zero at highest water level and maximum at the base. The hydrodynamic pressure due to the effect of earthquake is given by:

$$P_e = C w h \alpha_h$$

$$\text{and } C = \frac{C_m}{2} \left[ \frac{y_1}{h} \left( 2 - \frac{y_1}{h} \right) + \sqrt{\frac{y_1}{h} \left( 2 - \frac{y_1}{h} \right)} \right]$$

where,

$P_e$  = hydrodynamic pressure in  $\text{kg/m}^2$  at depth  $y_1$ ,

normal to the face

$C$  = pressure coefficient varying with shape and depth

$w$  = unit weight of water in  $\text{kg/m}^3$

$h$  = maximum depth of reservoir in meter

$\alpha_h$  = horizontal seismic coefficient

$C_m$  = maximum value of  $C$  obtained from IS: 1893

$y_1$  = depth of section below the water surface in meter

The effective seismic coefficient based on shear force at the base of the dam is considered for computing hydrodynamic pressure.

The values of compressive principal stresses are more or less same for all cases under all earthquakes. The reason is that the hydrostatic pressure remains the same for all cases. The little differences in the values are due to change in the value of seismic coefficients at the base for different cases and different earthquakes. The contribution of hydrostatic pressure is much greater as compared to hydrodynamic pressure.

The principal tensile stresses due to 'Koyna' earthquake at upstream face are mainly due to dynamic load. The maximum tensile stresses occurred at the crest in Case 1 while the minimum stresses occurred in Case 7 as shown in the Fig. 12(a). Near the base, the maximum and minimum principal stresses occur in Cases 3 and 1. The difference in stresses amongst all the cases is large at crest while it is reduced at and near the base.

The compressive principal stresses on downstream are due to static and dynamic vertical pressures. A drastic reduction of stresses is seen at the crest in all the cases as compared to Case 1 as shown in Fig. 12(b). The stresses are minimum for Case 7. At and near the base, the maximum and minimum stresses are developed for Cases 3 and 1 respectively. The difference in the stresses is also reduced at and near the base as compared to crest.

For reservoir empty condition, the maximum compressive principal stresses are due to both static and dynamic vertical stresses. The maximum and minimum stresses at the crest are developed in Cases 1 and 7 respectively. The difference in the values are also large at the crest as compared to base. At and near the base, maximum and minimum stresses are seen in Case 1 and Case 3 as shown in Fig. 12(c).

The principal tensile stresses are mainly due to dynamic effects. The variation of stresses along the height is similar to that of compressive principal stress.

The height versus principal stresses are plotted for 'Koyana Elongated' earthquake as shown in Fig. 15(a) to Fig. 15(c). For reservoir full conditions, the principal tensile stresses near the crest at upstream faces are maximum and minimum for Case 1 and Case 7 respectively. At and near the bottom, maximum and minimum stresses are developed in Cases 3 and 5. The difference in the stresses is large at the crest as compared to the base.

The compressive principal stress at downstream face also shows the same type of variation as shown in Fig. 15(b).

For reservoir empty condition, compressive principal stresses are maximum and minimum for Cases 1 and 7. The difference in the stresses for all the cases are much larger at the crest as compared to the base.

The principal tensile stresses at the crest are maximum and minimum for Cases 1 and 7. The difference in the values of stresses is reduced at and near the base of the dam as compared to the crest as shown in Fig. 15(c).

The principal stresses caused due to 'Koyna', 'El Centro' and 'Average Spectra' are compared in Figs. 12, 13 and 14. The largest and smallest tensile principal stresses at the upstream face are developed due to 'Koyna' and 'Average Spectra' earthquakes respectively for reservoir full condition as shown in Fig. 12(a), Fig. 13(a) and Fig. 14(a). The difference in stresses and reduction in stresses as compared to Case 1 is found to be maximum at the crest due to 'Koyna' earthquake while minimum is due to 'Average Spectra' earthquake. At and near the base, the maximum stresses are observed due to 'El Centro' while the minimum is due to 'Average Spectra'.

The same variation holds good for the compressive principal stresses at the crest as shown in Fig. 12(b), Fig. 13(b) and Fig. 14(b). The difference between the stresses is large in case of 'Koyna' earthquake as compared to the remaining two.

The large compressive and tensile principal stresses are observed at the crest due to 'Koyna' earthquake while minimum stresses are developed due to 'Average Spectra' earthquake as shown in Fig. 12(c), Fig. 13(c) and Fig. 14(c) for reservoir empty condition at upstream and downstream faces. The difference in the stresses for all cases is maximum at the crest while minimum at and near the base.

## 4. SUMMARY AND CONCLUSIONS

### 4.1 SUMMARY OF RESULTS

The analysis of all the dam sections indicates that the static principal stresses remain more or less same for reservoir full as well as empty conditions. Small tensile principal stresses are developed at upstream face otherwise the nature of principal stresses is generally compressive. For reservoir full condition, the large static vertical stresses are developed in all cases at the downstream face as compared to upstream face. For empty reservoir condition, large static vertical stresses are developed at the upstream face as compared to the downstream face.

The dynamic responses like deflection, shear, moment etc., are largest for 'Koyana Elongated' earthquake for both the conditions. The simple reason for this is the large spectral displacement values for the corresponding time periods as compared to the remaining three earthquakes which can be easily seen in Fig. 6.

The modal deflections are found to be increased at and near the top when the crest weight is reduced as compared to the solid crest. This is true for all the modes considered.

The total dynamic deflections are increased at and near the top in other cases as compared to Case 1 for reservoir full condition. For reservoir empty condition, the deflections in all the cases are reduced at and near the top as compared to Case 1.

The effect of reservoir is generally to increase the deflection at the top. This does not hold good for cases 1 and 2 when subjected to 'Koyana' earthquake. This is mainly due to increase in mode participation factors for first two modes in Case 1 and for first three modes in Case 2. Moreover, the 'Koyana' displacement spectrum has a sharp peak corresponding to 0.4 sec. time period. The 'Koyana Elongated' and 'Average spectra' earthquakes are responsible for causing maximum and minimum deflection at the top of the dam.

The dynamic shears are reduced at and near the top but they are found to be increased at and near the base as compared to Case 1 for reservoir full condition as shown in Fig. 10(a). For reservoir empty condition also the shears are reduced at and near the top as compared to Case 1. The reduction is large and occurs upto a greater distance measured from the top as compared to full reservoir condition. At and near the base, the largest shear occurs in Case 1 as compared to other cases. The maximum and minimum dynamic shears are caused by 'Koyana Elongated' and 'Average Spectra' earthquakes respectively.

The dynamic moments are reduced at and near the top as compared to Case 1 while at and near the bottom they are found to be somewhat increased for reservoir full condition. For reservoir empty condition, the moments are reduced throughout the height of the dam, as compared to Case 1. As compared to reservoir full condition, the dynamic moments are generally reduced except for cases 1 and 2, wherein the base moments in empty condition work out



to be more. The maximum and minimum dynamic moments are caused by 'Koyna Elongated' and 'Average Spectra' earthquakes respectively for both conditions.

For reservoir full condition, the compressive principal stresses at upstream face are more or less same. The tensile principal stresses are mainly due to dynamic effect of earthquake. A considerable reduction in tensile stresses near the crest is seen in other cases as compared to Case 1. At and near the base slight increase in stresses is also observed in other cases as compared to Case 1 when the dam is subjected to any of the earthquakes except 'El Centro'.

For empty reservoir condition, the tensile principal stresses at the downstream face are mainly due to earthquake dynamic effects. The maximum compressive principal stresses are developed at the upstream face. Near the crest, the compressive principal stresses are considerably smaller in other cases as compared to Case 1. The same variation also holds good for tensile stresses at the downstream face. The differences in the stresses at upstream and downstream faces at lower sections in all the cases are considerably smaller as compared to the differences near the crest.

#### 4.2 CONCLUSIONS

- (1) The static vertical and principal stresses at both the faces remain more or less unaltered due to reduction in the crest weight.

- (2) The reduction of mass at the crest also affects the moment of inertia and cross sectional area at the sections. Due to this, the time periods in all other cases are found to be decreased as compared to Case 1 as shown in Table 1.
- (3) For reservoir full condition, the mode participation factors for other cases do not show significant difference in first mode as compared to Case 1. But for second and third mode, the value of the factors is found to be increased considerably as compared to Case 1. This becomes more significant in third mode. For reservoir empty condition, generally the mode participation factors are found to be increased as compared to reservoir full condition in all the cases and modes.
- (4) Due to the reduction of crest weight, the modal deflections are found to be increased for both the conditions as compared to Case 1.
- (5) For reservoir full condition, the horizontal dynamic deflections at the top for other cases are found to be increased as compared to Case 1, while for empty reservoir condition the deflections are found to be decreased as compared to Case 1.
- (6) The tendency of the reservoir is to increase the horizontal dynamic deflection at the top except in Case 1 and Case 2 when analysed for the 'Koyna' earthquake.

- (7) The dynamic shear and moments are reduced near the top with the reduced weight of crest system but are found to be increased at and near the base as compared to Case 1 due to mode shape and participation factor effects. The shears and moments are found to be decreased at the top and near the base as compared to Case 1 for reservoir empty condition. The effect of the reservoir is to increase dynamic shears in all cases while the moments are found to be increased except in case 1 and case 2.
- (8) The principal stresses are found to be reduced in other cases as compared to Case 1 at top. The maximum reductions of stresses are observed in Case 3 and Case 7 for both the conditions and for all earthquakes. A little increase in stresses is observed in case of 'Koyna' earthquake for full reservoir condition at the base as compared to Case 1. The difference in principal stresses at and near the base is not significant for other earthquakes.
- (9) The more critical tensile stresses occur in the upper parts of the dams. The practice of decreasing the concrete strength at higher elevations in dams which is apparently common in our country does not appear to be sound one; on the contrary, relatively higher concrete strength is required in the upper parts of dams from seismic point of view.

#### 4.3 SCOPE FOR FURTHER INVESTIGATION

The method adopted for dynamic analysis is the shear beam approach which takes into account only the transverse vibrations and the principal stresses have been calculated only at the upstream and downstream faces. For more accurate method, a finite element technique in which the dam section is discretised by introducing finite elements may be used. It considers coupled vibrations in transverse and vertical directions. The principal stresses due to static and dynamic loads may be calculated across the width at number of sections. For still better accuracy, the time wise superposition of modal values may be used for evaluating dynamic response of the structure.

5. REFERENCES

- (1) Arya, A.S. and Agarwal, R.K., "Optimum Design of Concrete Gravity Dam Sections Considering Earthquake Forces," Earthquake Engineering Studies, S.R.T.E.E., November 1970 (Unpublished).
- (2) Arya, A.S., Krishna, J. and Thakkar, S.K., "Dynamic Analysis and Model Studies of Ganga Bridge at Allahabad for Earthquake Motions", Earthquake Engineering Studies, S.R.T.E.E., October 1969 (Unpublished).
- (3) Arya, A.S. and Thakkar, S.K., "Response of the Substructure of A Major Bridge to Earthquake Motions", Journal of the Indian Roads Congress, Volume XXXIII-2, September, 1970, pp. 377-392.
- (4) Chandrasekaran, A.R. and Mathur, B.C., "Pseudo Earthquakes Derived from Recorded Accelerograms", Bulletin of the Indian Society of Earthquake Technology, Vol. VII, No. 2, June 1970, pp. 97-101.
- (5) Chopra, A.K. and Chakrabarti, P., "The Koyna Earthquake of December 11, 1967 and The Performance of Koyna Dam", Report No. EERC 71-1, Earthquake Engineering Research Centre, University of Colifornia, pp. 12-45.
- (6) Chopra, A.K., "Earthquake Response of Concrete Gravity Dams", Journal of the Engineering Mechanics Division, Proc. ASCE, Vol. 96, No. EM4, August 1970, pp. 443-453.

- (7) Chopra, A.K., "Hydrodynamic Pressure on Dams during Earthquake", Journal of the Engineering Mechanics Division, Proc. ASCE, Vol. 93, No. EM6, December 1967, pp.205-221.
- (8) Chopra, A.K., "The Importance of the Vertical Component of Earthquake Motions", Bulletin of the Seismological Society of America, Vol.56, No.5, October 1966, pp.1163-1175.
- (9) Chopra, A.K., Wilson E.L. and Farhoomand, I., "Earthquake Analysis of Reservoir Dam Systems", Proc. Fourth World Conference on Earthquake Engineering, Vol. II, Santiago Chile, 1969, pp.B-4-1 - B-4-8.
- (10) Creager, W.P., Hinds, J. and Justin, J.D., "Engineering for Dams", Vol. II, Willey Eastern Private Limited, New Delhi, 1968, pp.247-312 and 401-413.
- (11) Davis, C.V., "Handbook of Applied Hydraulics", McGraw Hill Publication, 1952, pp.23-33.
- (12) Dixit, M.K., "Stress Analysis of Concrete Gravity Dams", M.E. Thesis, University of Roorkee, Roorkee, October 1971.
- (13) Holmes, W.H., "Determination of Principal Stresses in Buttress and Gravity Dams", Proc. ASCE, Vol. 98, 1933, pp.971-1038.
- (14) Housner, G.W. and Keightley, W.O., "Vibration of Linearly Tapered Cantilever Beams", Journal of the Engineering Mechanics Division, Proc. ASCE, Vol.88, EM2, April 1962, pp. 95-123.
- (15) Krishna, J., Chandrasekaran, A.R. and Saini, S.S., "Static and Dynamic Stress Analysis of Koyna Dam", Report not released for publication, S.R.T.E.E., University of Roorkee, Roorkee, March 1962.

- (16) Krishna, J., Chandrasekaran, A.R. and Saini, S.S., "Stress Analysis of Overflow Section of Koyna Dam", Earthquake Engineering Studies, S.R.T.E.E., April 1969, (Unpublished).
- (17) Krishna, J., Chandrasekaran, A.R. and Saini, S.S., "Earthquake Stress Analysis of Koyna Dam Monoliths", Proc. Fourth Symposium on Earthquake Engineering, Roorkee, India, 1970, pp. 99-106.
- (18) Saini, S.S., "Vibration Analysis of Dams", Ph.D. Thesis, University of Roorkee, Roorkee, September 1968.
- (19) Zangaar, C.N., "Hydrodynamic Pressure on Dams Due to Horizontal Earthquake Effects", Proc. of the Society for Experimental Stress Analysis, Vol.X, No.2, 1953, pp.93-101.
- (20) "Design and Construction of Dams", Joint ASCE-USCOLD Committee on Current United States Practice in the Design and Construction of Arch Dams, Embankment Dams, Concrete Gravity Dams, 1967, pp.87-104.
- (21) "Design of Small Dams", Chapter-7, United States Department of the Interior Bureau of Reclamation, 1968, pp.231-245.
- (22) IS:1893-1966, Indian Standard Criteria for Earthquake Resistant Design of Structures, Indian Standard Institution, New Delhi, India.
- (23) IS:1893-1970, Indian Standard Criteria for Earthquake Resistant Design of Structures, Indian Standards Institution, New Delhi.
- (24) "Treatise on Dams", Design Standard No.2, chapter-9, Part II, Gravity Dams, United States Department of the Interior Bureau of Reclamation, Denver, Colorado, pp.9-55.

APPENDIX - A



TIME PERIOD (T.P.) AND MODE PARTICIPATION FACTOR (P.F.) FOR  
FIRST THREE MODES

RESERVOIR FULL CONDITION

CASE	I MODE		II MODE		III MODE		Elongation in T.P. % due to Reservoir effect		
	T.P.	P.F.	T.P.	P.F.	T.P.	P.F.	I MODE	II MODE	III MODE
1	0.474	2.54	0.219	-2.88	0.130	2.22	28.10	20.30	19.30
2	0.463	2.57	0.206	-3.30	0.120	3.62	28.60	24.00	20.00
3	0.440	2.68	0.194	-3.99	0.124	4.14	33.33	34.70	32.50
4	0.440	2.60	0.193	-3.55	0.121	3.49	33.33	33.33	30.10
5	0.450	2.58	0.198	-3.36	0.121	3.36	32.40	28.50	23.40
6	0.452	2.53	0.197	-3.11	0.118	2.94	31.80	28.00	24.20
7	0.446	2.42	0.191	-2.94	0.113	3.11	33.10	30.80	30.30

RESERVOIR EMPTY CONDITION

1	0.370	2.66	0.182	-2.93	0.109	2.11			
2	0.360	2.74	0.166	-3.81	0.100	4.95			
3	0.330	2.73	0.144	-4.37	0.094	5.10			
4	0.330	2.68	0.145	-3.97	0.093	4.37			
5	0.340	2.71	0.154	-3.79	0.098	3.91			
6	0.343	2.65	0.154	-3.47	0.095	3.47			
7	0.335	2.47	0.146	-2.97	0.087	3.04			

Table - 2

T2

STATIC PRINCIPAL STRESSES IN Kg/cm<sup>2</sup>

## RESERVOIR FULL CONDITION

Section No.	Case 1		Case 3		Case 7	
	u/s	d/s	u/s	d/s	u/s	d/s
1	0.407	10.310	-1.060	2.481	0.070	3.123
3	1.839	8.363	-1.074	9.213	-0.260	8.831
5	1.109	13.636	-1.022	14.702	-0.4657	14.377
7	0.820	19.226	-1.077	20.171	-0.657	19.908
9	0.353	24.836	-1.180	25.635	-0.844	25.434
11	-0.1849	30.433	-1.310	31.145	-1.029	30.958

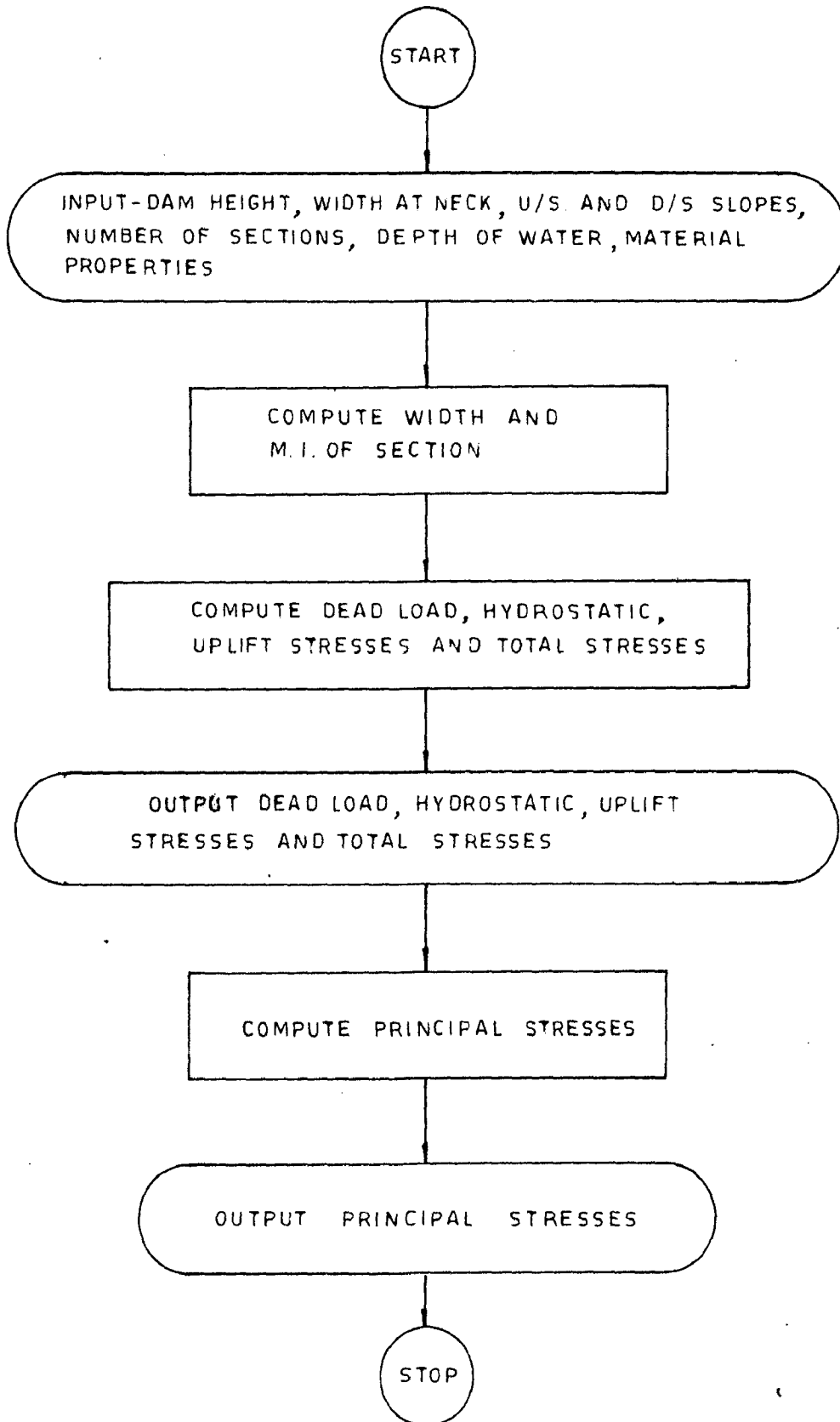
## RESERVOIR EMPTY CONDITION

1	3.572	7.265	2.1047	-0.564	3.235	0.078
3	10.216	0.314	7.303	1.1643	8.117	0.782
5	14.698	0.583	12.567	1.649	13.123	1.325
7	19.373	1.170	17.724	2.115	18.144	1.852
9	24.171	1.777	22.832	2.593	23.169	2.375
11	29.040	2.3709	27.915	3.082	28.196	2.896

+ compressive

- tensile

APPENDIX - B



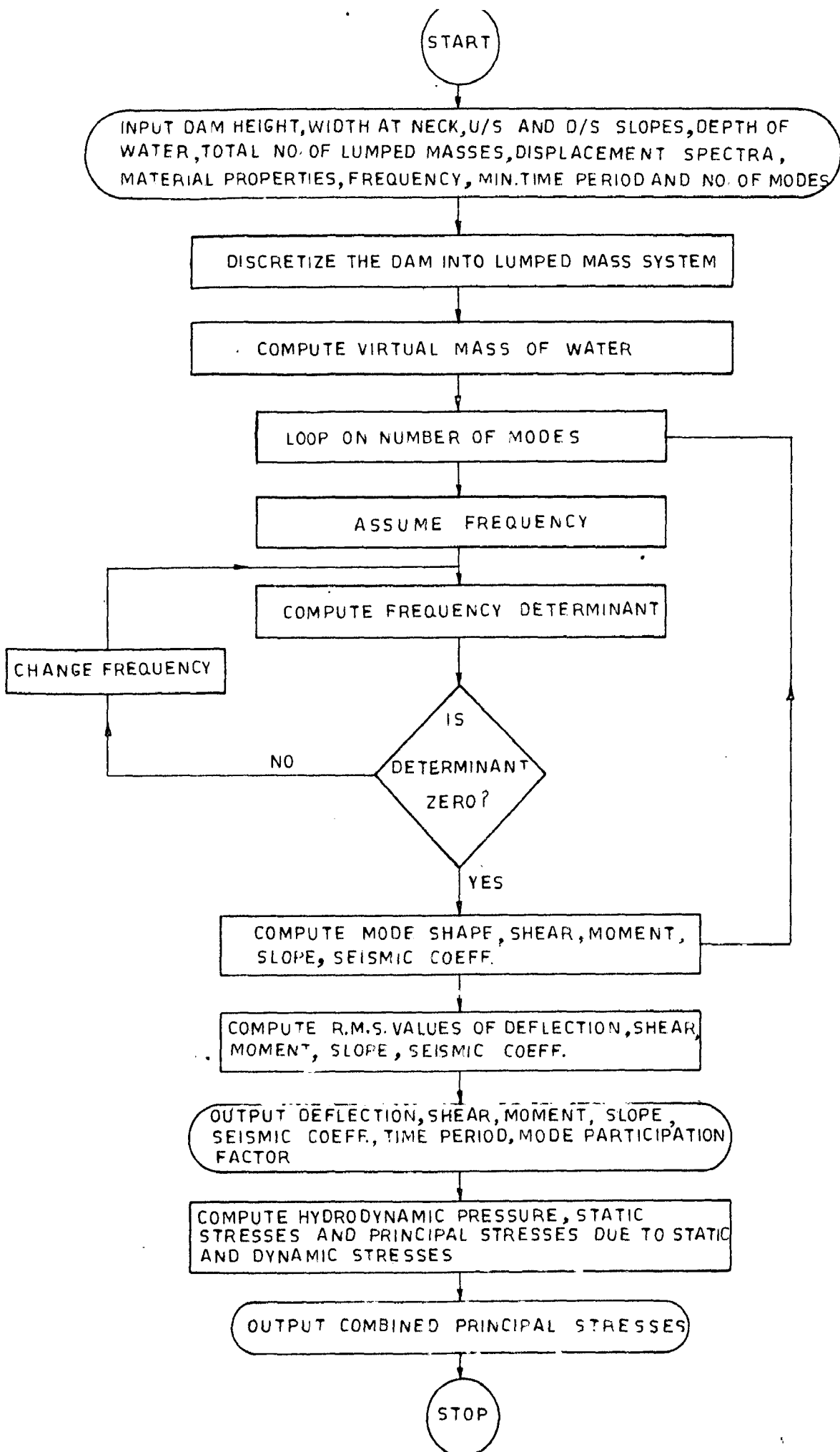
FLOW CHART FOR STATIC STRESSES PROGRAM

```

C C CALCULATION OF STRESSES
  DIMENSION BASE(15),GI(15),TUS(15),TDS(15),TDUS(15),TDDS(15)
  DIMENSION THUUS(15),THDUS(15),UPLUS(15),UPLDS(15)
  DIMENSION P1U(15),P2U(15),P1D(15),P2D(15)
55 READ11,NS,IPN
  READ12,B,H,ALPHA,BETA,ROH,ROHW,ZN,YZ
  READ12,WNEK,PA,DSL
  11 FORMAT(6I3)
  12 FORMAT(8F10.0)
  PUNCH111,IPN
111 FORMAT(12HPROBLEM NO.=I3)
  AN=NS
  SH=H/AN
  NN=NS+1
  X=0.0
  PUNCH112
112 FORMAT(35HVERTICAL STRESSES IN TONNES PER MSQ)
  DO 114 I=1,NN
  C=(ALPHA+BETA)*X
  BASE(I)=B+C
  GI(I)=6./(3BASE(I)**2)
  WT=0.5*(B+BASE(I))*X*ROH+WNEK
  C1=ALPHA*X
  C2=BETA*X
  B1=0.5*C2*X*C2*0.666667
  B2=B*X*(C2+0.5*B)
  B3=0.5*C1*X*(C2+B+0.33333*C1)
  B4=WNEK*(PA+C2)
  RES=((B1+B2+B3)*ROH+B4)/WT
  E=RES-0.5*BASE(I)
  FUS=-WT*E*GI(I)
  DS=WT/BASE(I)
  TDUS(I)=DS+FUS
  TDDS(I)=DS-FUS
  X1=ZN+X-DSL
  IF(X1)115,115,116
115 THUUS(I)=0.0
  THDUS(I)=0.0
  UPLUS(I)=0.0
  UPLDS(I)=0.0
  GO TO 117
116 D1=X1*BETA
  WTW=0.5*X1*D1*ROHW
  DS=WTW/BASE(I)
  DMONT=-WTW*(0.5*BASE(I)-0.33333*D1)+ROHW*X1*X1*X1*0.166667
  FUS=-DMONT*GI(I)
  THUUS(I)=DS+FUS
  THDUS(I)=DS-FUS
  UPLUS(I)=-ROHW*X1
  UPLDS(I)=0.0
117 TUS(I)=TDUS(I)+THUUS(I)+UPLUS(I)
  TDS(I)=TDDS(I)+THDUS(I)+UPLDS(I)
  X=X+SH
  PUNCH118,I,TDUS(I),TDDS(I),THUUS(I),THDUS(I),UPLUS(I),UPLDS(I),
  1TUS(I),TDS(I)

```

```
114 CONTINUE
118 FORMAT(1X,I2,8F9.4)
    THETA=ATAN(BETA)
    SECU=1./COS(THETA)
    UU=SECU*SECU
    BR=BETA*BETA
    PHI=ATAN(ALPHA)
    SECD=1./COS(PHI)
    DD=SECD*SECD
    BRD=ALPHA*ALPHA
    DO 99 I=1,NN
    P1U(I)=-0.1*UPLUS(I)
    P2U(I)=0.1*TUS(I)-P1U(I)*BR
    P1D(I)=0.0
    P2D(I)=0.1*TDS(I)*DD-P1D(I)*BRD
99 CONTINUE
PUNCH100
100 FORMAT(10X,29HPRINCIPAL STRESSES IN KG/CM2)
999 PUNCH126,(I,P1U(I),P2U(I),P1D(I),P2D(I), I=1,NN)
126 FORMAT(5X,I5,4F10.4)
    GO TO 55
END
```



FLOW CHART FOR DYNAMIC ANALYSIS AND COMBINED PRINCIPAL STRESSES PROGRAM

```

C C MAIN PROGRAM DYNAMIC ANALYSIS G I PRAJAPATI
  DIMENSION VR(35),BMR(35),YR(35),TOS(35),ALFA(35),AREA(35)
  DIMENSION AMASS(35),SI(35)
  DIMENSION HI(35),TRE(35),NAMP(6),SDD(100),Y(35),T(35),BM(35)
  DIMENSION V(35),C(2,2),Z(2)
  COMMON B,H,ALPHA,BETA,ROH,ANMAS,N,NTOP,G,AREA,SI,HI
  COMMON AMASS,RO,NMS,ROHW,ZN,YZ,CM,NT,BMR,ALFA
C INPUT
151 READ1,N,NPONT,NDAMP,NTOP,IPN,NM
  M=NPONT*NDAMP
C SPECTRAL DATA
  READ2,(TRE(I), I=1,NPONT)
  READ2,(SDD(I), I=1,M)
C DAMPING VALUES
  READ1,(NAMP(I), I=1,NM)
C DAM PROFILE (TOP ABOVE NECK)
  READ3,(AREA(I),AMASS(I),SI(I),HI(I),I=1,NTOP)
  READ3,ZN,YZ,CM,ROHW
  READ2,B,H,ALPHA,BETA,ROH,ANMAS
C DAM PROPERTIES
  READ2,AE,POISO,SIGMA,TMIN
C TRIAL FREQ.,ACCUFACY,INCREMENT IN FREQ
  READ2,PR,ACC,DP
  1 FORMAT(6I3)
  2 FORMAT(8F10.0)
  3 FORMAT(4F10.0)
  PRINT 175, IPN
175 FORMAT(3X,12HPROBLEM NO. I3)
  G=1./9.80665
  PI=3.14159265
  RO=ROH*G
  NMS=N+NTOP
  NT=NMS+1
  DO 59 I=1,NT
  VR(I)=0.
  BMR(I)=0.
59 YR(I)=0.
  AEN=1./AE
  AG=AE*0.5/(1.+POISO)
  NM1=0
  CALL DEDAM
  N1=NTOP+1
  AMASS(N1)=AMASS(N1)+ANMAS
  CALL HYDYN
  5 LX=2
  S1=0.
  S2=0.
  RT1=0.
  RT2=0.
  7 Z(2)=0.
17 AP=PR*PR
  P1=PR
  Z(1)=1.
  DO 22 J=1,LX
  VN=0.
  BMO=0.

```



```

V(1)=0.
BM(1)=0.
YN=Z(1)
T0=Z(2)
Y(1)=Z(1)
T(1)=Z(2)
DO 21 I=1,NMS
  I1=I+1
  AN=AREA(I)
  AM=AMASS(I)
  HN=HI(I)
  AIN=SI(I)
  EIN=AEN/AIN
  VN=VN+AM*AP*YN
  AMN=BMO+VN*HN-RO*AIN*AP*TO*HN
  TN=TO+0.5*(BMO+AMN)*EIN*HN
  YN=YN+TO*HN+(BMO+AMN*0.5)*HN*HN*EIN/3.
  YN=YN-SIGMA*VN*HN/(AG*AN)
  BMO=AMN
  TO=TN
  Y(I1)=YN
  T(I1)=TN
  BM(I1)=AMN
  V(I1)=VN
21 CONTINUE
  C(1,J)=YN
  C(2,J)=TN
  Z(1)=0.
22 Z(2)=1.
  GO TO(70,80),LX
70 DO 30 I=1,NMS
  S1=S1+Y(I)*AMASS(I)
30 S2=S2+Y(I)*Y(I)*AMASS(I)
  GO TO 90
80 DT=C(1,1)*C(2,2)-C(1,2)*C(2,1)
C INTERPOLATION
  IF(DT)60,66,61
60 RT1=DT
  Q1=PR
  IF(RT2)64,64,65
61 RT2 =DT
  Q2=PR
  IF(RT1)65,64,64
64 PR=PR+DP
  GO TO 7
65 PR=(RT1*Q2-RT2*Q1)/(RT1-RT2)
  P1=(PR-P1)/PR
  IF(ABS(P1)-ACC)66,66,7
66 F=0.5*PR/P1
  NM1=NM1+1
  TP=1./F
  PRINT6,PR,F,TP,ACC
6 FORMAT(1X,2HP=E12.5,3X,2HF=E12.5,3X,2HT=E12.5,3X,4HACC=F10.6)
  IF(TP-TMIN)89,67,67
80 DO 97 I=1,NT
  VR(I)=SQRT(VR(I))

```

```

BMR(I)=SQRT(PMR(I))
97 YR(I)=SORT(YR(I))
DO 93 I=1,NMS
  I1=I+1
  TOS(I)=VR(I1)-VR(I)
93 TOS(I)=TOS(I)/AMASS(I)
  TOS(NT)=0.
  S=0.
  ALFA(I)=0.
  DO 98 I=1,NMS
    S=S+AMASS(I)/G
    I1=I+1
98 ALFA(I1)=VR(I1)/S
  M3=NM1-1
  PRINT44,M3
44 FORMAT(2X,10HR.M.S. OF=I3,2X,5HMODES)
  PRINT42
42 FORMAT(2X,5HJOINT,2X,5HSHEAR,9X,6HMOMENT,8X,5HACCLN,8X,5HDEFLN,
  1 9X,4HALFA)
  PRINT43,(I,VR(I),BMR(I),TOS(I),YR(I),ALFA(I), I=1,NT)
43 FOPMAT(2X,I2,5E14.5)
  CALL STRESS
  GO TO 151
67 LX=1
  Z(2)=-C(1,1)/C(1,2)
  GO TO 17
90 SUM=S1/S2
  PRINT9,NM1,SUM
  9 FORMAT(1X,5HMODE=I2,3X,5HP.F.=E12.5)
  PRINT 88
88 FORMAT(6X,5HJOINT,6X,5HSHEAR,11X,6HMOMENT,10X,5HSLOPE,10X,5HDEFLN)
  8 FORMAT(5X,I3,4(2X,E14.6))
  DO 79 I=1,NT
    PRINT8,I,V(I),BM(I),T(I),Y(I)
79 CONTINUE
C CALCULATE SD VALUE
  SD1=0.
  T1=0.
  TY=TP
  MPAD=NAMP(NM1)
  K1=NPONT*MPAD
  DO 91 J=1,NPONT
    K=K1+J
    T2=TRE(J)
    IF(TY-T2)92,99,94
94 T1=T2
    SD1=SDD(K)
91 CONTINUE
92 SD2=SDD(K)
  X1=(SD2-SD1)/(T2-T1)
  X1=X1*(TY-T1)
  SD=SD1+X1
  GO TO 96
99 SD=SDD(K)
96 CR=SUM*SD
  CR=CR*CR

```

```

DO 41 I=1,NT
VR(I)=VR(I)+V(I)*V(I)*CR
BMR(I)=BMR(I)+BM(I)*BM(I)*CR
41 YR(I)=YR(I)+Y(I)*Y(I)*CR
PR=PR+DP
GO TO 5
END
SUBROUTINE DEDAM
DIMENSION ARFA(35),SI(35),HI(35),AMASS(35),BMR(35),ALFA(35)
COMMON B,H,ALPHA,BETA,ROH,ANMAS,N,NTOP,G,AREA,SI,HI
COMMON AMASS,RO,NMS,ROHW,ZN,YZ,CM,NT,BMR,ALFA
AN=N
SH=H/AN
X=0.5*SH
N1=NTOP+1
NMS=NTOP+N
C=ALPHA+BETA
DO 100 I=N1,NMS
AREA(I)=R+X*C
SI(I)=0.083333*AREA(I)**3
AMASS(I)=0.5*X*(AREA(I)+R)*RO
HI(I)=SH
B=AREA(I)
X=SH
100 CONTINUE
RETURN
END
SUBROUTINE HYDYN
DIMENSION AREA(35),SI(35),HI(35),AMASS(35),VM(35),BMR(35),ALFA(35)
COMMON B,H,ALPHA,BETA,ROH,ANMAS,N,NTOP,G,AREA,SI,HI
COMMON AMASS,RO,NMS,ROHW,ZN,YZ,CM,NT,BMR,ALFA
RHT=H+ZN-YZ
CONST=0.5*CM*ROHW*G*RHT
DO 100 I=1,NMS
IF(I=1)5,5,6
5 Y1=0.
HT=0.
GO TO 7
6 HT=HT+HI(I=1)
Y1=HT-0.5*HI(I=1)-YZ
7 Y2=HT+0.5*HI(I)=YZ
IF(Y2)50,50,8
50 VM(I)=0.
GO TO 99
8 IF(Y1)9,10,10
9 Y1=0.
10 C=Y1*Y1/RHT
D=0.333333*C*Y1/RHT
CC=Y1/(2.*RHT)
X=SQRT(CC)
XX=SQRT(1.-CC)
Z=X/XX
ZZ=ATAN(Z)
A=C-D+RHT*(ZZ-SIN(4.*ZZ))*0.25)
C=Y2*Y2/RHT
D=0.333333*C*Y2/RHT
CC=Y2/(2.*RHT)

```

```

X=SQRT(CC)
XX=SQRT(1.-CC)
Z=X/XX
ZZ=ATAN(Z)
B=C-D+RHT*(ZZ-SIN(4.*ZZ))*0.25)
VM(I)=(B-A)*CONST
99 AMASS(I)=VM(I)+AMASS(I)
100 CONTINUE
RETURN
END
SUBROUTINE STRESS
DIMENSION HI(35), AMASS(35), BMR(35), ALFA(35)
DIMENSION TUS(11), TDS(11), TDUS(11), TDDS(11), THUUS(11)
DIMENSION THDUS(11), UPLUS(11), UPLDS(11), BASE(35), GI(35)
DIMENSION P1U(11), P2U(11), P1D(11), P2D(11)
COMMON B,H,ALPHA,BETA,ROH,ANMAS,N,NTOP,G,BASE,GI,HI
COMMON AMASS,RO,NMS,ROHW,ZN,YZ,CM,NT,BMR,ALFA
EQUIVALENCE(AMASS(1),P1U(1)),(AMASS(12),P2U(1))
EQUIVALENCE(AMASS(23),P1D(1)),(BASE(12),P2D(1))
READ111,R,WNEK,PA,DSL,NS
111 FORMAT(4F10.0,I2)
AN=NS
SH=H/AN
NN=NS+1
X=0.0
PRINT112
DO 114 I=1,NN
C=(ALPHA+BETA)*X
BASE(I)=B+C
GI(I)=6.0/(BASE(I)**2)
WT=0.5*(B+BASE(I))*X*ROH+WNEK
C1=ALPHA*X
C2=BETA*X
B1=0.5*C2*X*C2*0.666667
B2=B*X*(C2+0.5*R)
B3=0.5*C1*X*(C2+B+0.33333*C1)
B4=WNEK*(PA+C2)
RES=((B1+B2+B3)*ROH+B4)/WT
E=RES-0.5*BASE(I)
FUS=-WT*E*GI(I)
DS=WT/BASE(I)
TDUS(I)=DS+FUS
TDDS(I)=DS-FUS
X1=ZN+X-DSL
IF(X1)115,115,116
115 THUUS(I)=0.0
THDUS(I)=0.0
UPLUS(I)=0.0
UPLDS(I)=0.0
GO TO 117
116 D1=X1*BETA
WTW=0.5*X1*D1*ROHW
DS=WTW/BASE(I)
DMONT=-WTW*(0.5*BASE(I)-0.33333*D1)+ROHW*X1*X1*X1*0.166667
FUS=-DMONT*GI(I)
THUUS(I)=DS+FUS

```

```

      THDUS(I)=DS=FUS
      UPLUS(I)=-ROHW*X1
      UPLDS(I)=0.0
117 TUS(I)=TDUS(I)+THUUS(I)+UPLUS(I)
      TDS(I)=TDDS(I)+THDUS(I)+UPLDS(I)
      X=X+SH
      PRINT118,I,TDUS(I),TDDS(I),THUUS(I),THDUS(I),UPLUS(I),UPLDS(I),
1      ITUS(I),TDS(I)
114 CONTINUE
112 FORMAT(1X,35HVERTICAL STRESSES IN TONNES PER MSC)
118 FORMAT(1X,I2,8F9.4)
      THETA=ATAN(BETA)
      SECU=1./COS(THETA)
      UU=SECU*SECU
      BB=BETA*BETA
      PHI=ATAN(ALPHA)
      SECD=1./COS(PHI)
      DD=SECD*SECD
      BBD=ALPHA*ALPHA
      NJ=NT-N
      IF(DSL=ZN)119,119,120
119 RHT=H+ZN=YZ
      HI(1)=ZN=YZ
      DO 121 I=2,NN
121 HI(I)=HI(I-1)+SH
      CONST=0.5*CM*RHT*ALFA(NT)
      DO 122 I=1,NN
      A=HI(I)/RHT*(2.-HI(I)/RHT)
      AA=SQRT(A)
      PDYN=CONST*(A+AA)
      P1U(I)=0.1*(-UPLUS(I)+PDYN*SECU)
      DYSTR=BMR(NJ)*GI(I)
      P2U(I)=0.1*(TUS(I)-DYSTR)*UU-P1U(I)*BB
      P1D(I)=0.0
      P2D(I)=0.1*(TDS(I)+DYSTR)*DD
      NJ=NJ+3
122 CONTINUE
      PRINT123
123 FORMAT(10X,33HPRINCIPAL STRESSES RESERVOIR FULL)
      GO TO 999
120 DO 124 I=1,NN
      P1U(I)=0.0
      DYSTR=BMR(NJ)*GI(I)
      P2U(I)=0.1*(TUS(I)+DYSTR)*UU
      P1D(I)=0.0
      P2D(I)=0.1*(TDS(I)-DYSTR)*DD
      NJ=NJ+3
124 CONTINUE
      PRINT125
125 FORMAT(10X,34HPRINCIPAL STRESSES RESERVOIR EMPTY)
999 PRINT126,(I,P1U(I),P2U(I),P1D(I),P2D(I), I=1,NN)
126 FORMAT(5X,I5,4F10.4)
      RETURN
      END

```

INPUT AND OUTPUT FOR DYNAMIC ANALYSIS AND COMBINED PRINCIPAL  
STRESSES PROGRAM

\*\*\*\*\*

\*INPUT\*

\*\*\*\*\*

N	NUMBER OF DISCRETISED MASSES BELOW CREST
NPONT	TOTAL NUMBER OF TIME PERIODS
NDAMP	DAMPING PERCENTAGE IN DIFFERENT MODES
NTOP	NUMBER OF DISCRETISED MASSES ABOVE CREST
IPN	PROBLEM NUMBER
NM	NUMBER OF MODES
TRE	TIME PERIODS OF DISPLACEMENT SPECTRA
SDD	SPECTRAL DISPLACEMENT
NAMP	DAMPING VALUES
AREA	CROSS SECTIONAL AREA
AMASS	DISCRETISED MASS
SI	MOMENT OF INERTIA
HI	DISTANCE BETWEEN TWO CONSECUTIVE MASSES
ZN	HEIGHT OF THE CREST
YZ	FREE BOARD
CM	CONSTANT
ROHW	UNIT WEIGHT OF WATER
B	WIDTH AT THE NECK
H	HEIGHT BELOW THE NECK UPTO BASE
ALPHA	DOWNSTREAM SLOPE
BETA	UPSTREAM SLOPE
ROH	UNIT WEIGHT OF CONCRETE
ANMAS	MASS ABOVE THE NECK
AE	MODULUS OF ELASTICITY
POISO	POISSONS RATIO
SIGMA	SHAPE FACTOR
TMIN	MINIMUM TIME PERIOD
FR	ASSUMED FREQUENCY
ACC	ACCURACY
DP	INCREMENT IN FREQUENCY
WNEK	WEIGHT OF CREST
PA	POINT OF APPLICATION OF CREST WEIGHT
DSL	RESERVOIR WATER LEVEL MEASURED FROM TOP OF DAM
NS	NUMBER OF SECTIONS BEGINING FROM CREST

\*\*\*\*\*

\*OUTPUT\*

\*\*\*\*\*

IPN	PROBLEM NO.
P	NATURAL FREQUENCY IN DIFFERENT MODES
T	TIME PERIODS IN DIFFERENT MODES
ACC	ACCURACY
P.F.	MODE PARTICIPATION FACTORS FOR DIFFERENT MODES
I	JOINT NUMBER
V	MODAL SHEAR
BM	MODAL MOMENT
T	MODAL SLOPE
Y	MODAL DEFLECTION
VR	TOTAL DYNAMIC SHEAR
BMR	TOTAL DYNAMIC MOMENT
TOS	SLOPE

YR	DYNAMIC DEFLECTION
ALFA	EQUIVALENT SEISMIC COEFFICIENT
TDUS	STATIC VERTICAL STRESS DUE TO D.L. AT U/S FACE
TDDS	STATIC VERTICAL STRESS DUE TO D.L. AT D/S FACE
THUUS	STATIC VERTICAL STRESS DUE TO HYDROSTATIC PRESSURE AT U/S FACE
THDUS	STATIC VERTICAL STRESS DUE TO HYDROSTATIC PRESSURE AT D/S FACE
UPLUS	VERTICAL STRESS DUE TO UPLIFT PRESSURE AT U/S FACE
UPLDS	VERTICAL STRESS DUE TO UPLIFT PRESSURE AT D/S FACE
TUS	TOTAL VERTICAL STRESS AT U/S FACE
TDS	TOTAL VERTICAL STRESS AT D/S FACE
I	NUMBER OF SECTIONS FOR STRESS CALCULATION
P1U	MAJOR COMBINED PRINCIPAL STRESS AT U/S FACE
P2U	MINOR COMBINED PRINCIPAL STRESS AT U/S FACE
P1D	MAJOR COMBINED PRINCIPAL STRESS AT D/S FACE
P2D	MINOR COMBINED PRINCIPAL STRESS AT D/S FACE

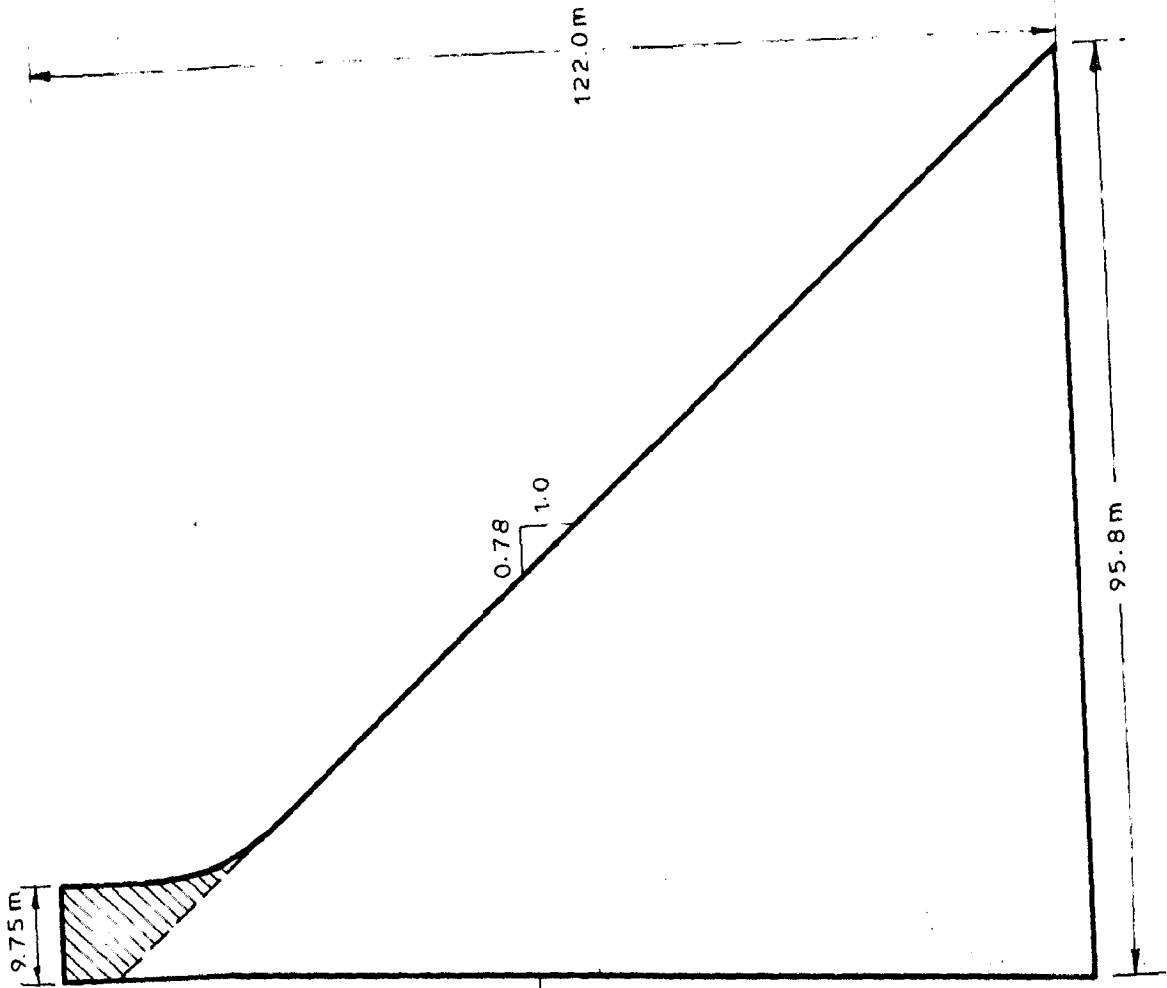


FIG. 2 - PINE FLAT DAM

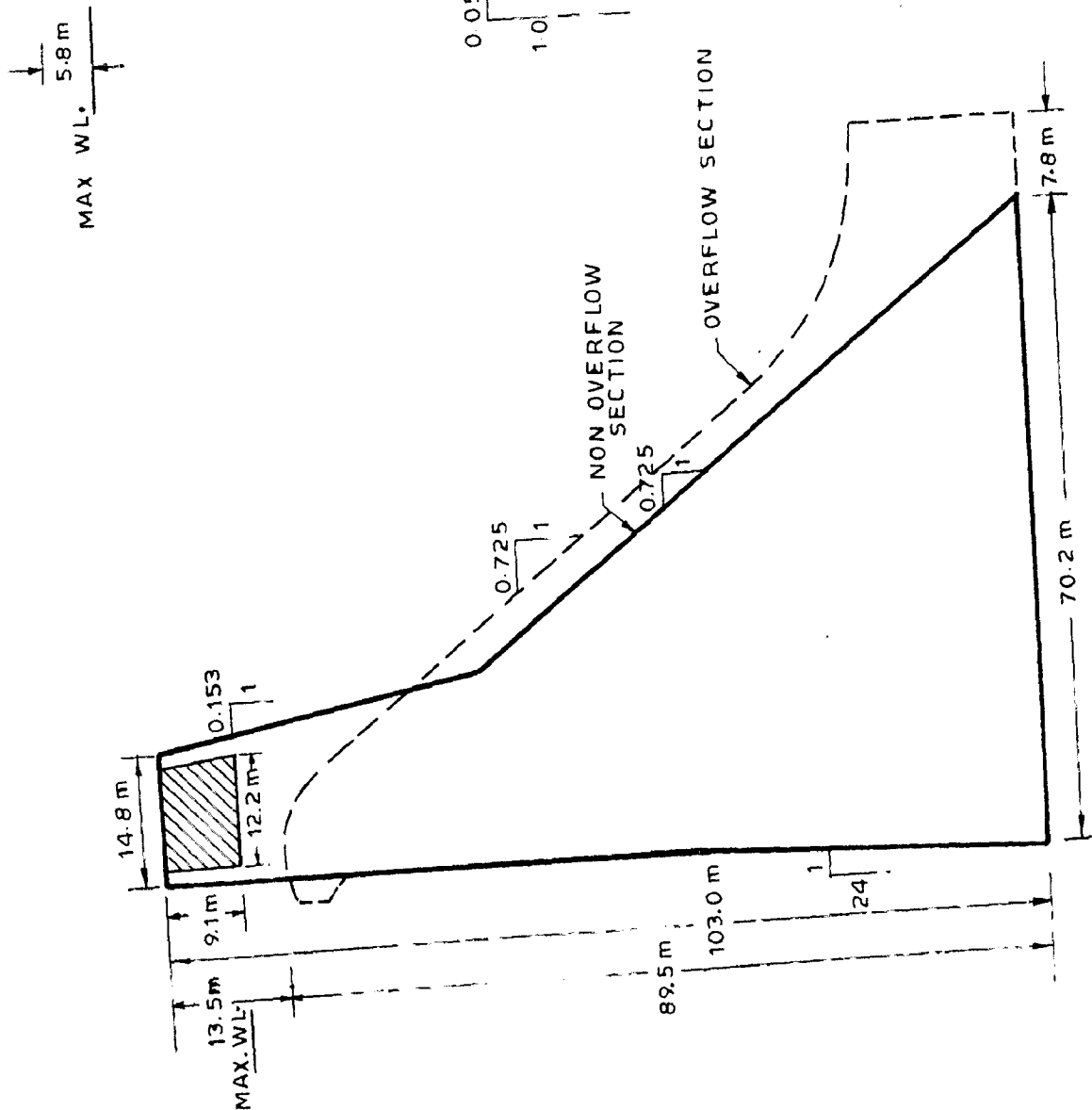
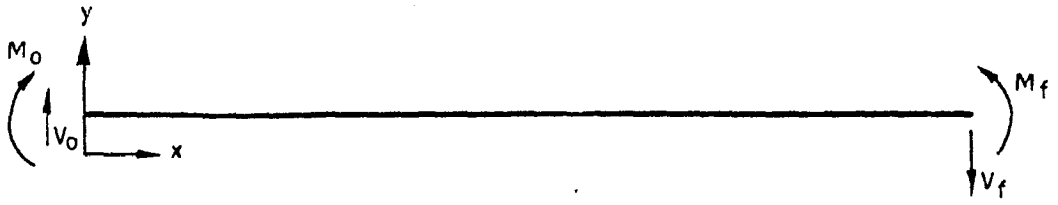
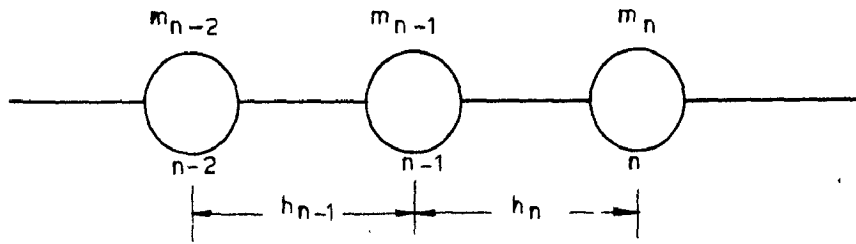


FIG. 1 - OVERFLOW AND NON OVERFLOW SECTIONS OF KOYNA DAM

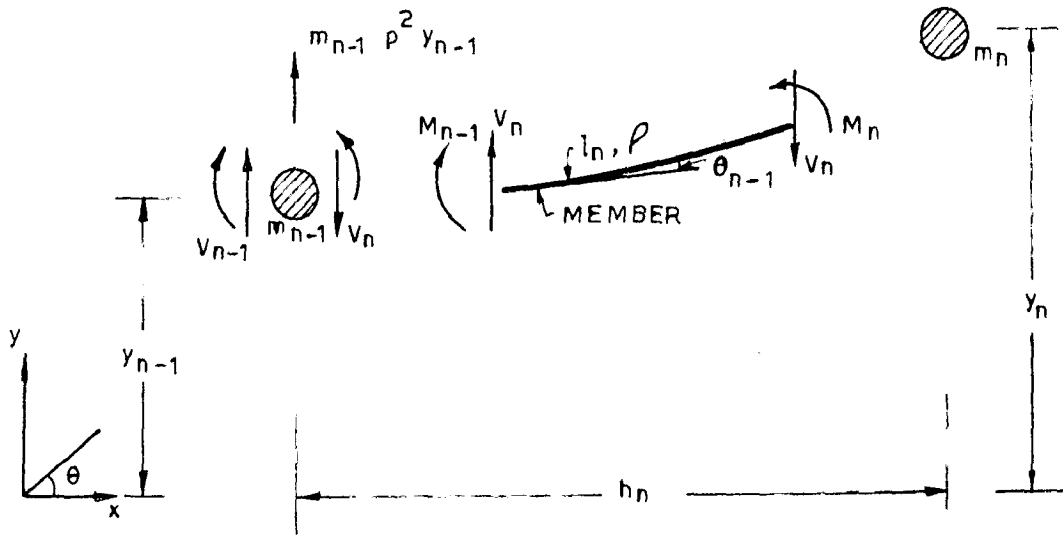




a - TAPERED CANTILEVER BEAM



b - DISCRETISED LUMPED MASS SYSTEM



c - FREE BODY DIAGRAM

FIG. 3

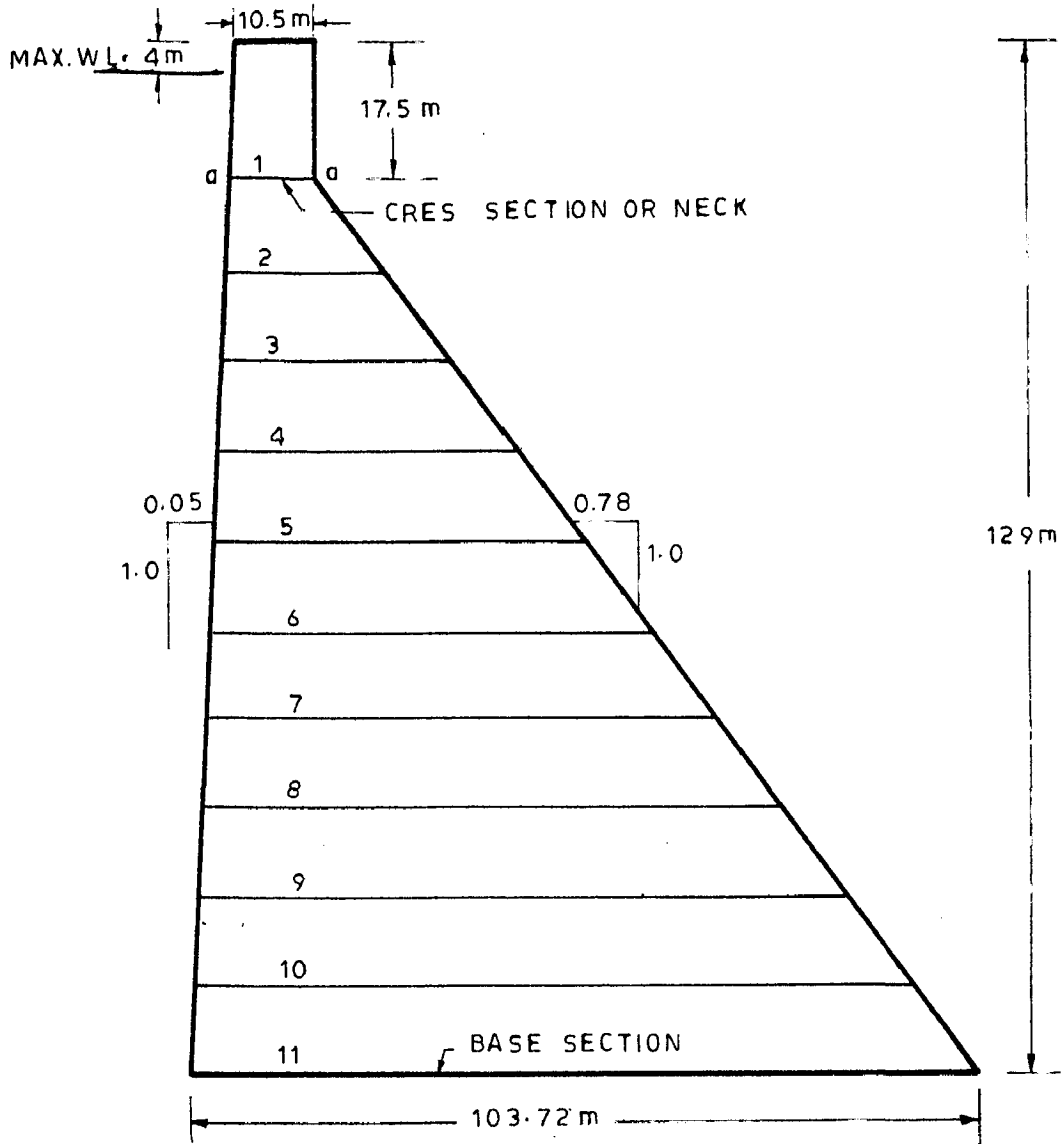


FIG. 4 \_ MODIFIED PINE FLAT DAM

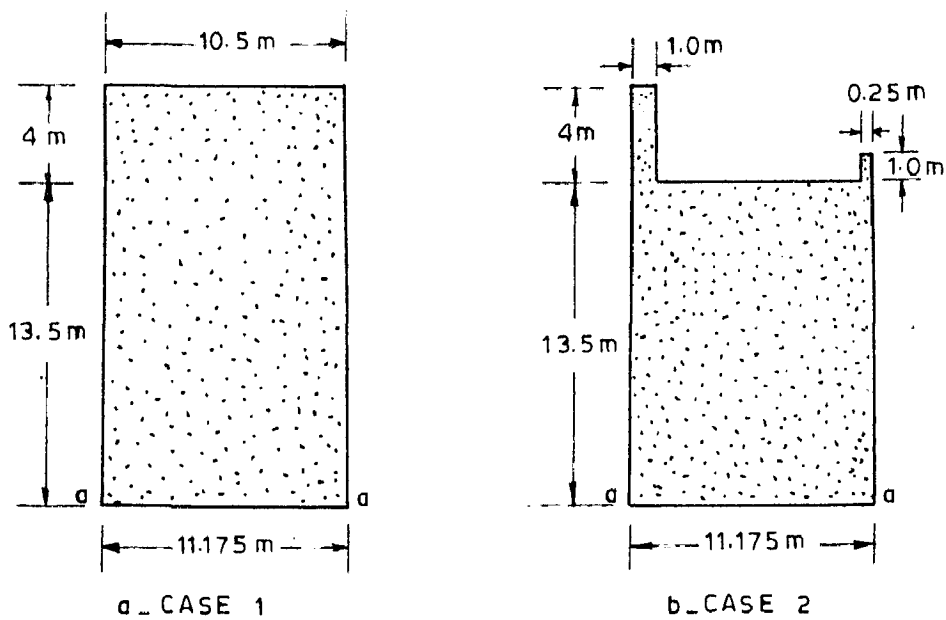
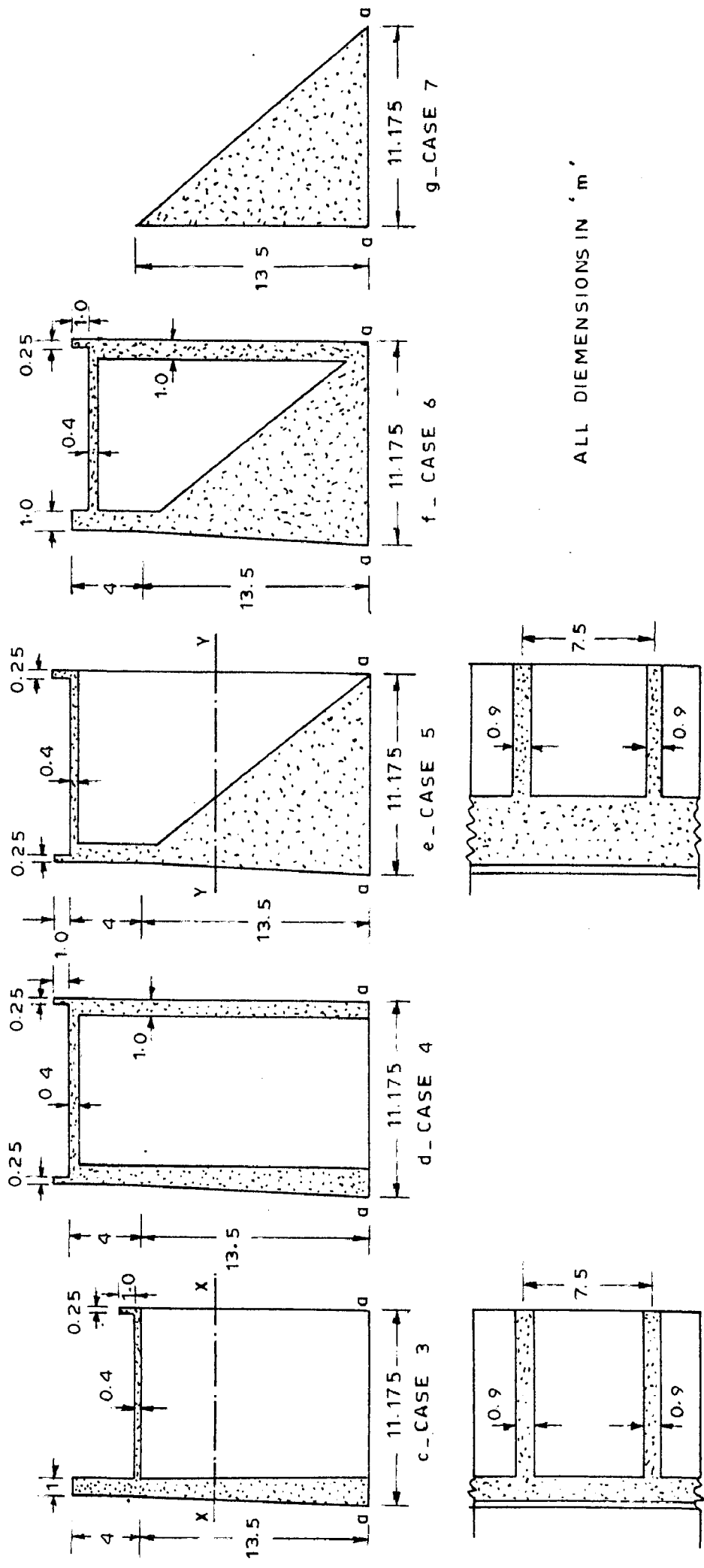


FIG. 5



ALL DIMENSIONS IN 'm'

SECTIONAL PLAN YY

SECTIONAL PLAN XX

FIG. 5 - CASES OF STRUCTURAL SYSTEMS AT TOP OF DAM

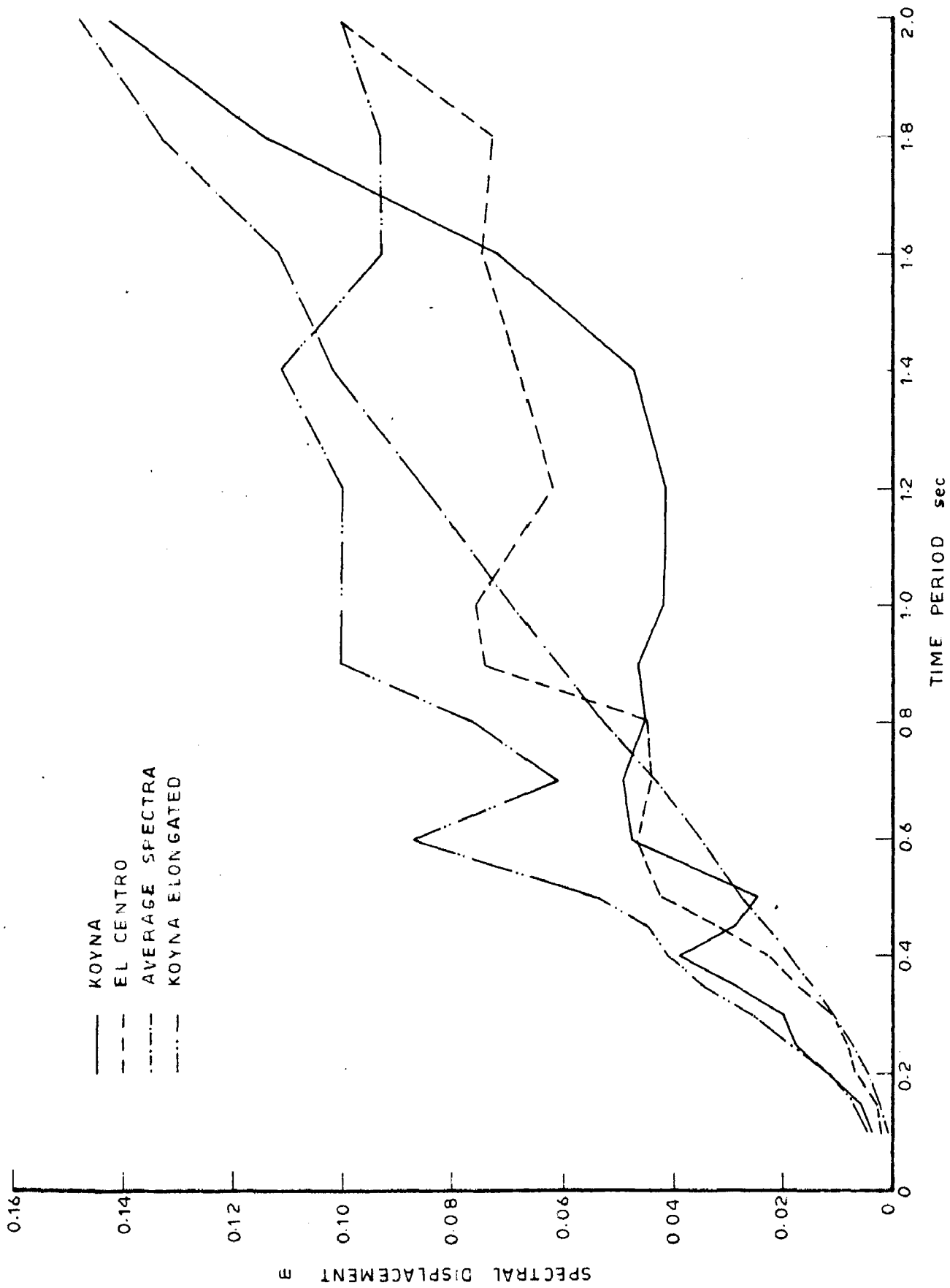


FIG. 6 - DISPLACEMENT RESPONSE SPECTRUM FOR EARTHQUAKES

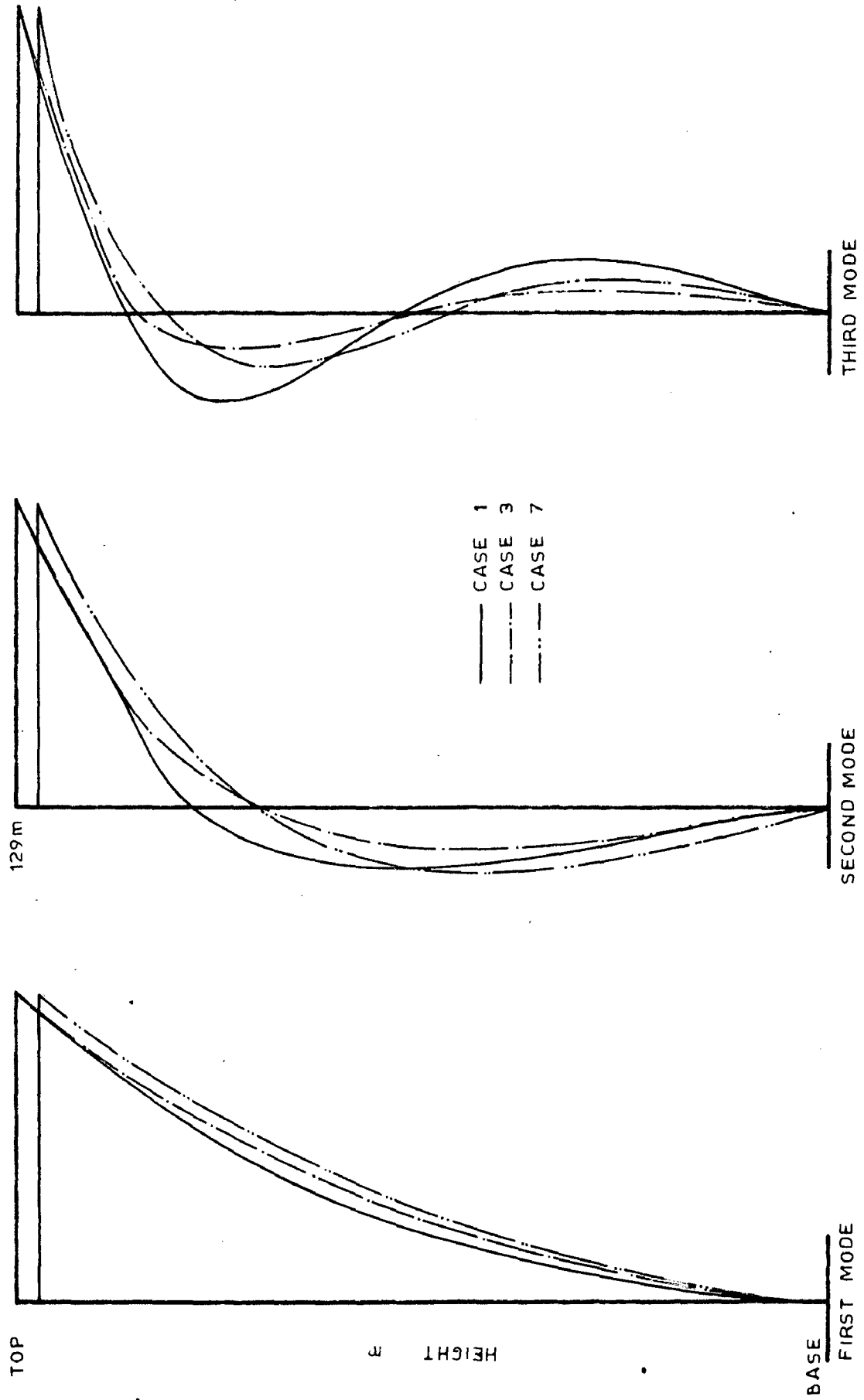


FIG. 7(a) - MODE SHAPES FOR FULL RESERVOIR CONDITION

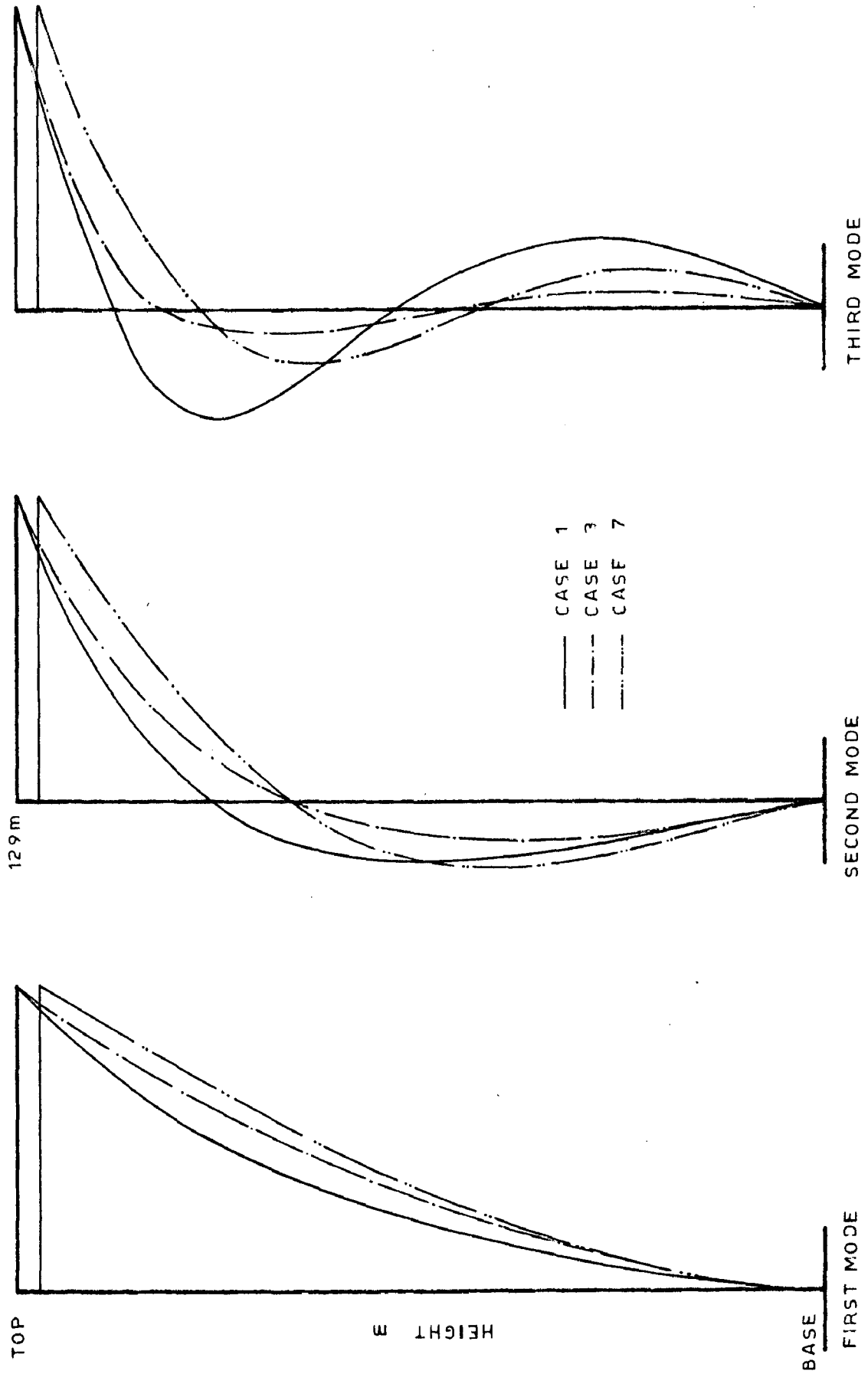


FIG. 7(b) - MODE SHAPES FOR EMPTY RESERVOIR CONDITION

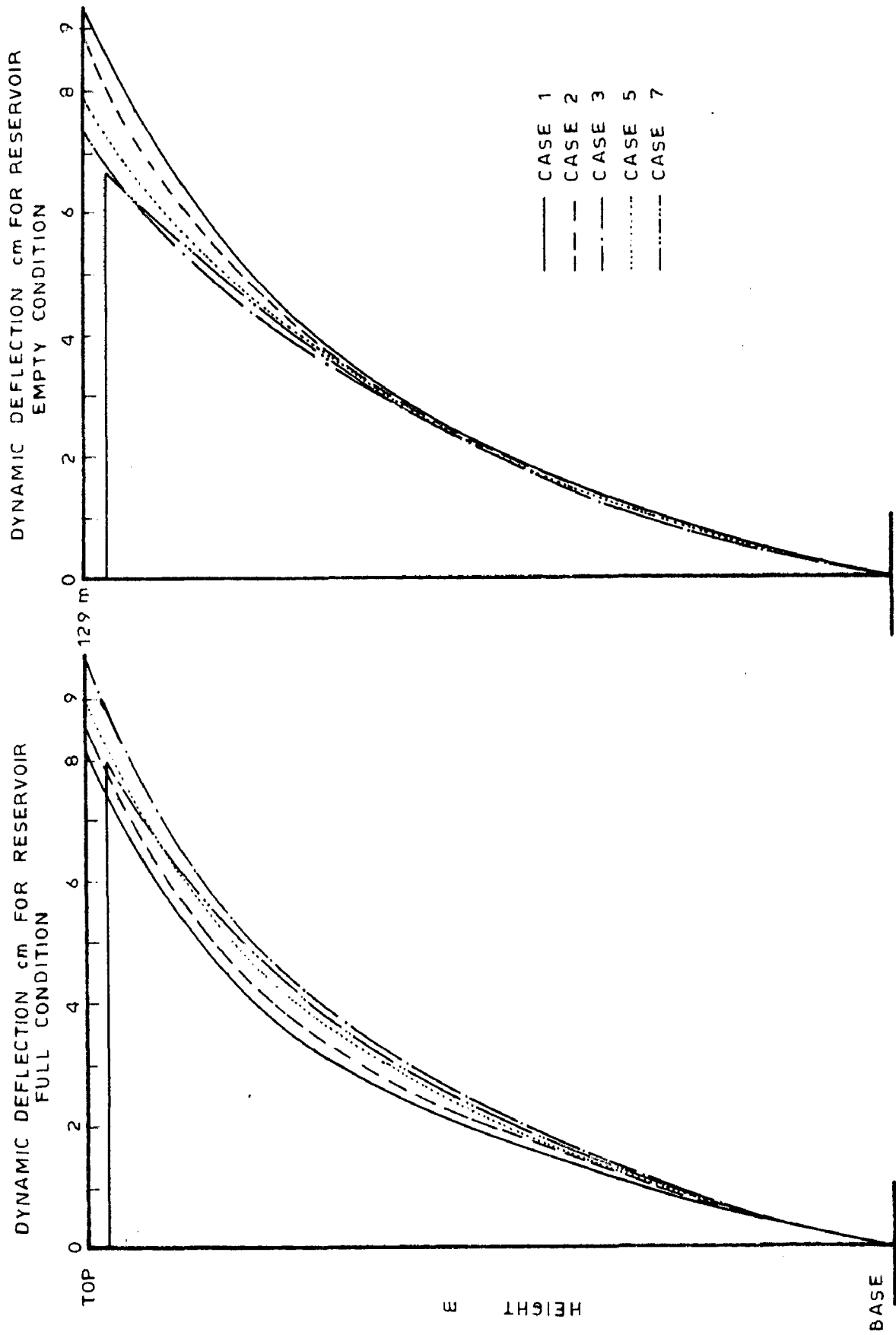


FIG. 8 - DYNAMIC DEFLECTION FOR VARIOUS CASES DUE TO KOYNA EARTHQUAKE

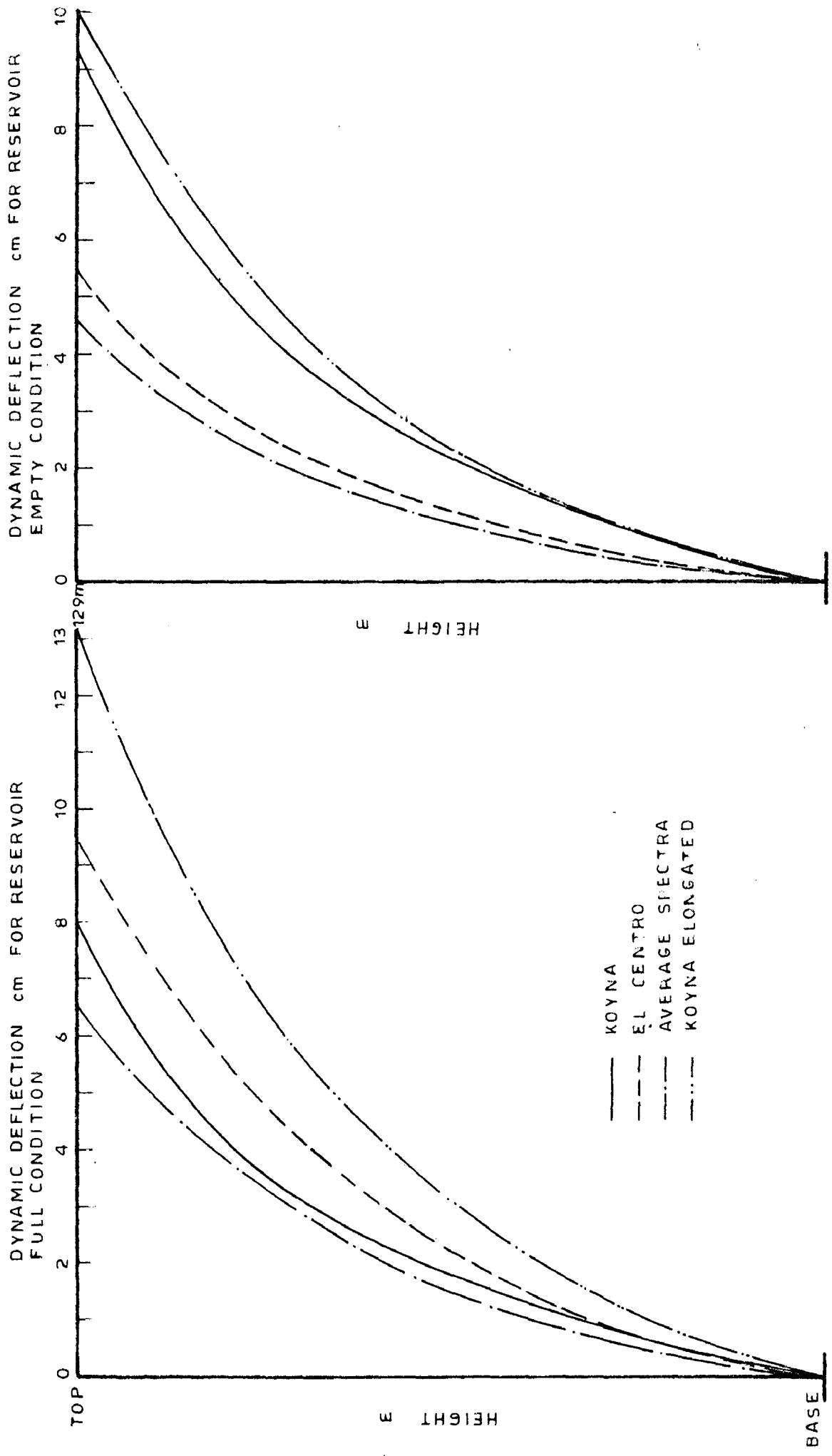


FIG. 9(a) - DYNAMIC DEFLECTION FOR CASE 1 DUE TO DIFFERENT EARTHQUAKES



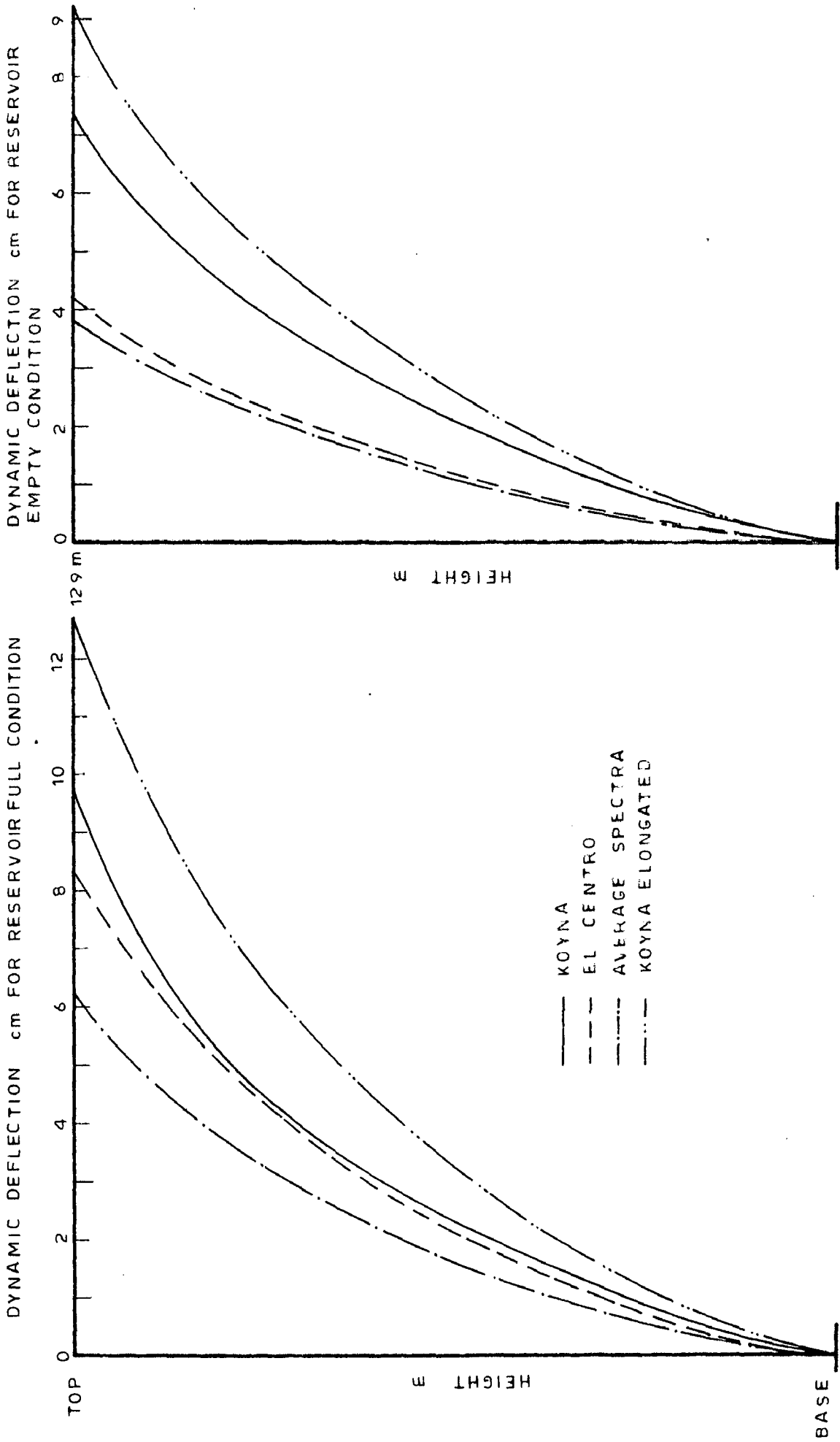


FIG. 9(b) - DYNAMIC DEFLECTION FOR CASE 3 DUE TO DIFFERENT EARTHQUAKES

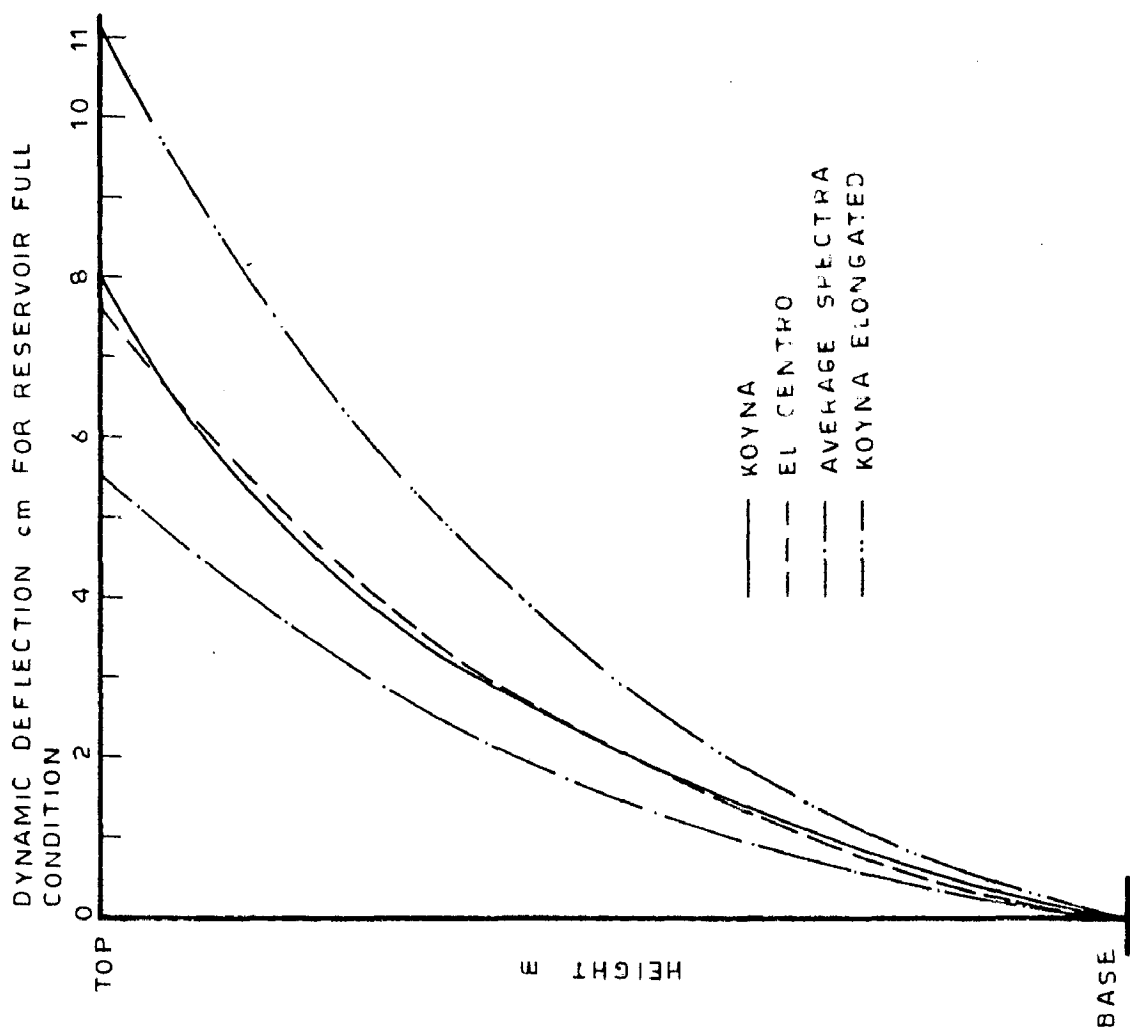
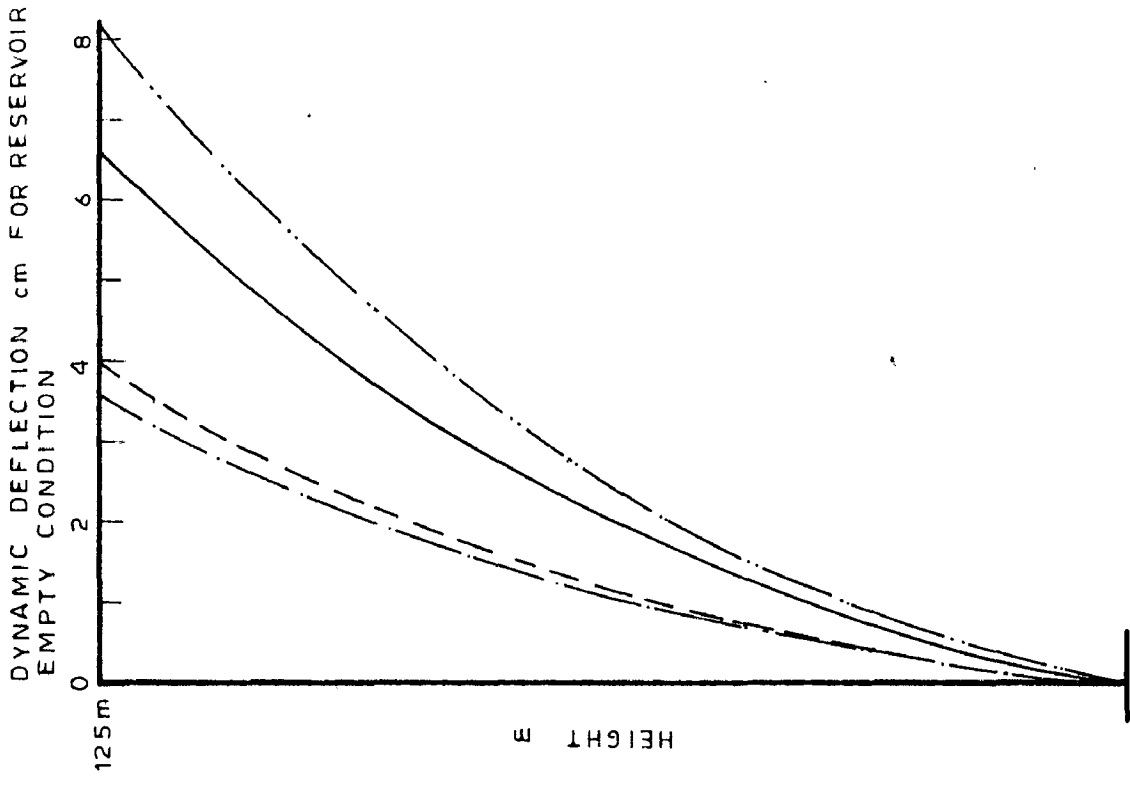


FIG. 9(c) - DYNAMIC DEFLECTION FOR CASE 7 DUE TO DIFFERENT EARTHQUAKES

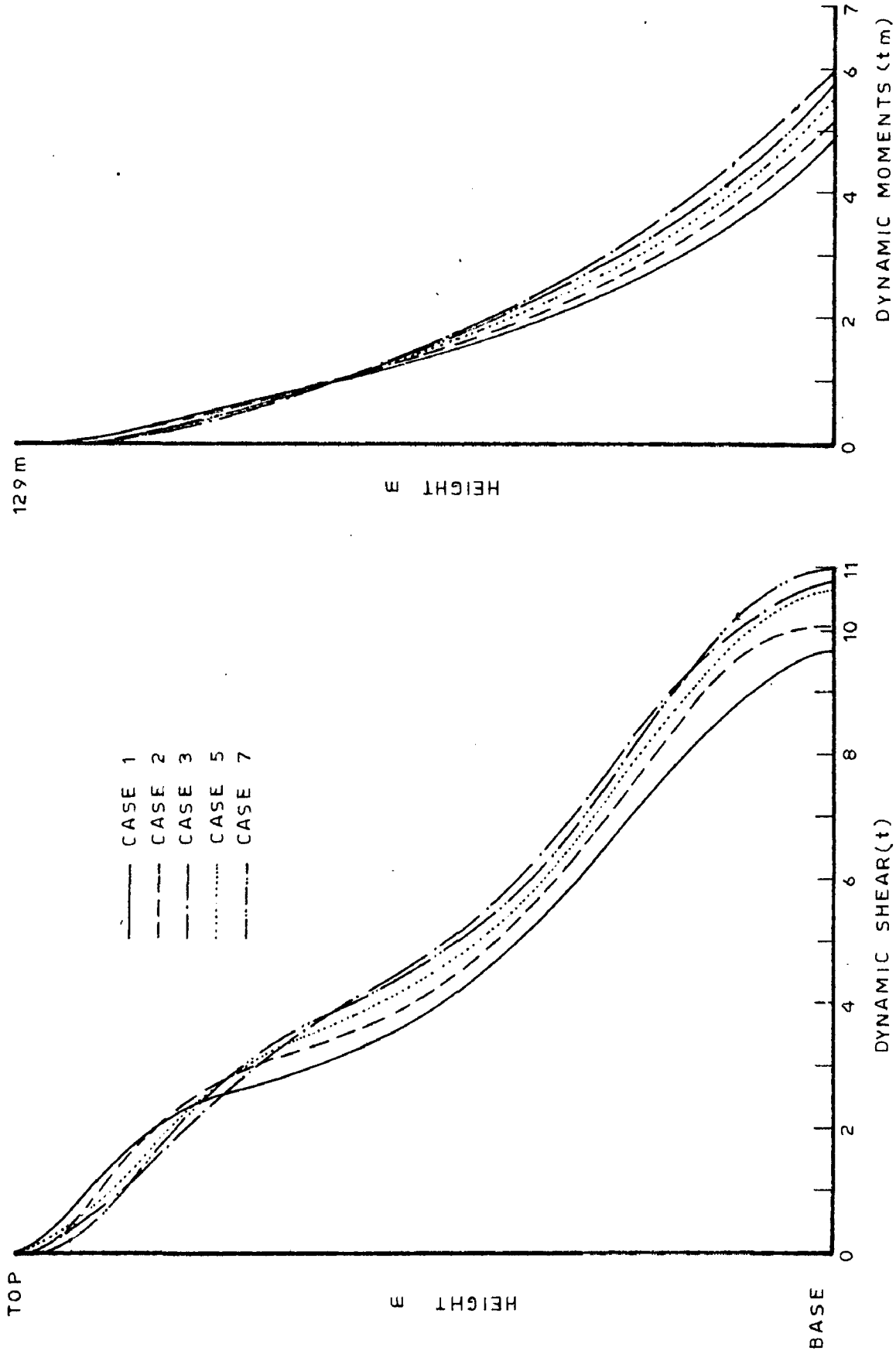


FIG. 10 (a)\_ DYNAMIC SHEAR AND MOMENT FOR VARIOUS CASES DUE TO KOYNA EARTHQUAKE FOR FULL RESERVOIR CONDITION

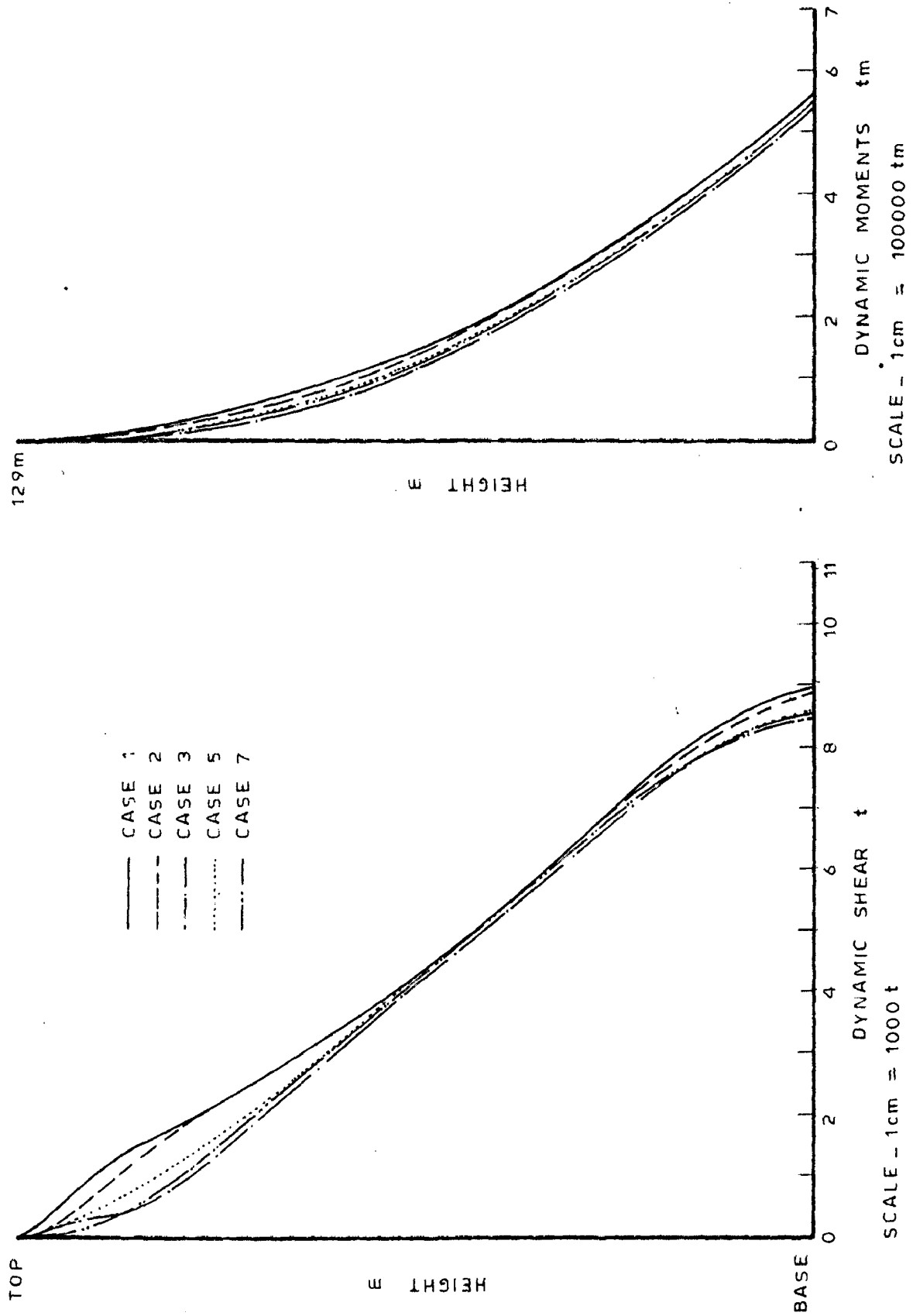


FIG. 10(b)-DYNAMIC SHEAR AND MOMENT FOR VARIOUS CASES DUE TO KOYNA EARTHQUAKE FOR EMPTY RESERVOIR CONDITION

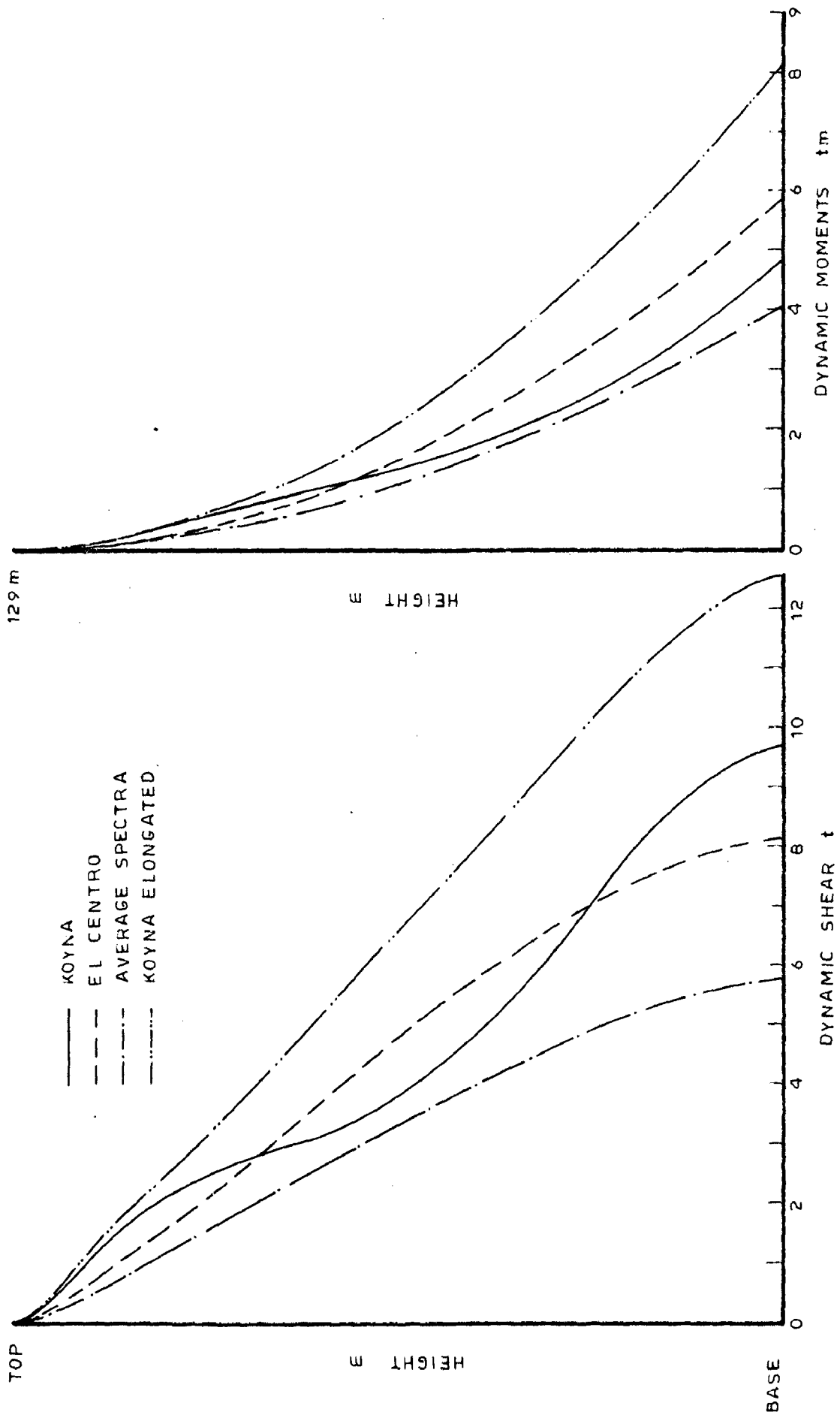


FIG.11(a) - DYNAMIC SHEAR AND MOMENT FOR CASE 1 DUE TO DIFFERENT EARTHQUAKES FOR FULL RESERVOIR CONDITION

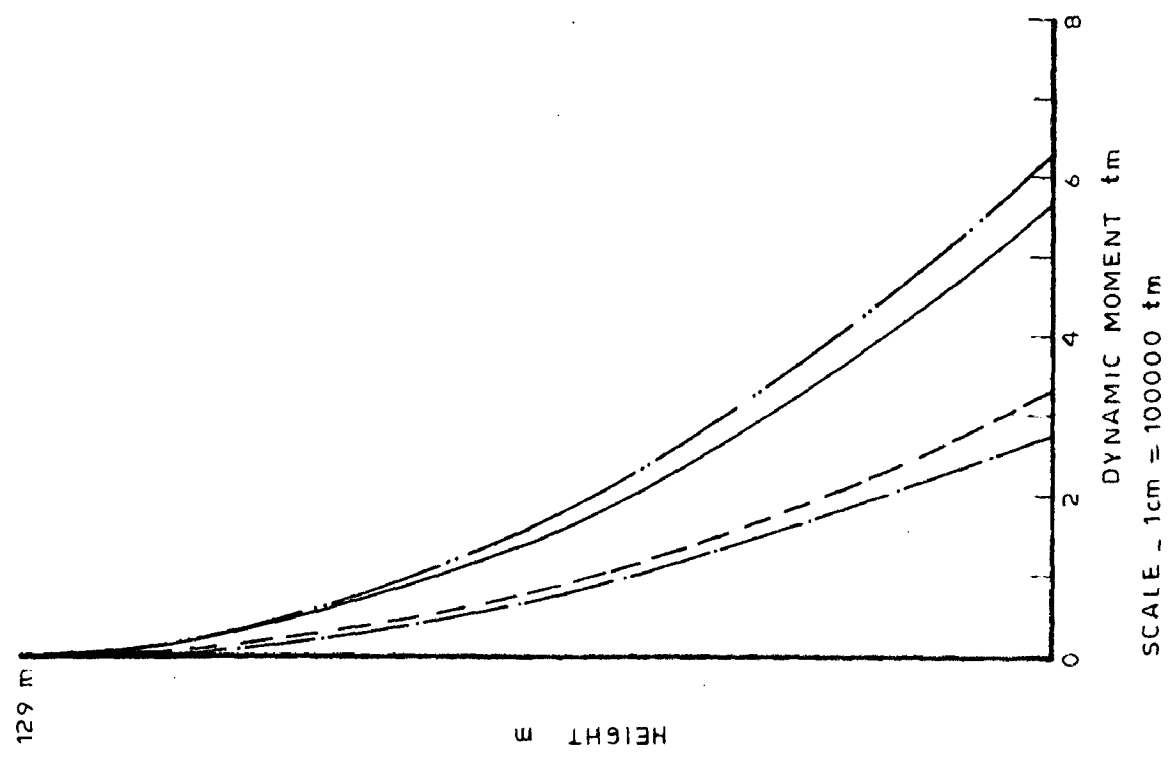
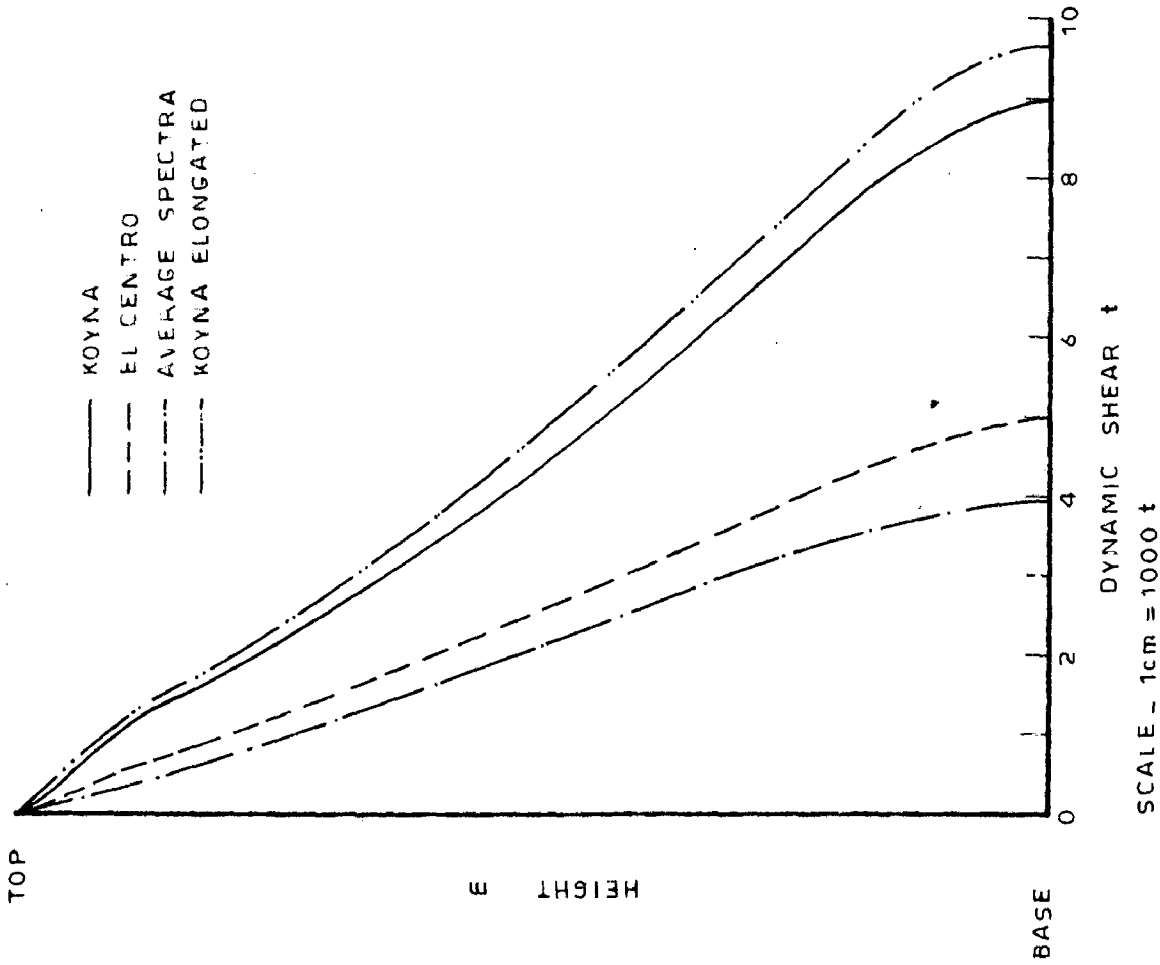
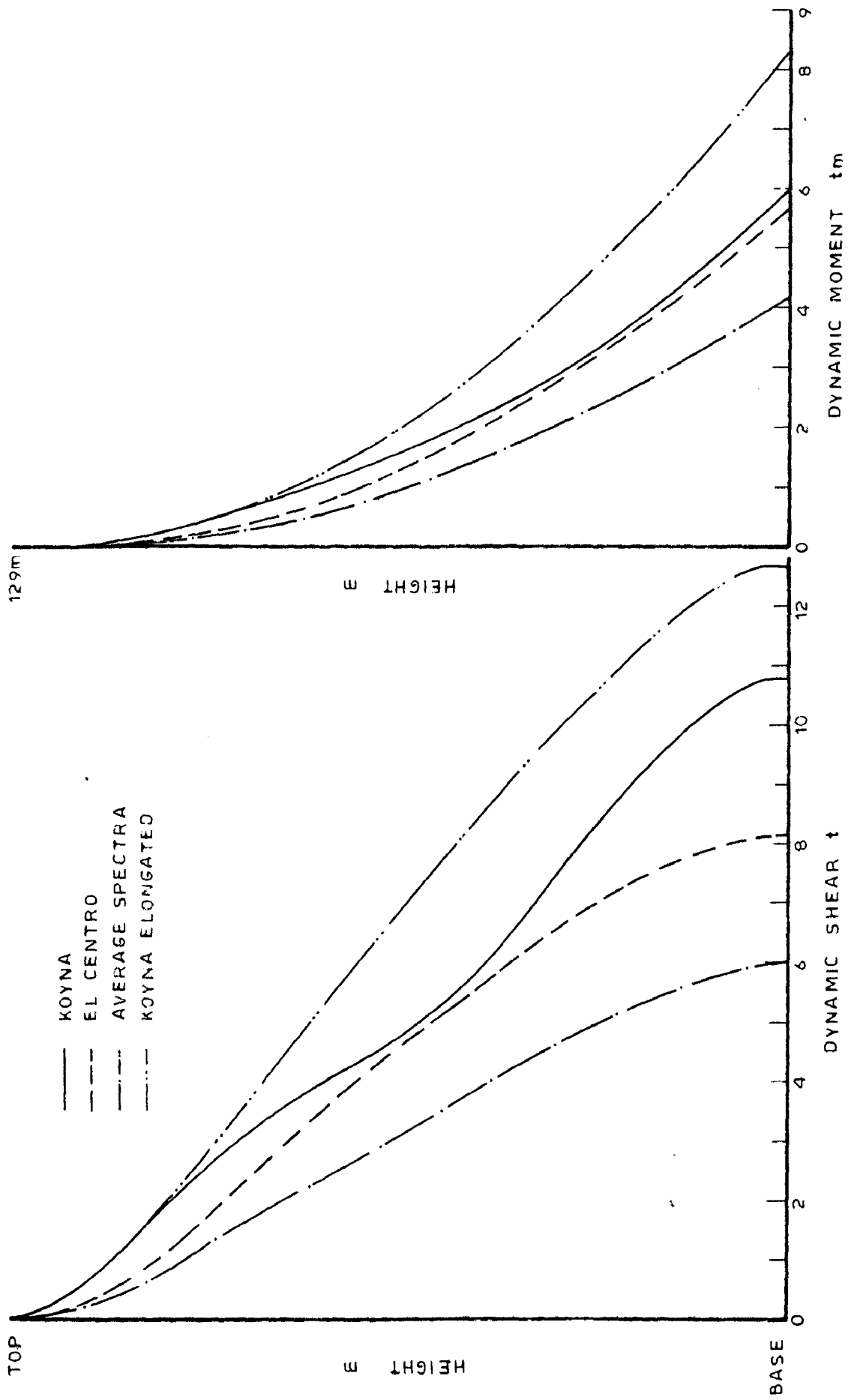


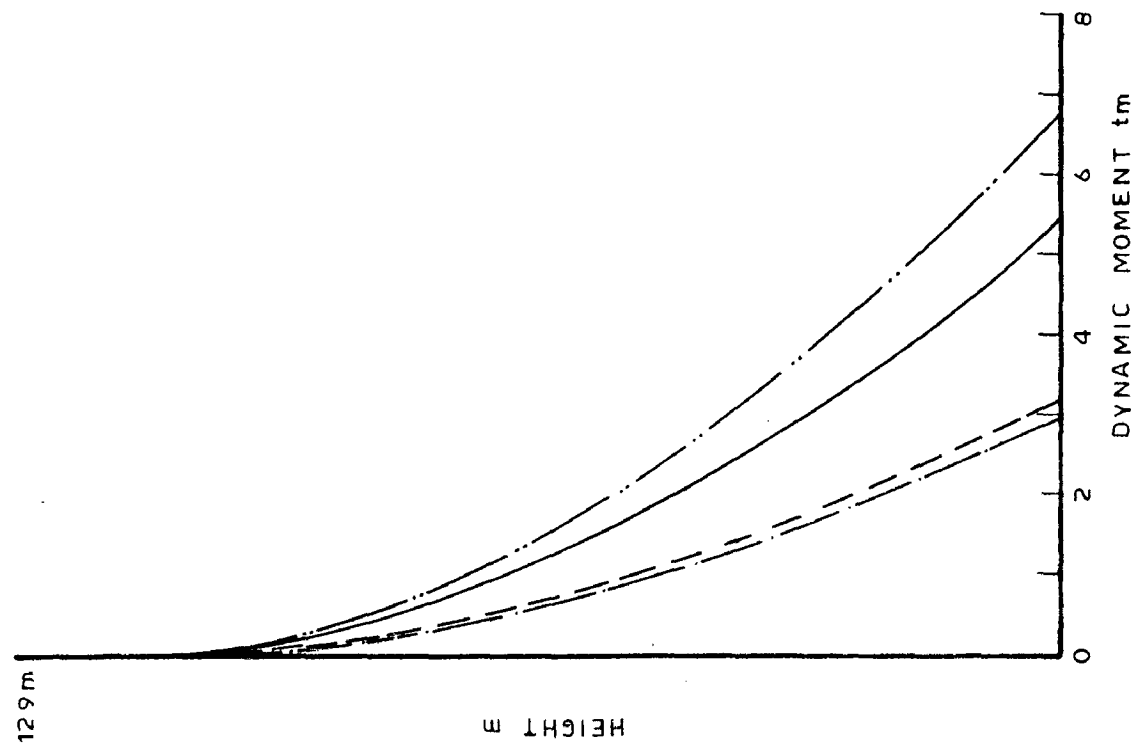
FIG.11(b) - DYNAMIC SHEAR AND MOMENT FOR CASE 1 DUE TO DIFFERENT EARTHQUAKES FOR EMPTY RESERVOIR CONDITION



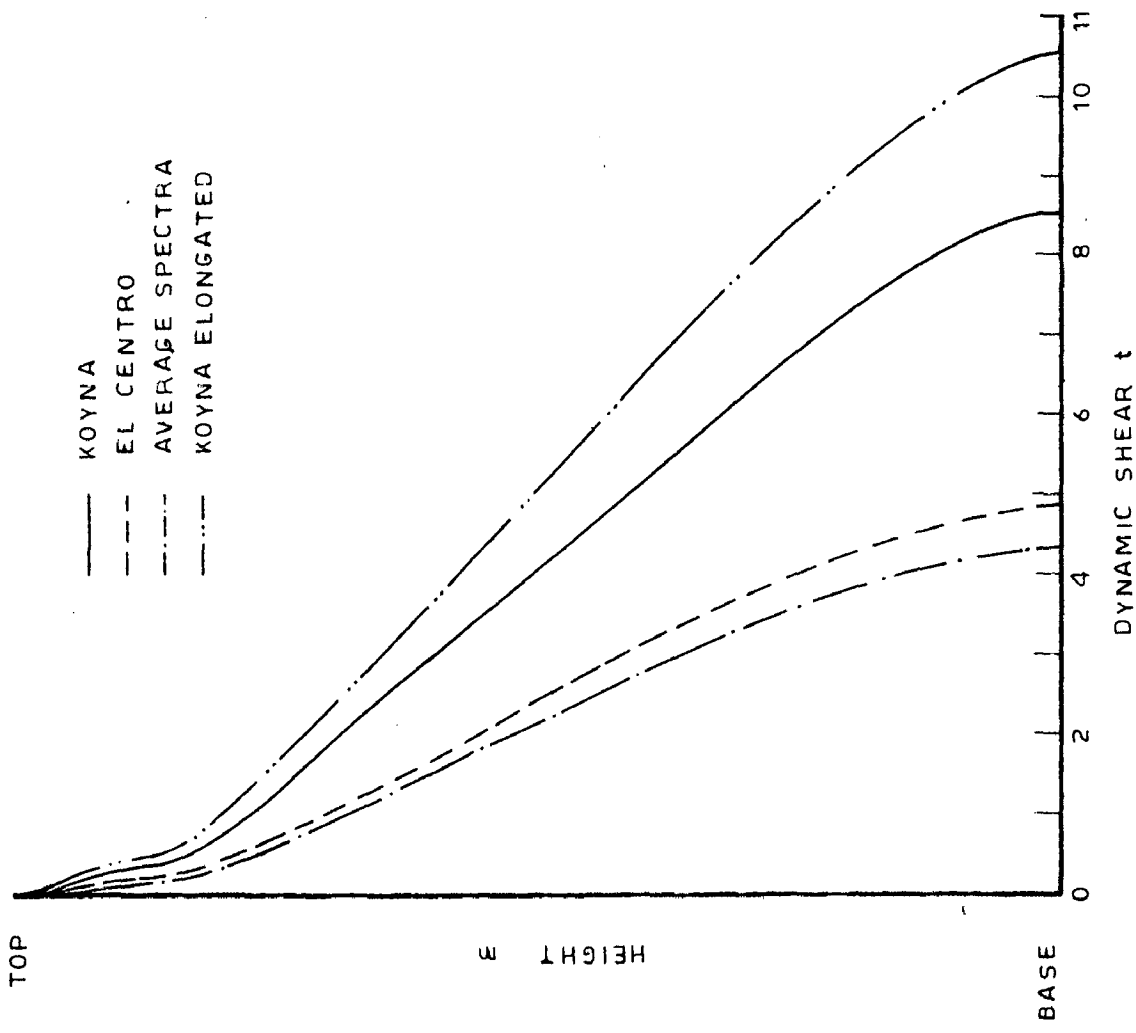
SCALE - 1 cm = 1000 t

SCALE - 1 cm = 100000 tm

FIG. 11(c) - DYNAMIC SHEAR AND MOMENT FOR CASE 3 DUE TO DIFFERENT EARTHQUAKES FOR FULL RESERVOIR CONDITION



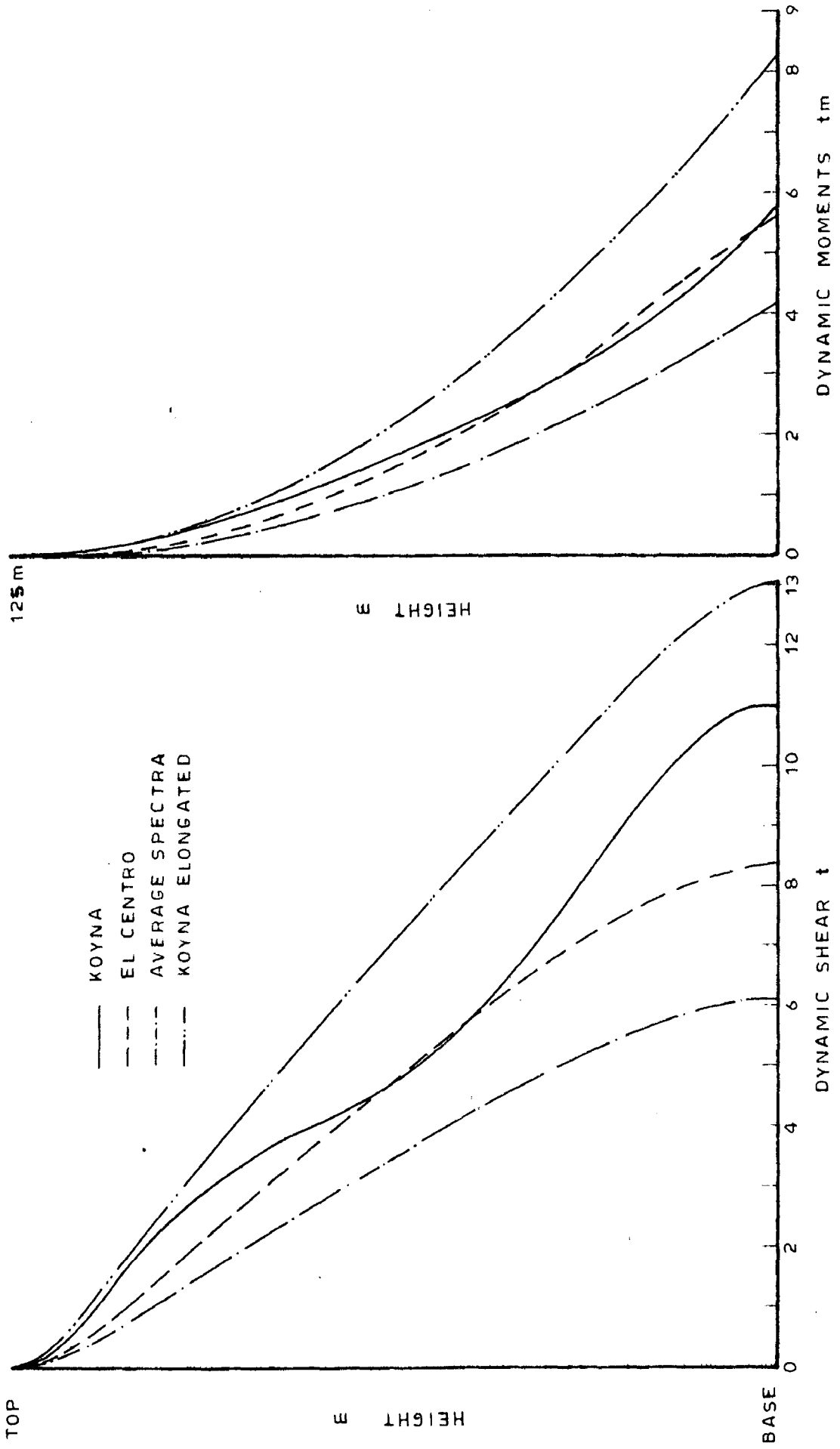
SCALE - 1cm = 100000 t m



SCALE - 1cm = 1000 t

FIG.11(d) - DYNAMIC SHEAR AND MOMENT FOR CASE 3 DUE TO DIFFERENT EARTHQUAKES FOR EMPTY RESERVOIR CONDITION





SCALE - 1cm = 1000 t

SCALE - 1cm = 100000 tm

FIG. 11(e) - DYNAMIC SHEAR AND MOMENT FOR CASE 7 DUE TO DIFFERENT EARTHQUAKES FOR FULL RESERVOIR CONDITION

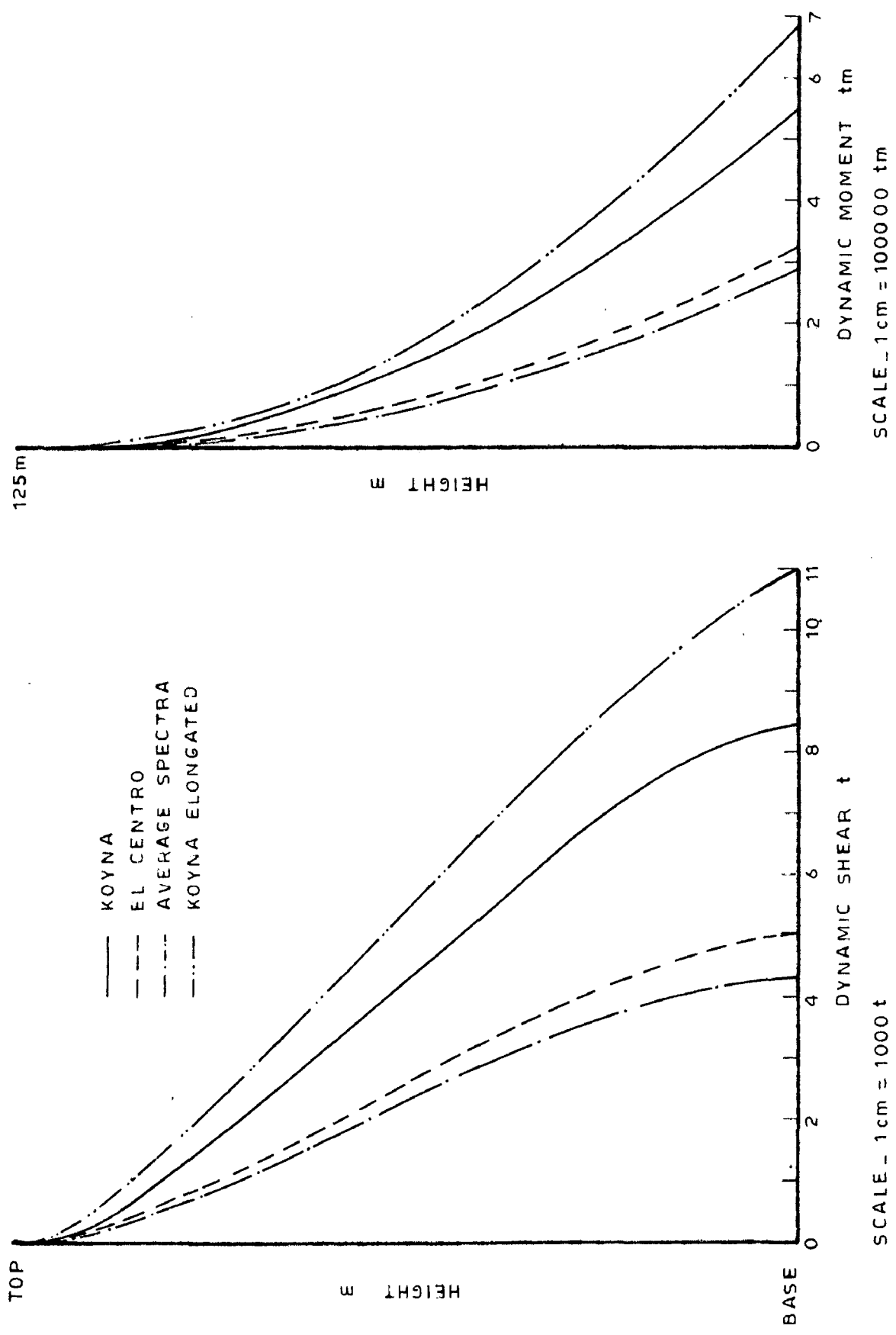


FIG.11(f)- DYNAMIC SHEAR AND MOMENT FOR CASE 7 DUE TO DIFFERENT EARTHQUAKES FOR EMPTY RESERVOIR CONDITION

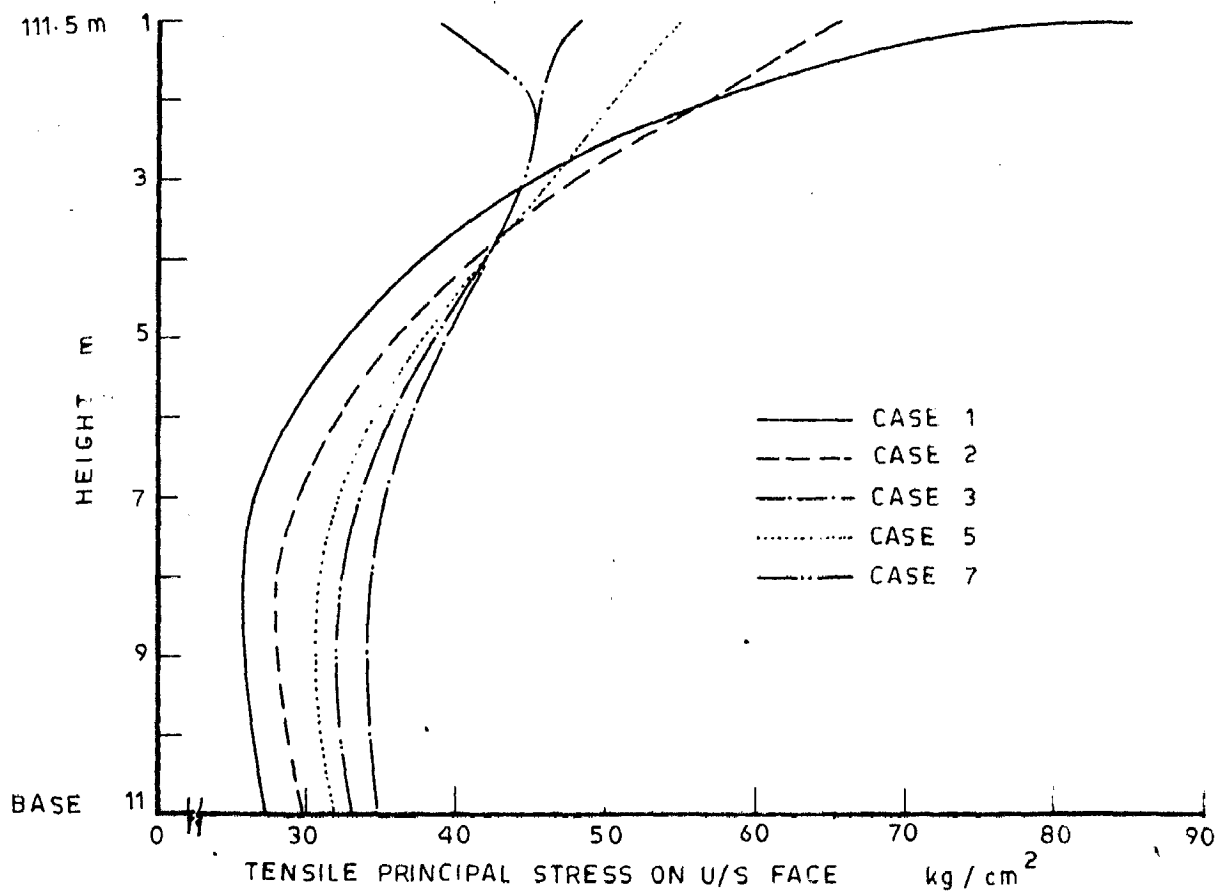
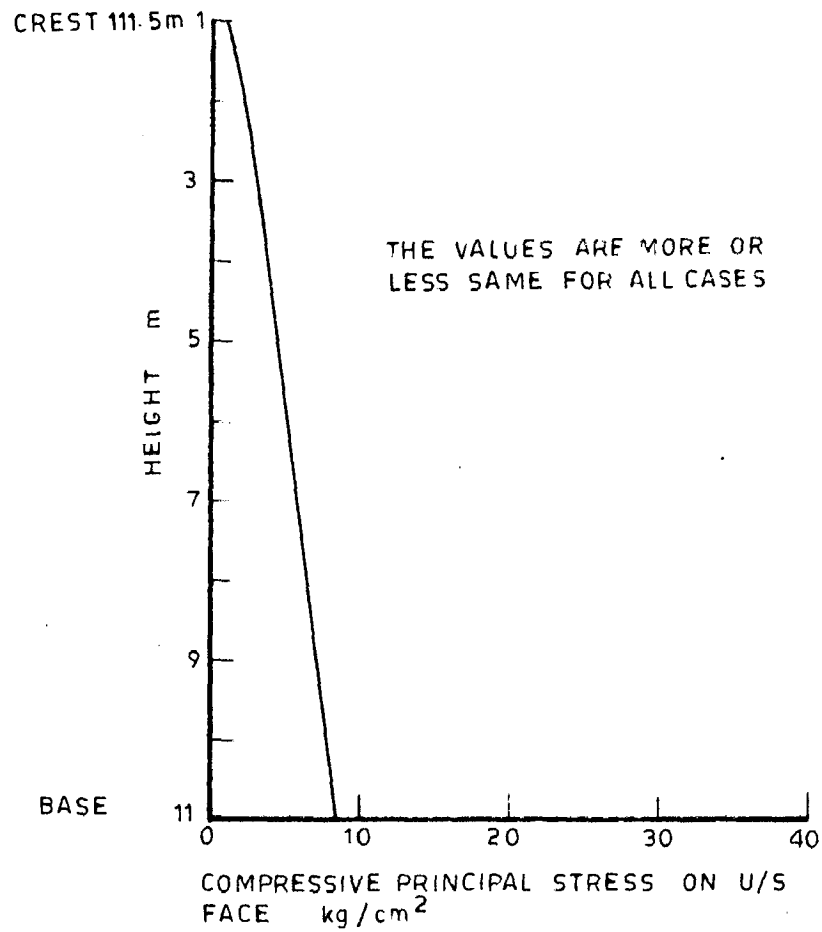


FIG 12(a)\_COMBINED PRINCIPAL STRESSES FOR VARIOUS CASES DUE TO KOYNA EARTHQUAKE FOR FULL RESERVOIR CONDITION

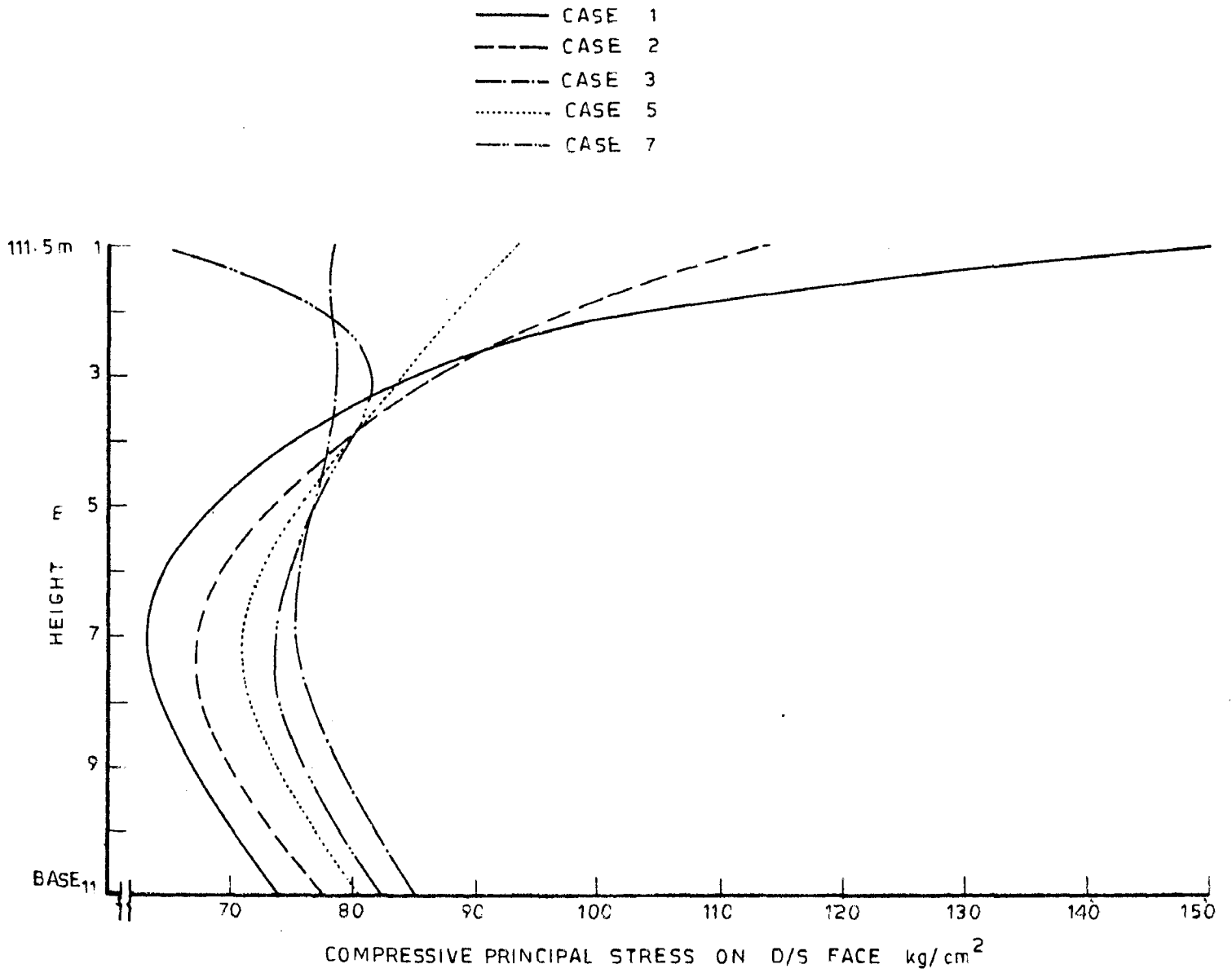


FIG. 12 (b)\_COMBINED PRINCIPAL STRESSES FOR VARIOUS CASES  
DUE TO KOYNA EARTHQUAKE FOR FULL RESERVOIR  
CONDITION

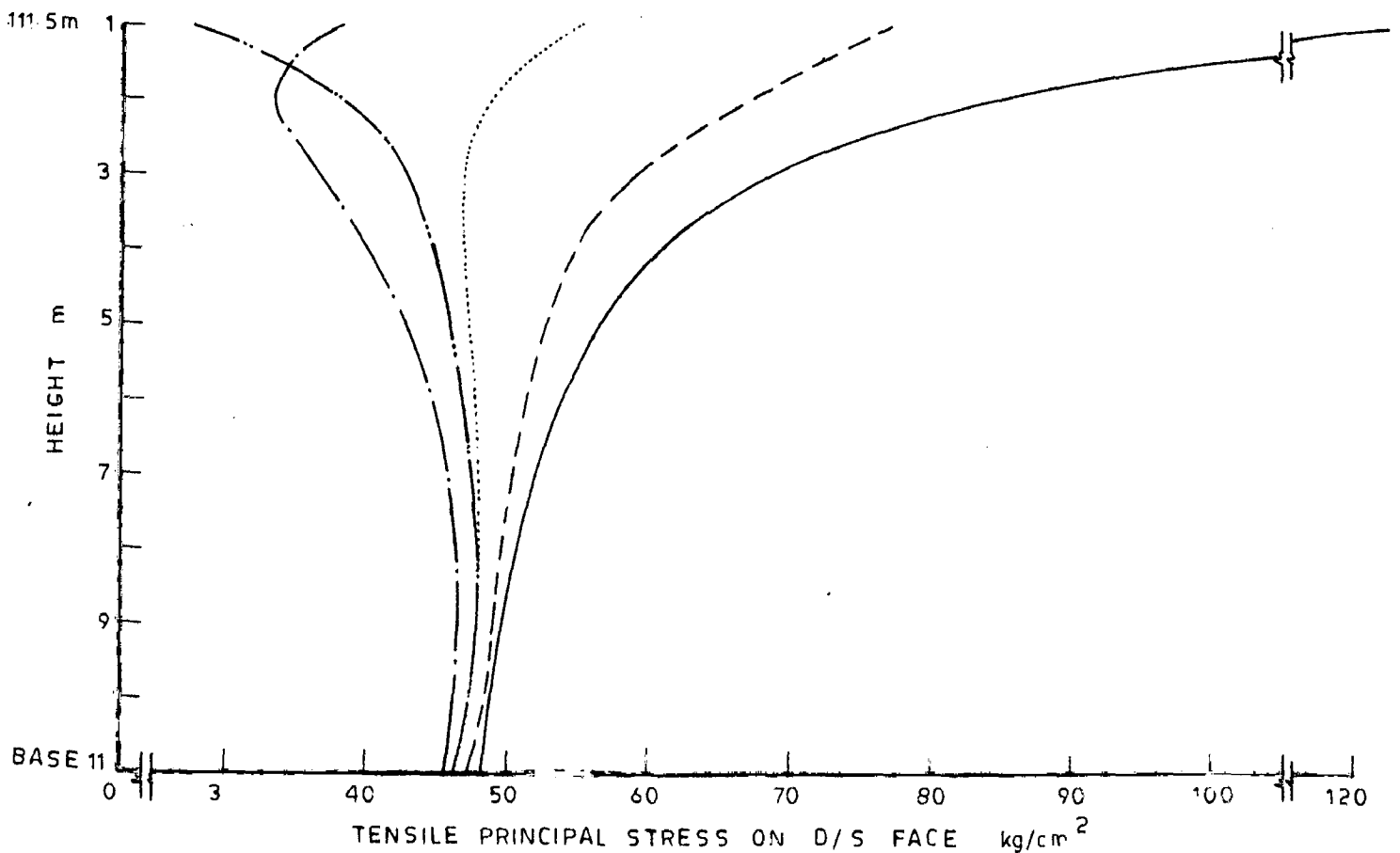
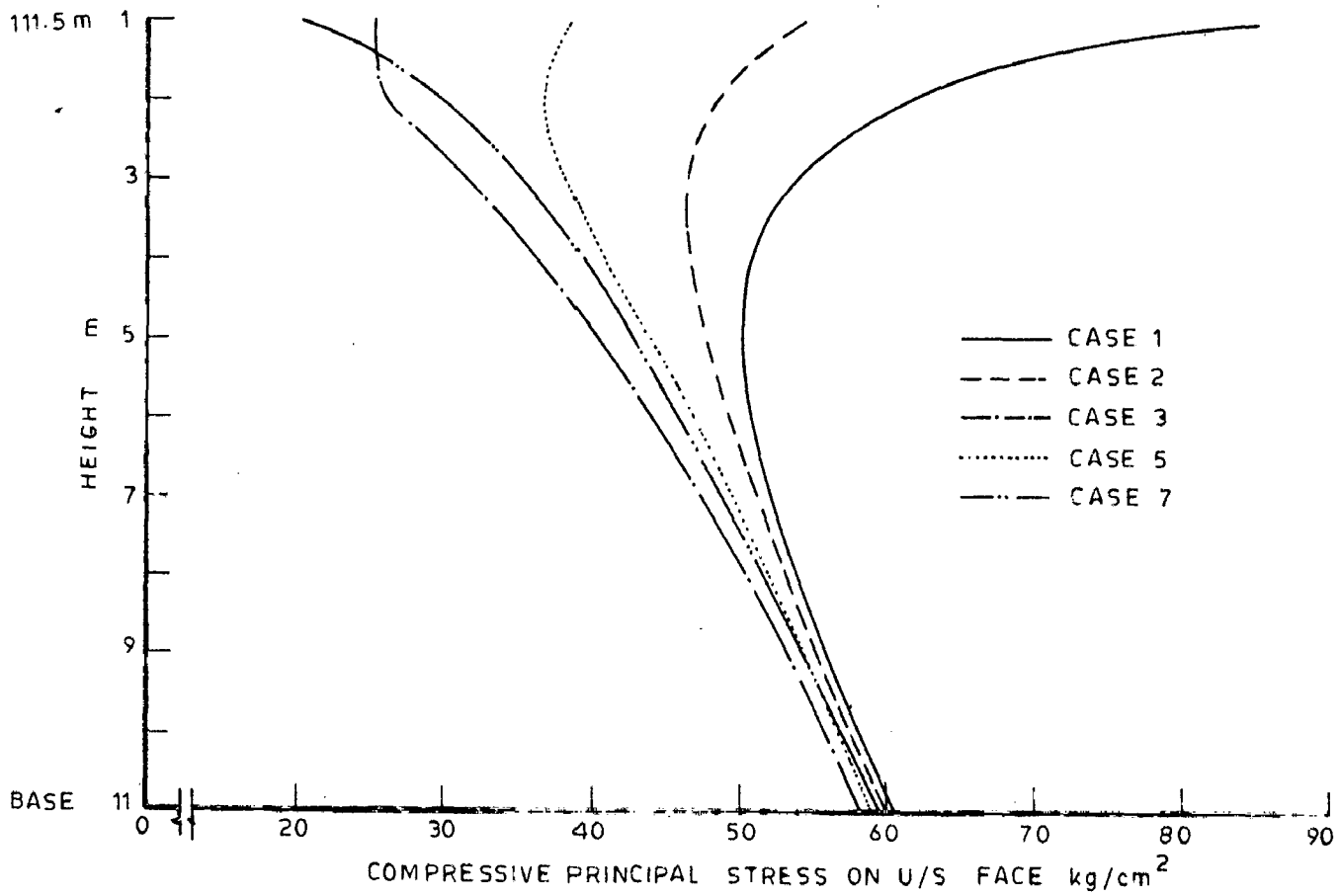


FIG 12 (c) COMBINED PRINCIPAL STRESSES FOR VARIOUS CASES DUE TO KOYNA EARTHQUAKE FOR EMPTY RESERVOIR CONDITION

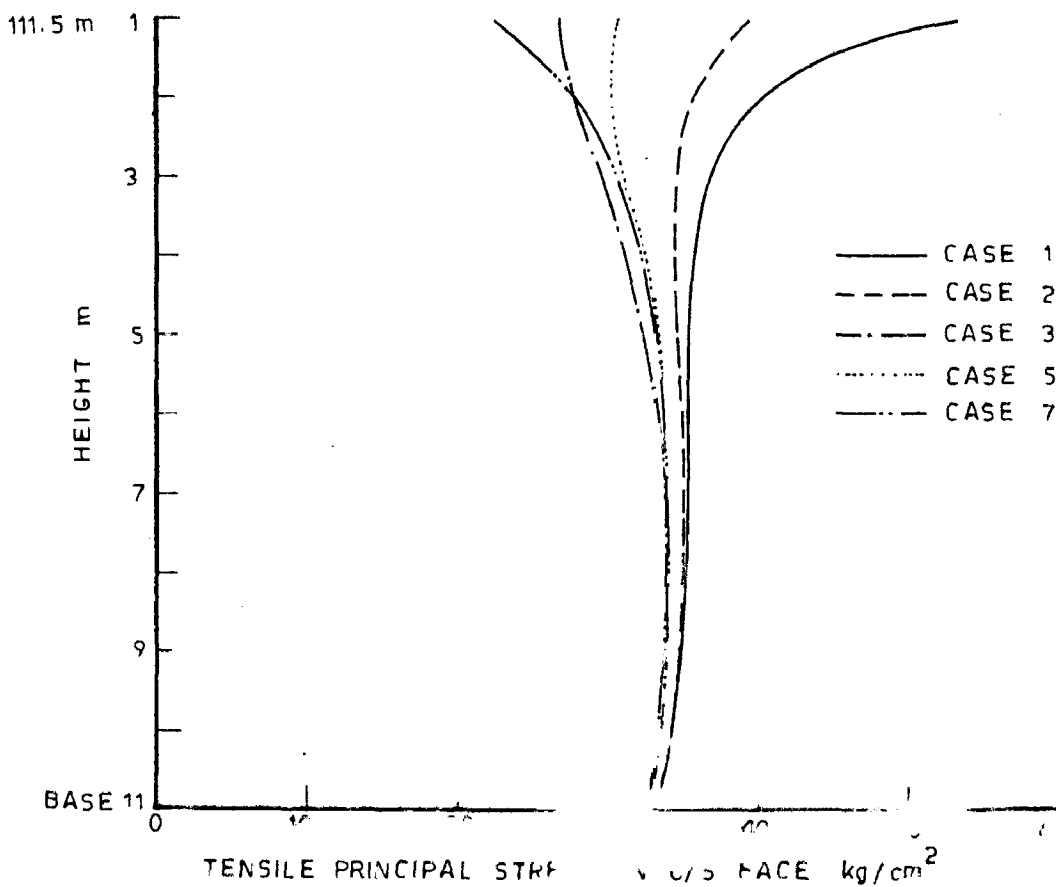
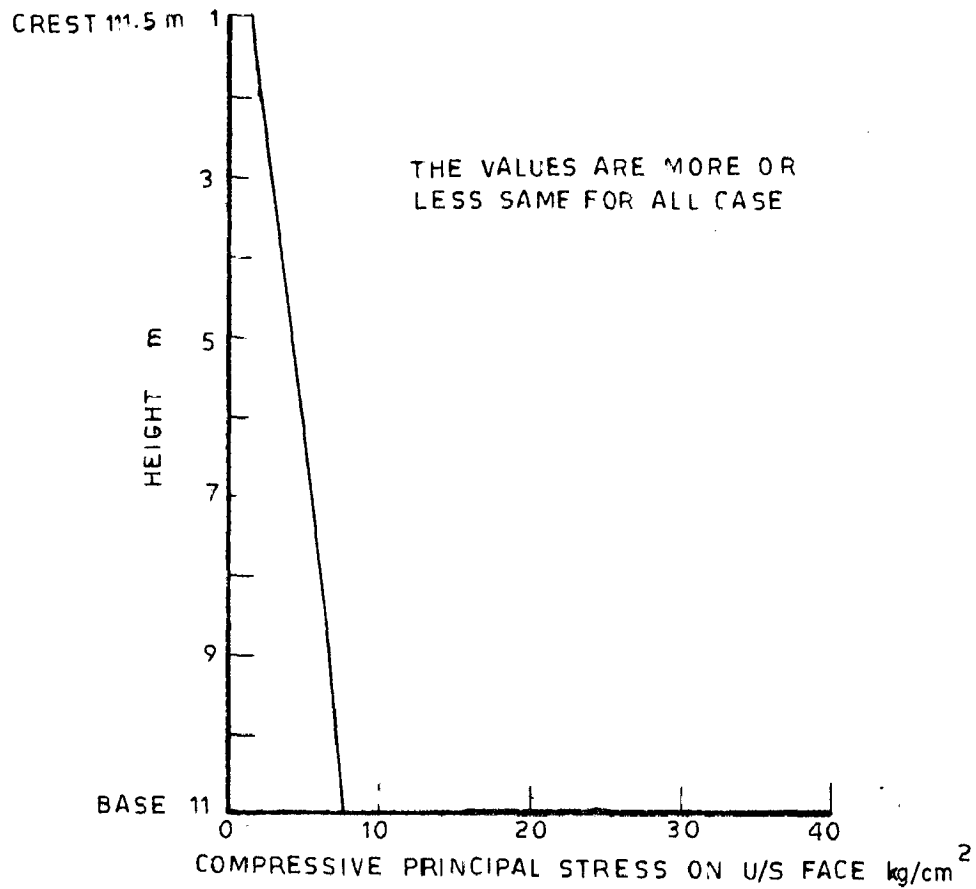


FIG. 13(a) COMBINED PRINCIPAL STRESSES FOR VARIOUS CASES DUE TO EL CENTRO EARTHQUAKE FOR FULL RESERVOIR CONDITION

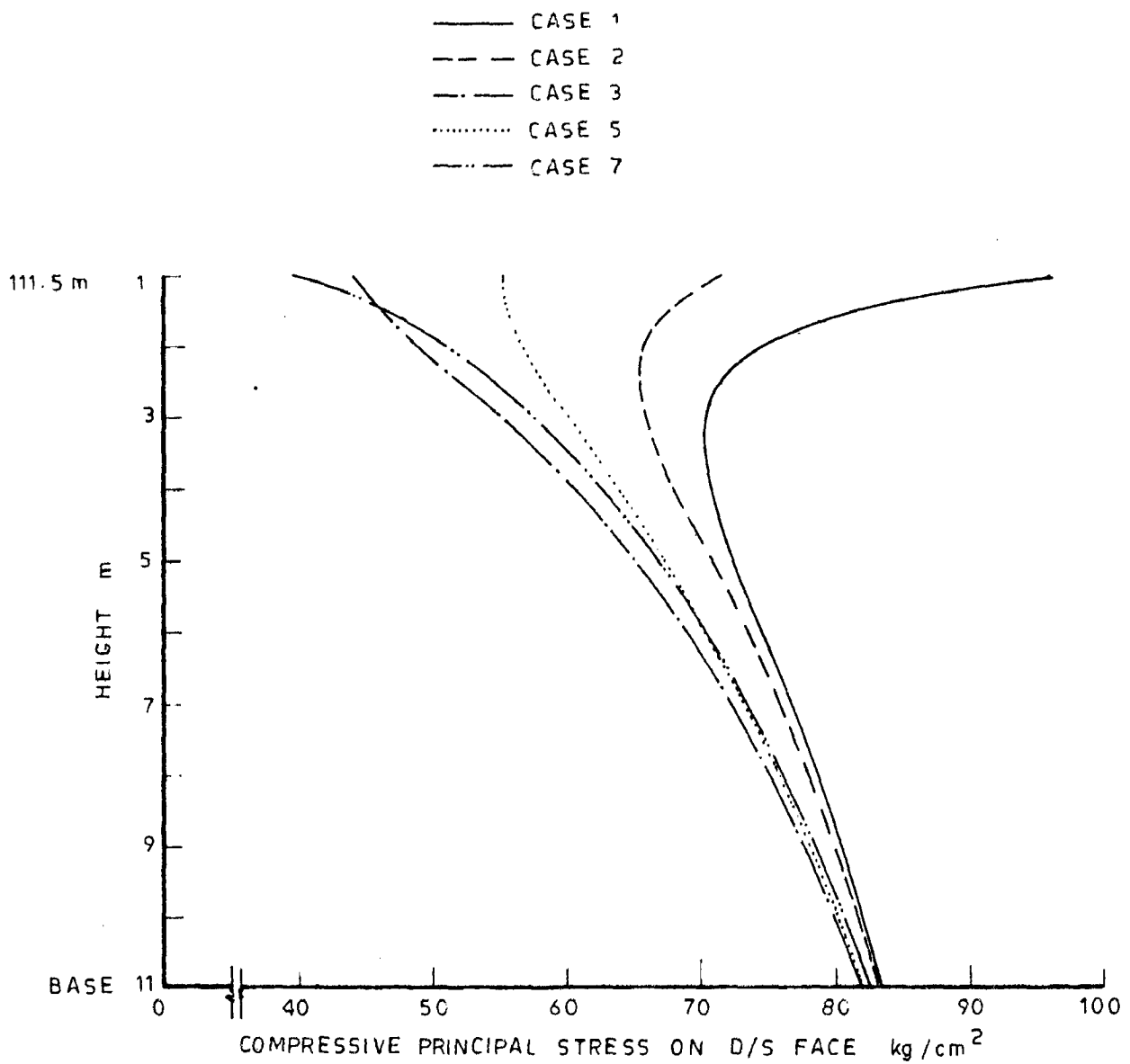


FIG. 13(b) COMBINED PRINCIPAL STRESSES FOR VARIOUS CASES DUE TO EL CENTRO EARTHQUAKE FOR FULL RESERVOIR CONDITION

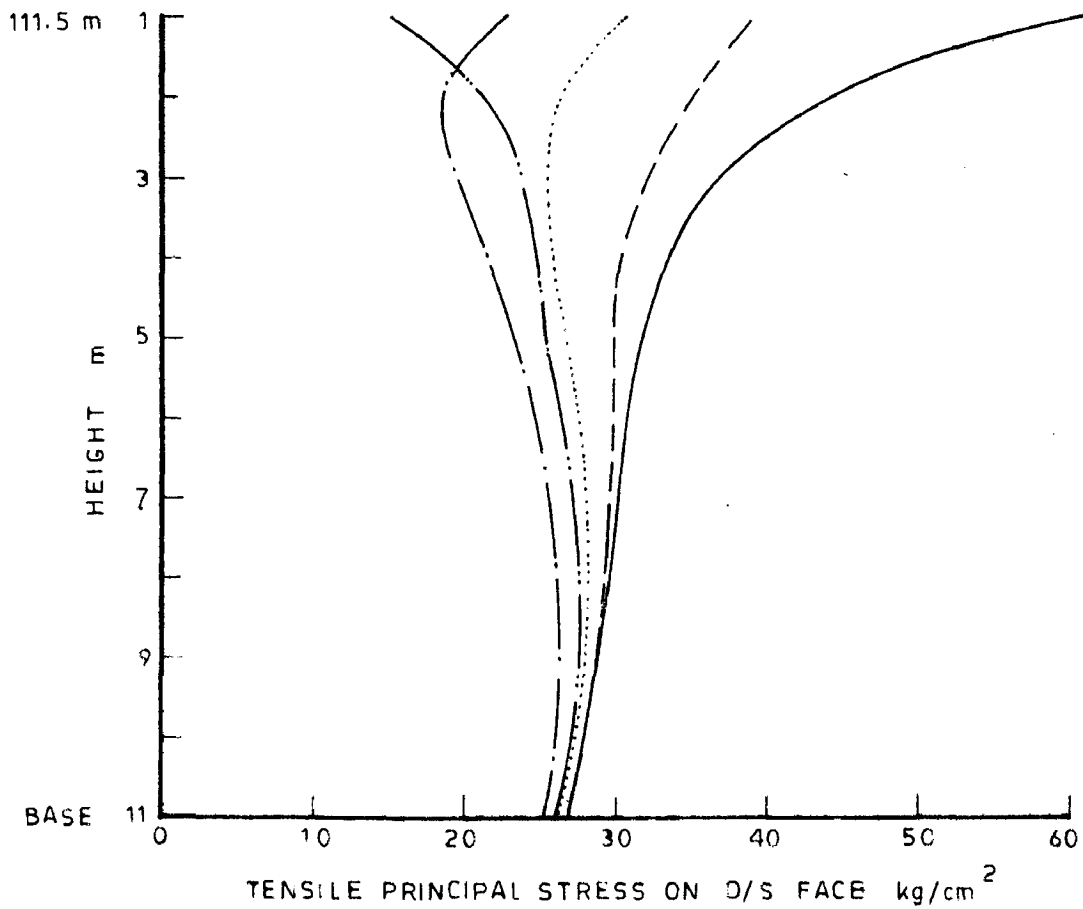
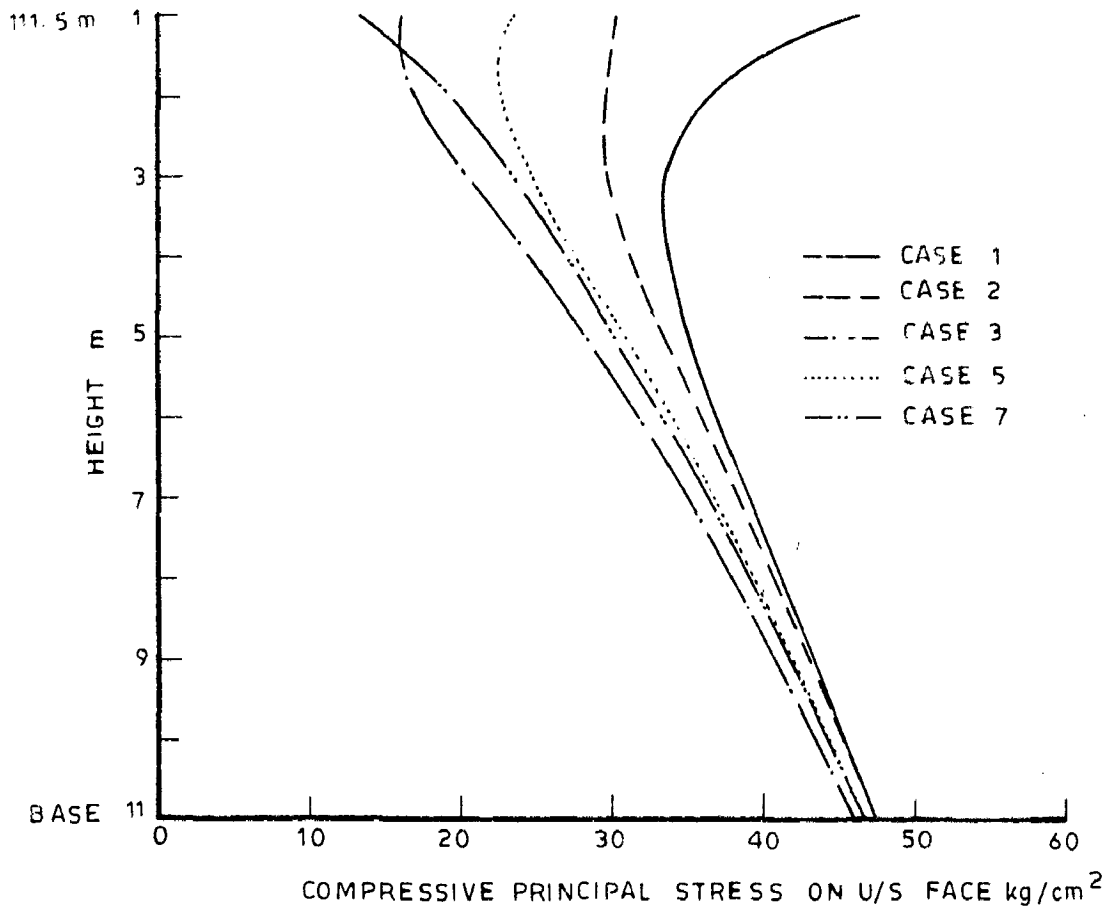


FIG. 13(c) COMBINED PRINCIPAL STRESSES FOR VARIOUS CASES DUE TO EL CENTRO EARTHQUAKE FOR EMPTY RESERVOIR CONDITION



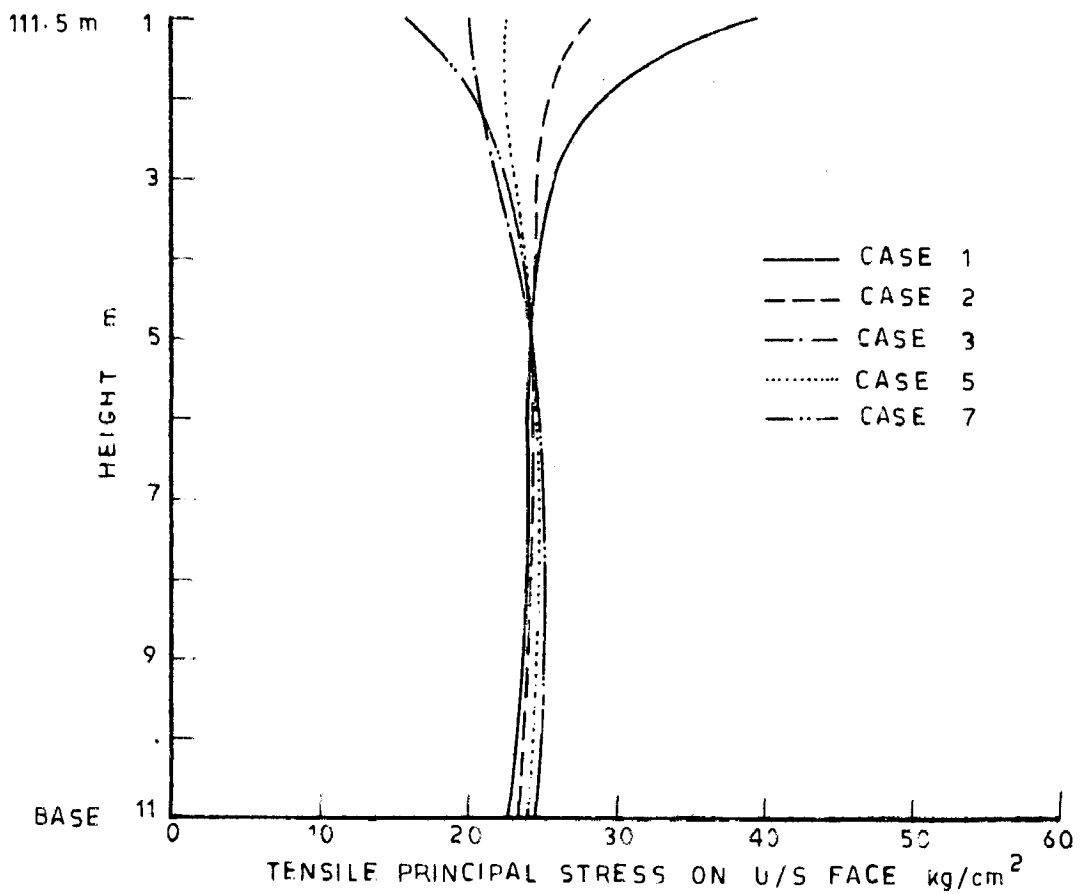
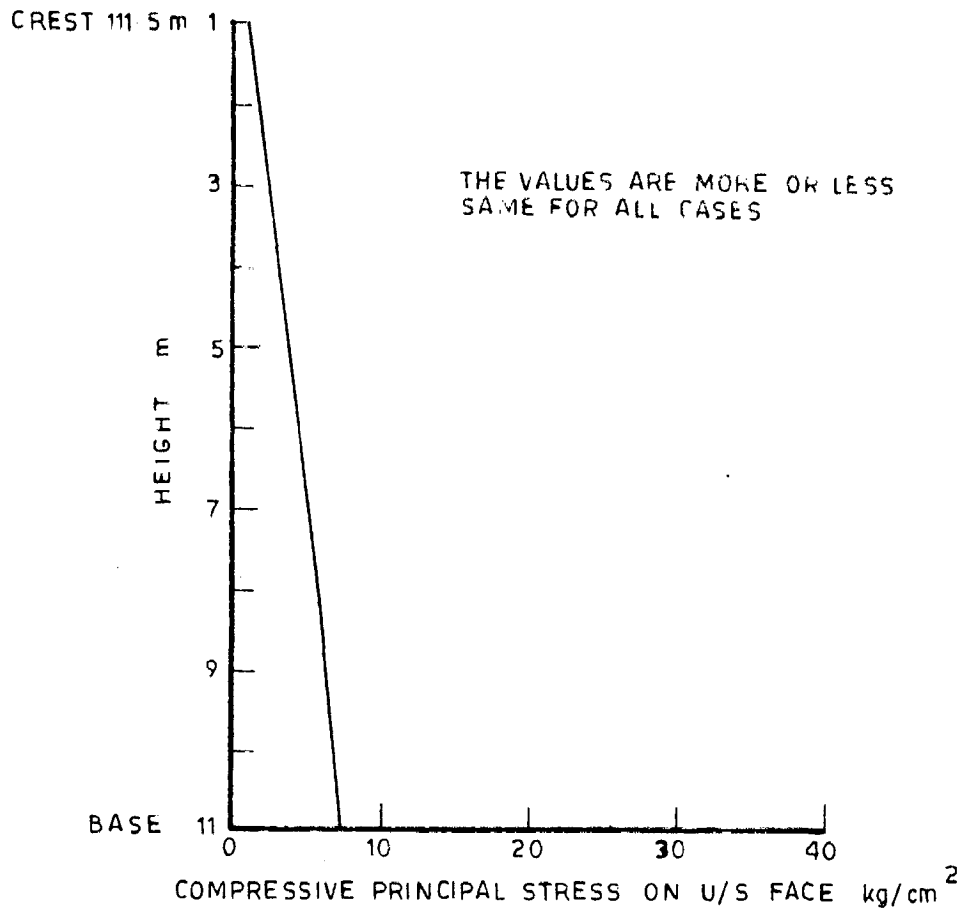


FIG.14 (a) - COMBINED PRINCIPAL STRESSES FOR VARIOUS DUE TO AVERAGE SPECTRA EARTHQUAKE FOR FULL RESERVOIR CONDITION

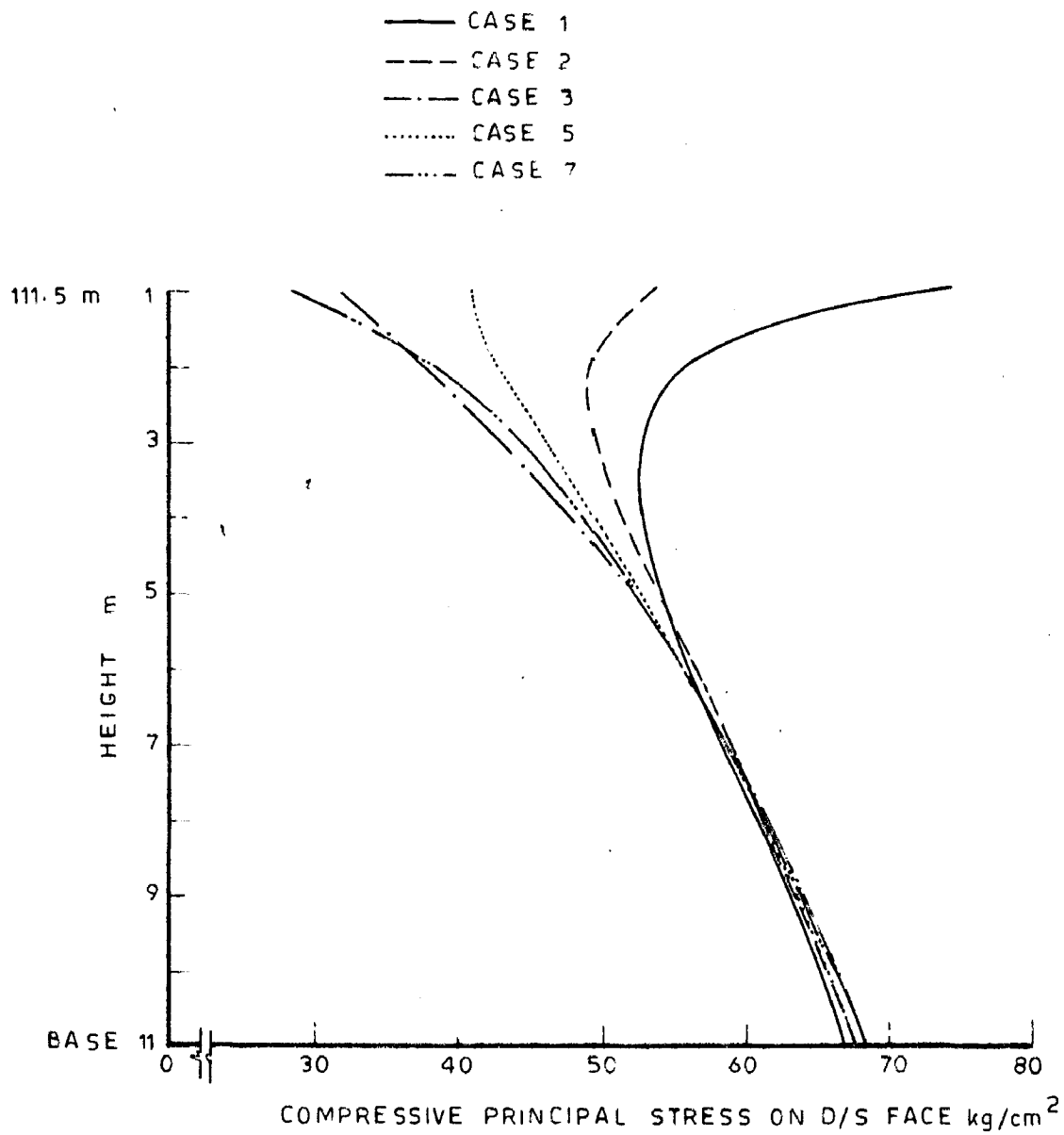


FIG.14 (b)\_COMBINED PRINCIPAL STRESSES FOR VARIOUS CASES DUE TO AVERAGE SPECTRA EARTHQUAKE FOR FULL RESERVOIR CONDITION

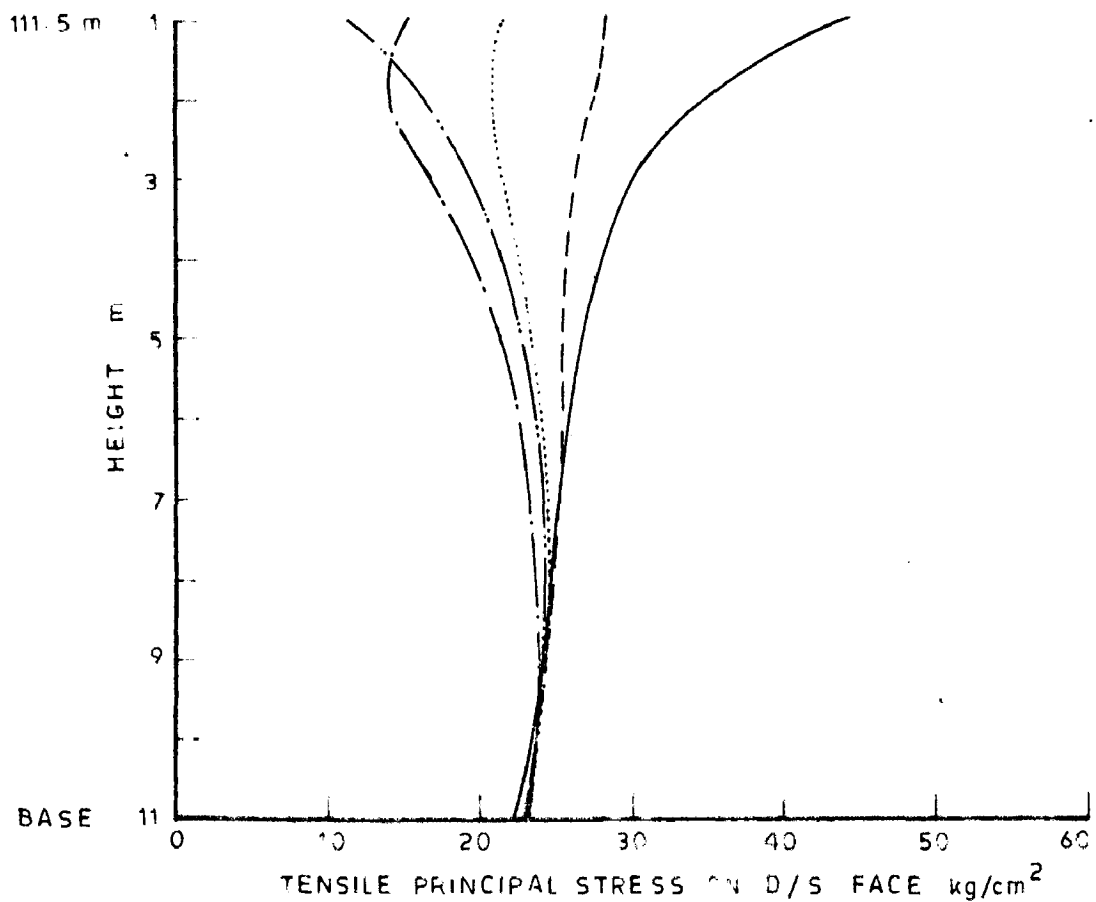
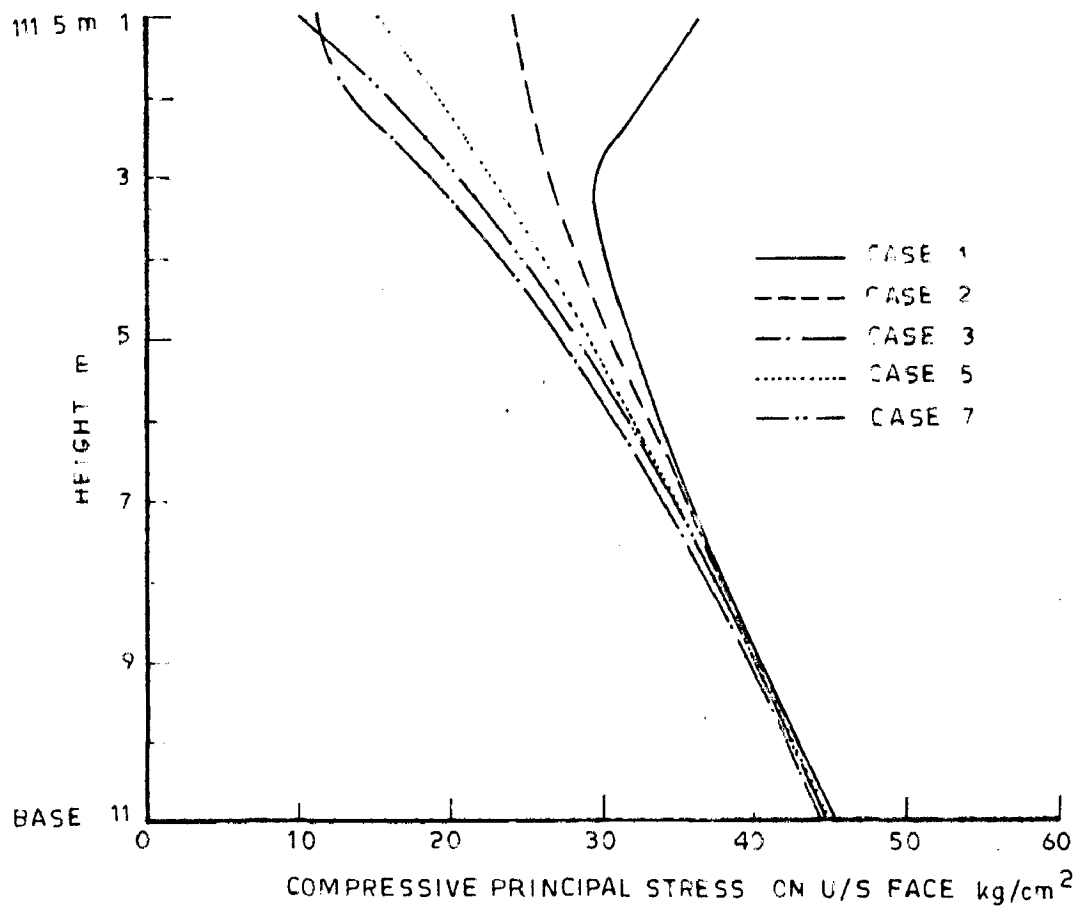


FIG.14(c) - COMBINED PRINCIPAL STRESSES FOR VARIOUS CASES DUE TO AVERAGE SPECTRA EARTHQUAKE FOR EMPTY RESERVOIR CONDITION

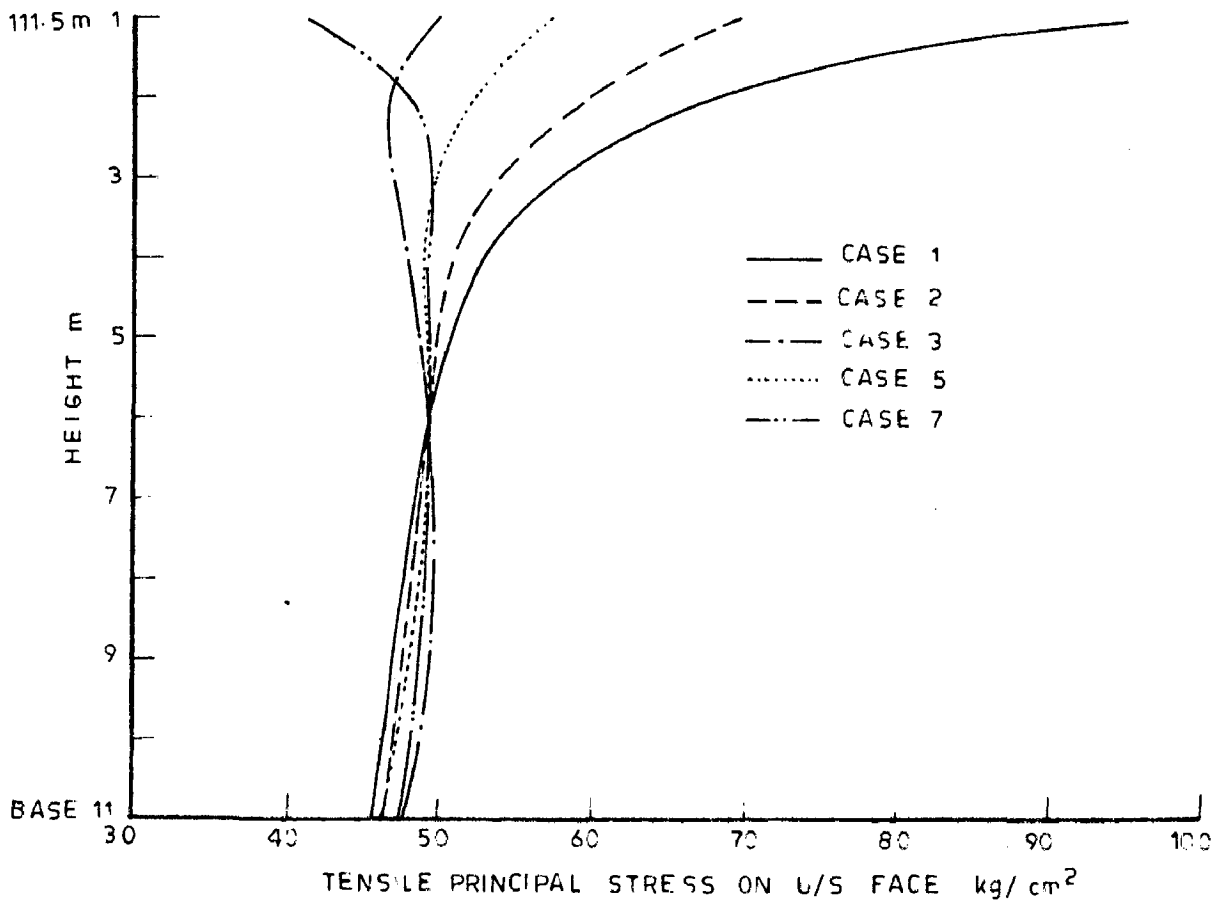
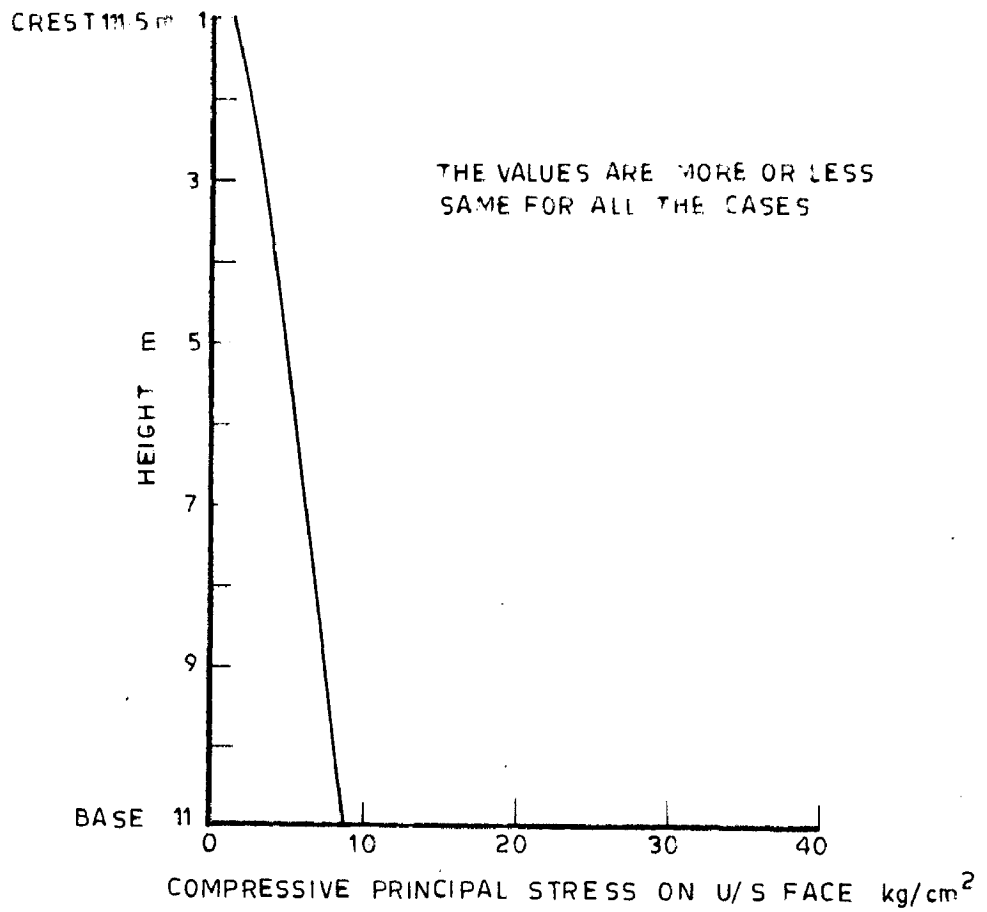


FIG. 15(a) COMBINED PRINCIPAL STRESSES FOR VARIOUS CASE DUE TO KOYNA ELONGATED EARTHQUAKE FOR FULL RESERVOIR CONDITION

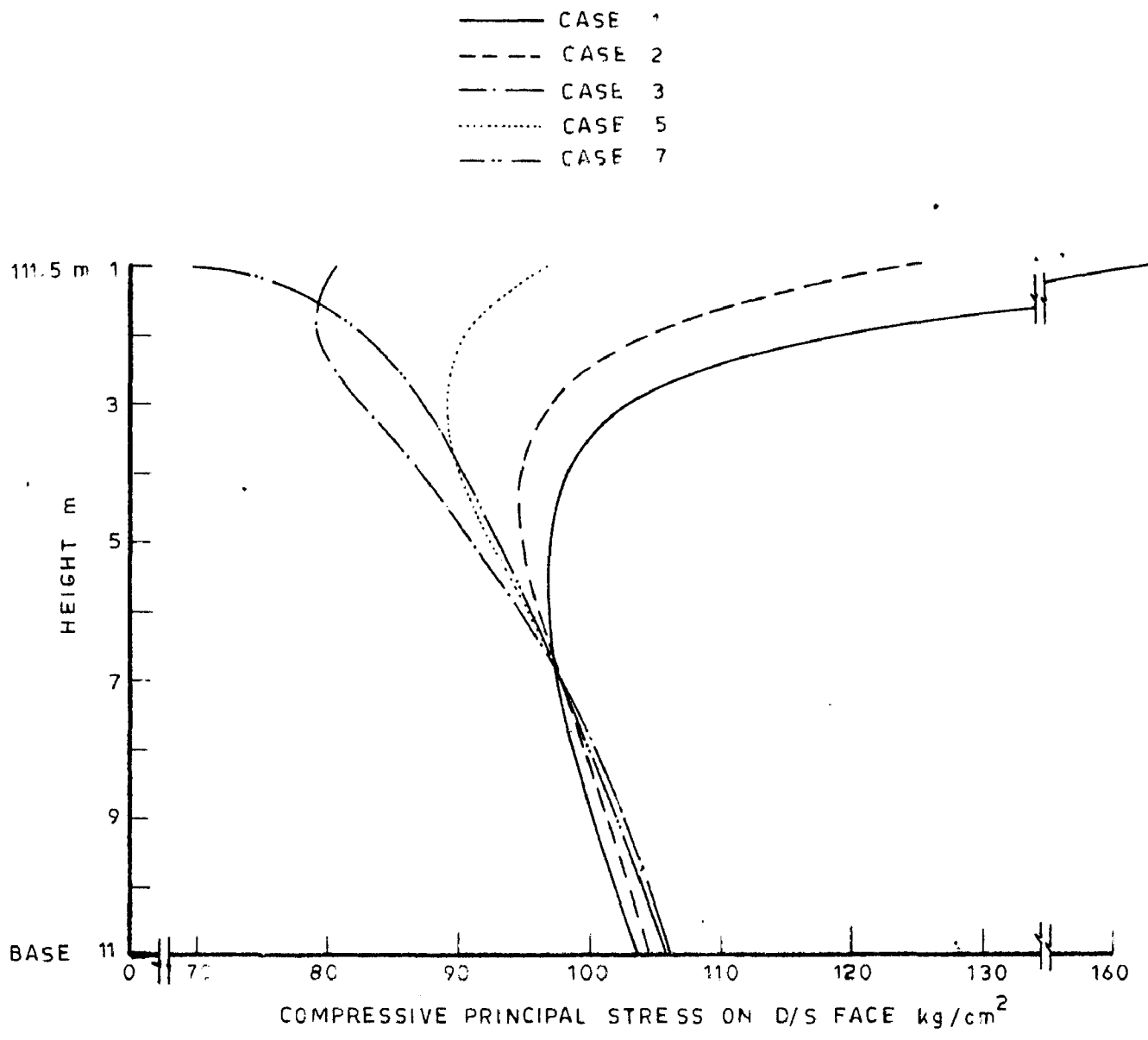


FIG.15(b)\_ COMBINED PRINCIPAL STRESSES FOR VARIOUS CASES DUE TO KOYNA ELONGATED EARTHQUAKE FOR FULL RESERVOIR CONDITION

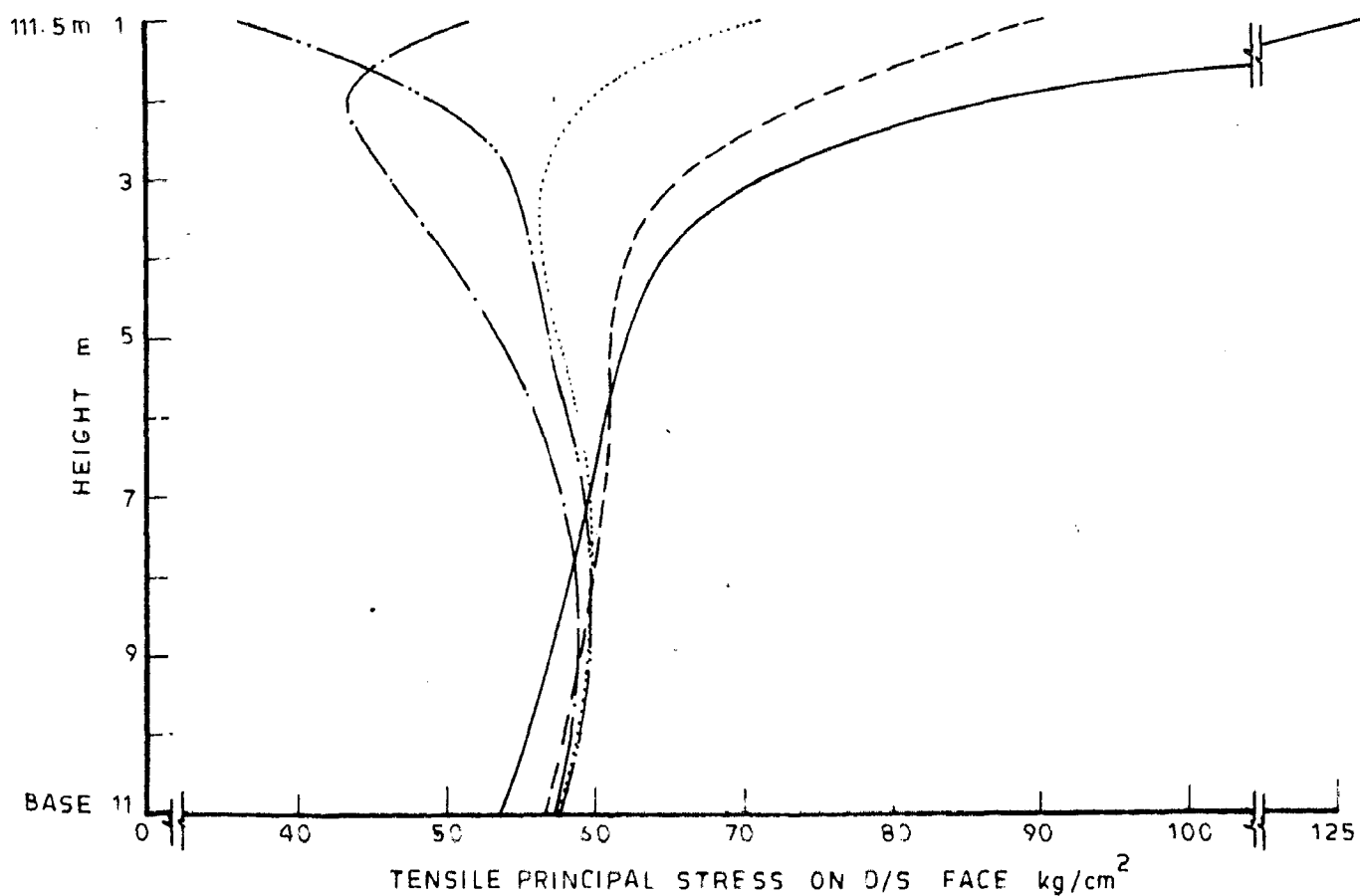
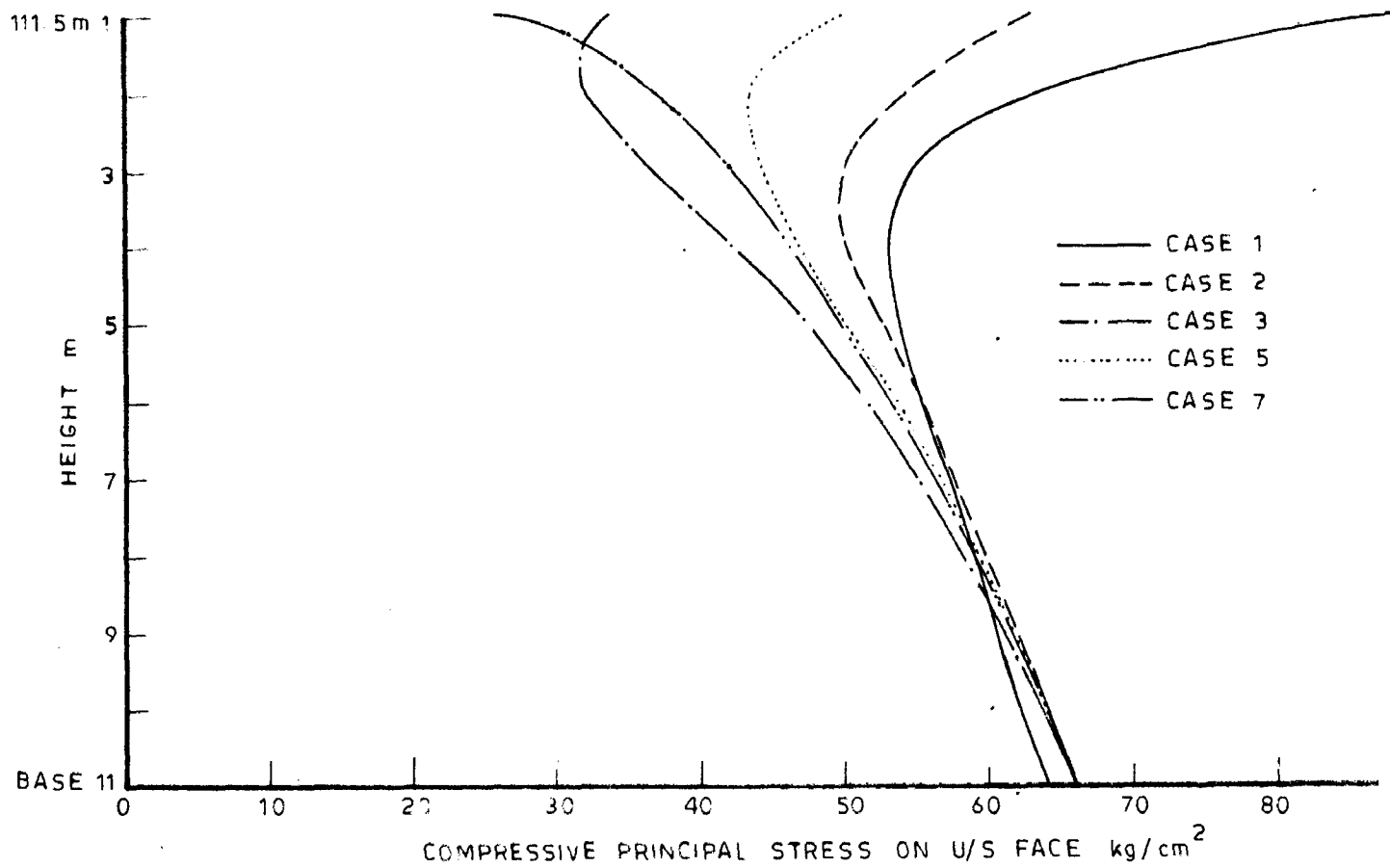


FIG. 15(c) COMBINED PRINCIPAL STRESSES FOR VARIOUS CASES DUE TO KOYNA ELONGATED EARTHQUAKE FOR RESERVOIR CONDITION